Structural studies of two solid steroid compounds

Abdullah Othman

Structural Studies of Two Solid Steroid Compounds

By

Abdullah Othman B.Sc., AMRSC

Ustinov College

Durham University

A thesis submitted in partial fulfillment of requirements for the degree of Masters of Science

Department of Chemistry

Durham University

2006

Abstract

Polymorphism (including solvated solid forms) is relatively common among steroids. Understanding the physical properties of each polymorph/ solvate is important for evaluating their relative stability and dissolution rates (related to bioavailability). In pharmaceutical industry powder X-ray Diffraction (XRPD), complemented by thermal methods, is the most widely used technique for characterising solid forms. However, these methods do not directly provide molecular-level information. Solid-state NMR here plays an important leading role.

A number of polymorphs and solvates of two steroids (androsterone and finasteride) have been studied. Solid-state NMR and XRPD were used to characterise the hemihydrate form and the anhydrous form 1 of androsterone. XRPD was also used to study the transformation between the hemihydrate and the anhydrous form at room temperature as a function of time. Furthermore, the ^{13}C CPMAS spectra of the two forms were assigned by applying specialised NMR pulse sequences.

A number of solid forms of finasteride have been described in the scientific and patent literature. Combined characterisation by solid-state NMR and X-ray diffraction has identified deficiencies in the patent literature, reflecting the limitations of characterisation based on XRPD alone. For instance, one of the patented finasteride "polymorphs" was proved to be a dioxane solvate hydrate. Solid-state NMR and single-crystal XRD have been used to define the structure in a number of newly prepared finasteride solvates. The solvates were found to be all isomorphous with each other as well as with another solvate reported in the literature. They appear to be bis (finasteride) monosolvate monohydrates. Preliminary proton spin-lattice relaxation measurements were done on the solvates and on form II (anhydrous). It is suggested that the relaxation is driven by reorientation of the methyl groups rather than by solvent dynamics. A new form X was characterised by solid–state NMR though the sample is of unknown origin. TGA and DSC experiments were also carried out on the various forms.

Memorandum

The research presented in this thesis has been carried out in the Chemistry Department, Durham University between October 2005 and September 2006. Unless otherwise stated, it is the original work of the author. None of this work has been submitted for any other degree.

Acknowledgments

First of all, I would like to thank my employer Hikma Pharmaceuticals Ltd. for giving me such a splendid opportunity to obtain an M.Sc. degree in such a great University. Second of all, I would like to thank my three supervisors; Dr. John S.O. Evans, prof. Robin K. Harris and Dr. Paul Hodgkinson for their wonderful academic support as well as standing up for me in my daily life. I would like to thank Dr. Alan Kenwright for his help with my study and with his support and suggestions in my research. I am glad for having the chance to collaborate with Dr. Robert Lancaster and for receiving beneficial consultation from him (especially on the androsterone work). I would like to thank also Dr. David Apperley and Dr. Ivana R. Evans for their technical support on solid-sate NMR and single crystal XRD, respectively.

A special thanks goes out to the "unforgettable" Dr. Vadim Zorin our dearest post-doc in the solid-state NMR group for his help basically with everything and for the rest of the solid-state NMR group (Andy, Fraiser, Anne and Tim). Last but not least, the incredibly nice group of XRPD; Loc, Lars, Graham and Sarah. Generally, I thank every single person in the Chemistry department for being such helpful people and all my Footy mates for such a great time.

Thanks to Allah mighty for giving me the strength to achieve this degree
and may Allah make it beneficial to all human beings

To all my beloved family
It wouldn't have been accomplished without your support.....

TABLE OF CONTENTS

Chapter 1: Introduction

1.1 Polymorphs

Structural properties of polymorphs have constituted an important research area with rapid development over the past few decades. A number of definitions are reported for the phenomenon of polymorphism[1,2]. The simplest and fairly classical definition for polymorphs is that they are solid forms of different crystal structures of the same chemical substance which produce indistinguishable solutions when dissolved. A number of annotations are used for labelling polymorphs; the most commonly used are Arabic or Roman numerals. It has been commented that "the number of known polymorphic forms for a given compound is proportional to the time and money spent in research on that compound"[2]. It is very important to distinguish between true polymorphs and other solid forms like solvates (see the following section). Mixing up the definitions of solid forms develops considerable confusion in the literature, hence complicating follow up on the research area.

1.2 Solvates/ Hydrates

Solvates (including hydrates) are different from true polymorphs because they include additional solvent molecules in the crystal structure in addition to the base molecule or host. Solvates have been also termed as pseudopolymophs although this terminology is not recommended[1]. Stoichiometric solvates, especially hydrates, are of comparable importance to that of polymorphs in the pharmaceutical industry because solvation or desolvation can occur during the manufacture formulation and storage of drugs. Some solvates are desolvated without destroying the basic structure whereas in other cases desolvation can lead to break down of the structure. Non-stoichiometric solvates are also reported to be of an interest[1] (e.g. hydrates of tartrate, sildenafil and thiamine hydrochloride). The characterisation of pharmaceutical hydrates must be sufficient to provide confidence that the behaviour of the hydrate is predictable and reproducible. It is reported for example that the smaller the particle size the more rapidly dehydration occurs, which is justified on the basis of surface area and/or the existence of crystal defects. Crystal defects can be encountered when the hydrate is subjected to high-energy particle size reduction, and can have consequent effects on storage and dosing.

1.2.1 Structural Classification of Hydrates[3]

1.2.1.1 Isolated lattice sites

This type of hydrate represents structures with water molecules isolated from direct contact with other water molecules by drug molecules. In cephradine dihydrate, for instance, no line can be drawn between separate water pairs without passing through a portion of cephradine molecule. The two water molecules adjacent to the cephradine molecule were found to be easily lost because presumably no hydrogen bonds network exists between water molecules. Correspondingly, the DSC thermogram showed two incompletely resolved, but sharp, endotherms at approximately 100°C. The TGA thermogram also showed a sharp weight loss.

1.2.1.2 Lattice Channels

Water in this class of hydrates occupies lattice channels, i.e. water molecules lie next to each other along a single direction forming channels (e.g. ampicillin trihydrate). Lattice hydrates often show different thermograms to those of isolated lattice site network. The DSC and TGA thermograms for ampicillin trihydrate for example show that the dehydration onset occurs earlier and the water loss is found to be continuous up to 125°C. The latter observations were attributed to the fact that dehydration begins at one end of the crystal and carries on through the channels towards the other end.

Lattice channel hydrates can be subdivided into different sets[3]:

(i) Expanded Channels (non-stoichiometric)

Hydrates of this class can accommodate additional moisture in the channels when exposed to high humidity (e.g. chromylin sodium).

(ii) Planar Hydrates (lattice planes)

This subclass of hydrates has water localised inside a two-dimensional plane. Examples of this class are sodium ibuprofen and nedocromil zinc.

1.2.1.3 Metal-ion Coordinated Water (Ion Associated Hydrates)

Hydrates of this type have metal ion coordinated water. The metal-water interaction can be quite strong compared to other molecular interactions in crystals, hence dehydration takes place at very high temperatures. Drugs with solubility, dissolution or handling problems are mostly crystallised as Na^{+}, K^{+}, Ca^{+2} or Mg^{+2} salts and often hygroscopic. The tetra-decahydrate and tetra-dihydrate of calteridol calcium are examples of this type of hydrates. Calteridol calcium is used as a chelating excipient in a parenteral formulation which has a metal cation and contains water in channels. In the tetra-decahydrate there are four water molecules associated with each central calcium and ten lattice water molecules associated with channels perpendicular to the *ac* plane.

1.3 Amorphous Forms

Amorphous materials are generally more energetic than crystalline materials; hence they tend to have higher solubilities and rates of dissolution, which makes amorphous forms important in pharmaceutical industry. Amorphous pharmaceutical materials are usually obtained by crystallisation procedures far from equilibrium such as rapid solidification from the melt, lyophilisation or spray drying, removal of solvent from a solvate, precipitation by changing pH or by mechanical processing like granulation, grinding or milling.

1.4 Literature Sources of Polymorphic and Solvated Forms[2]

There are a number of sources and databases for consultation on organic polymorphs and solvates. The Cambridge Structural Database (CSD) is one of the most important and it is continuously updated. The database includes crystal structures of organic and organometallic compounds along with their bibliographic information. The Crystallographic Information File (CIF) for each structure can be extracted from the database which contains the available crystallographic information on each compound or polymorph (unit cell parameters, space group, atomic positions, instrumental settings, etc...). A second crystallographic data base is the Powder Diffraction File (PDF) which consists of organic, organometallic and inorganic compounds. A third source is the patent literature, where enormous numbers of patent issues involve pharmaceutical polymorphs, crystalline forms and even amorphous forms.

1.5 Importance of Pharmaceutical Solid Forms

Pharmaceutical solid forms (polymorphs and solvates) are vital in industry as different forms exhibit different physical properties which influence their performance in formulation. Many pharmaceutical materials (active drug substances and excipients) are found to be polymorphic. Examples of such excipients are lactose, glucose, sucrose, magnesium stearate, calcium phosphates, and mannitol. Enormous numbers of examples of polymorphs and solvates for active ingredients are present in the literature[1,2,4,5]. The nature of solid excipients has an impact on the final physical properties of the formulation (e.g. tablets) or may induce a polymorphic conversion of the active ingredient. Pharmaceutical materials have been shown to have variable properties between different crystal modifications. The physical properties of each solid form are important for evaluation of the relative stability, efficacy and dissolution rates, which in turn are related to bioavailability.

Increasing attention is being paid by regulatory agencies to the preparation, identity, characterisation, purity, and properties of the crystal forms used in pharmaceutical products. Such information is now required by the US Food and Drug Administration (FDA) in a New Drug Application (NDA). The International Conference on Harmonisation (ICH) has also guidelines (Q6A) [6] on this issue.

1.6 Enantiotropic and Monotropic Polymorphs in The Pharmaceutical Industry

One of the key questions regarding polymorphic/ solvated systems is the relative stability of various crystal modifications and the changes in the thermodynamics accompanying a phase transformation. Polymorphs can be classified as one of two types; enantiotropic and monotropic. The latter is defined as a polymorphic system containing two forms in which one undergoes an irreversible phase change to the second form. The former type represents polymorphic systems of two forms in which the two phases can undergo a reversible transition. Increase in temperature for an enantiotropic system leads to the formation of a form at high temperatures which is metastable on cooling to ambient temperatures. Such forms can often exist for long periods of time before transforming to the stable form. Metastable forms are higher in energy and metastable with respect to the most stable forms below the transition temperature. Metastable and unstable forms typically have greater solubility than the more stable forms in a particular solvent and at a given temperature, i.e. stable forms are the least soluble. Consequently, metastable forms are of high importance in pharmaceutical industry and advantageous to selectively obtain and maintain in the formulation. Attempts are carried out to inhibit the growth of the stable form in order to favour the growth of a metastable form[2,7]. A pharmaceutical metastable solid form can relax to the more stable form during processing. Examples of pharmaceutical metastable forms which relax to a more stable form are commonly found in suspensions, in solid dosage forms, and of course via dissolution. Solid-state relaxation is more likely to be a slow process but is possible during storage. Accelerated stability studies may exceed the temperature of a polymorphic phase transition or dehydration, causing transformation of metastable forms to be rapid because of molecular mobility increase. Hydration of a drug can be induced by high humidity. Additionally, exceeding the glass temperature of an amorphous form can induce crystallisation and/or other mobility-related problems[3].

1.7 Hydrogen Bonding in Solid Forms

Hydrogen bonds are amongst the most important intermolecular interactions found in solids, and hence are the subject of several structural studies. Additionally, hydrogen bonds affect the stability and colligative properties (e.g. melting point) of a solid form. Hydrogen bonds are normally found in solid forms where potential hydrogen bond donors and hydrogen bond acceptors are available. Hydrogen bonding between drug molecules and water is very common in hydrates where water acts as a hydrogen bond donor and acceptor at the same time. A water molecule can form up to four hydrogen bonds; two from the two hydrogens (donor) and another two from the two lone pairs on the oxygen (acceptor). Knowing how water is occupying the crystal structure as well as information on hydrogen bonds is very important for hydrates (see hydrates section).

the oxygen (acceptor). Knowing how water is occupying the crystal structure as well as information on hydrogen bonds is very important for hydrates (see hydrates section).

1.8 Controlling the Preparation of Solid Forms; Disappearing Polymorphs

The basic experimental conditions that must be defined for targeting a certain solid form comprise the solvents, temperature range, rate for evaporation or cooling and many others. These conditions are called the occurrence domain. Control over the process of polymorph preparation is not easy to achieve. Moreover, there are crystal forms that are observed over a period of time but are apparently replaced by a more stable crystalline form in later preparations. This phenomenon is called "disappearing polymorphs"[8]. A classical example of this phenomenon in a pharmaceutical system is ritonavir[9,10]. There is a variety of conditions (mentioned above) controlling the reproducibility of crystallisation which makes identifying the factor responsible for this phenomenon a very hard task.

1.9 Analytical Techniques

Many analytical techniques have been used for the characterisation of solid forms. The definitive evidence for the identity of solid forms is provided by the crystal structure (obtained from X-ray or neutron diffraction)[11,12]. Other analytical techniques can be applied for routine analysis of solid forms. Most commonly used in the pharmaceutical industry are powder X-ray diffraction (XRPD) and thermal analysis (TGA, DSC and hot-stage microscopy). FT-IR, Raman and near-IR spectroscopy are used to a lesser extent. However, many researches have been carried out, in the past decade or so, using solid-state NMR (especially using ^{13}C cross polarization magic-angle spinning; ^{13}C CPMAS[1]). The huge development in the techniques relating to CPMAS NMR and the increase of the requirements of the regularity and patent authorities were the reason behind the increasing importance of solid-state NMR. In some cases, solid-state NMR has accurately identified different solid forms while X-ray methods falsely indicated only a single structure[13]. Molecular level mobility information has also been deduced from relaxation time measurements[1,14].

In practice, characterisation of polymorphs/ solvates should involve as many techniques as possible; the more information available from the analyses, the greater the understanding and possible control over the solid forms. For instance, single-crystal XRD analysis gives a definitive crystal structure of a certain form but it cannot generate information about the purity of the whole powder (very important in industry). XRPD assists phase identification as well as purity information (qualitative and quantitative), though it has been reported that it is hard to generate information at a molecular level. Moreover, there are many cases reported where XRPD for isomorphous solvates was unable to distinguish between them (e.g. neotame[13], aspartame[15], erythromycin[16],...etc). For molecular information, solid-state NMR plays a leading role. Additionally, solid-state NMR can

readily identify and quantify purity of different solid forms including amorphous materials. Information on solid mobility has been also obtained. However, other analytical techniques including thermal analysis and microscopy are normally important for quick complementary analysis, providing information on heat capacity, phase transitions and relative stability.

1.10 Steroids

Steroids are of considerable pharmaceutical importance and are of particular interest in the research reported. Hence, Polymorphs and solvates (including hydrates) are relatively common among steroids. Much research has been carried on steroids utilizing solid-state NMR[17-19]. Moreover, steroids are know to have stable hydrates and hemihydrates[20,21]. They generally crystallise well and give high-quality CPMAS spectra[22-27].

1.11 Thesis Overview

It was aimed in the reported research to study the structural properties of various solid modifications of two steroids (androsterone and finasteride) and to gain understanding of the relationship between the NMR chemical shifts of these forms and crystallography. To this end the study utilised XRD (powder, together with single-crystal where appropriate) and NMR (with magic-angle spinning methods for the solids, backed up by solution-state techniques where relevant). Thermal analysis (TGA and DSC) methods were also consulted where appropriate. In order for the investigation to proceed, it was decided to attempt to implement several preparation procedures to obtain samples of finasteride solvates, some of which are novel. The intention was to show that magic-angle spinning NMR can be used to detect the "solvent" molecules (and thus to readily characterise them) and to ascertain to what extent the stoichiometry of the solvates can be established.

1.12 References

1. Harris RK 2006. NMR studies of organic polymorphs & solvates. The Analyst 131:351-373.
2. Bernstein J. 2002. Polymorphism in molecular crystals. ed., Oxford: Oxford University Press. p 410.
3. Brittain HG. 1999. Polymorphism in Pharmaceutical Solids. ed.: Marcel Dekker. p 125-179.
4. Lee DC, Webb M editors. 2003. Pharmaceutical Analysis. ed., Oxford: Blackwell Publishing Ltd. p 364.
5. Hilfiker R editor 2006. Polymorphism in the pharmaceutical industry. ed., Weinheim: Wiley-VCH. p 414.
6. ICH 1999. Specifications: Test Procedures and Acceptance Criteria for New Drug Substances and New Drug Products: Chemical Substances (Q6A).
7. Gu CH, Chatterjee K, Young V, Grant DJW 2002. Stabilization of a metastable polymorph of sulfamerazine by structurally related additives. J Crystal Growth 235(1-4):471-481.
8. Dunitz JD, Bernstein J 1995. Disappearing Polymorphs. Acc Chem Res 28(4):193-200.
9. Bauer J, Spanton S, Henry R, Quick J, Dziki W, Porter W, Morris J 2001. Ritonavir: An Extraordinary Example of Conformational Polymorphism. Pharm Res 18(6):859.
10. Chemburkar SR, Bauer J, Deming K, Spiwek H, Patel K, Morris J, Henry R, Spanton S, Dziki W, Porter W, Quick J, Bauer P, Donaubauer J, Narayanan BA, Soldani M, Riley D, McFarland K 2000. Dealing with the Impact of Ritonavir Polymorphs on the Late Stages of Bulk Drug Process Development. Org Process Res Dev 4(5):413-417.
11. Raw AS, Furness MS, Gill DS, Adams RC, Holcombe JFO, Yu LX 2004. Regulatory considerations of pharmaceutical solid polymorphism in Abbreviated New Drug Applications (ANDAs). Adv Drug Delivery Rev 56(3):414.
12. Threlfall TL 1995. Analysis of Organic Polymorphs - a Review. Analyst 120(10):2435-2460.
13. Padden BE, Zell MT, Dong ZD, Schroeder SA, Grant DJW, Munson EJ 1999. Comparison of solid-state C-13 NMR spectroscopy and powder X-ray diffraction for analyzing mixtures of polymorphs of neotame. Anal Chem 71(16):3325-3331.
14. Byrn SR, Xu W, Newman AW 2001. Chemical reactivity in solid-state pharmaceuticals: formulation implications. Adv Drug Delivery Rev 48(1):136.
15. Zell MT, Padden BE, Grant DJW, Schroeder SA, Wachholder KL, Prakash I, Munson EJ 2000. Investigation of Polymorphism in Aspartame and Neotame Using Solid-State NMR Spectroscopy. Tetrahedron 56(36):6616.
16. Stephenson GA, Stowell JG, Toma PH, Pfeiffer RR, Byrn SR 1997. Solid-state investigations of erythromycin A dihydrate: Structure, NMR spectroscopy, and hygroscopicity. Journal of Pharmaceutical Sciences 86(11):1239-1244.
17. Park JS, Kang HW, Park SJ, Kim CK 2005. Use of CP/MAS solid-state NMR for the characterization of solvate molecules within estradiol crystal forms. Eur JPharmaceut Biopharmaceut 60(3):407-412.
18. Variankaval NE, Jacob KI, Dinh SM 2000. Characterization of crystal forms of beta-estradiol - thermal analysis, Raman microscopy, X-ray analysis and solid-state NMR. J Crystal Growth 217(3):320-331.

19. Wawer I, Nartowska J, Cichowlas AA 2001. C-13 cross-polarization MAS NMR study of some steroidal sapogenins. Solid State Nucl Magn Reson 20(1-2):35-45.
20. Salole EG 1987. The Physicochemical Properties of Estradiol. J Pharm Biomed Anal 5(7):635-648.
21. Hulme AT, Lancaster RW, Cannon HF 2006. Clarification of the crystalline forms of androsterone. Crystengcomm 8(4):309-312.
22. Fletton RA, Harris RK, Kenwright AM, Lancaster RW, Packer KJ, Sheppard N 1987. A Comparative Spectroscopic Investigation of 3 Pseudopolymorphs of Testosterone Using Solid-State Ir and High-Resolution Solid-State Nmr. Spectrochimica Acta 43(9):1111-1120.
23. Harris RK, Say BJ, Yeung RR, Fletton RA, Lancaster RW 1989. Cross-Polarization Magic-Angle Spinning Nmr-Studies of Polymorphism - Androstanolone. Spectrochimica Acta 45(4):465-469.
24. Harris RK, Kenwright AM, Say BJ, Yeung RR, Fletton RA, Lancaster RW, Hardgrove GL 1990. Cross-Polarization Magic-Angle Spinning Nmr-Studies of Polymorphism - Cortisone-Acetate. Spectrochimica Acta 46(6):927-935.
25. Christopher EA, Harris RK, Fletton RA 1992. Assignments of solid-state 13C resonances for polymorphs of cortisone acetate using shielding tensor components. Solid State Nucl Magn Reson 1(2):101.
26. Harris RK, Joyce SA, Pickard CJ, Cadars S, Emsley L 2006. Assigning carbon-13 NMR spectra to crystal structures by the INADEQUATE pulse sequence and first principles computation: a case study of two forms of testosterone. Phys Chem Chem Phys 8(1):137-143.
27. Carss SA, Harris RK, Fletton RA 1995. C-13 Nmr Investigations of 3 Fluorinated Steroids. Magn Reson Chem 33(7):501-505.

Chapter 2: Experimental

2.1 Nuclear Magnetic Resonance (NMR)

2.1.1 Solid-State NMR

2.1.1.1 ^{13}C Cross Polarisation and Magic Angle Spinning NMR (^{13}C CPMAS NMR)

The Cross Polarization (CP) pulse sequence (Figure 2.1) is normally used to enhance the signal-to-noise ratio for spectra and to obtain shorter recycle times by transferring magnetisation from naturally abundant nuclei (normally ^{1}H) to dilute nuclei (e.g. ^{13}C and ^{15}N).[1-3]

The ^{13}C CPMAS NMR spectrum of androsterone hemihydrate was measured at ambient temperature using a VARIAN Inova spectrometer, which operates at 75.40 MHz for ^{13}C and 299.18 MHz for ^{1}H. All other spectra were measured at ambient probe temperature using a Varian InfinityPlus spectrometer, which operates at 125.65 MHz for ^{13}C and 499.70 MHz for ^{1}H. Samples were packed, with light grinding, into 5.0 mm o.d. rotors (except for the acetic acid solvate, for which a 2.5 mm rotor was used).

For finasteride samples, the contact times were in the range 1-5 ms, with spin rates 8.5 kHz, recycle delays of 4 s and acquisition times of 40 ms. The duration of the proton 90° pulse was 4.4 μs. Proton decoupling was carried out with the TPPM[4] method (except for the acetic acid solvate, for which SPINAL[5] was used). The proton decoupling power was equivalent to 55-63 kHz for all spectra except for the acetic acid solvate, for which 100 kHz was applied. Good quality spectra could be obtained with accumulation of 150-220 transients for the 5 mm probe, though 10000 transients were used for the 2.5 mm probe (acetic acid solvate).

For androsterone samples, the contact times were in the range 1 ms, with spin rates of 5 and 9 kHz (for the hemihydrate and form 1, respectively), recycle delays of 60 s and acquisition times of 40 and 75 ms (for form 1 and the hemihydrate, respectively). The duration of the proton 90° pulse was 4.3 μs. Proton decoupling was carried out with TPPM[4] using proton decoupling power equivalent of about 60 kHz. The hemihydrate form spectrum was acquired over 240 transients and for form 1; 900 transients were recorded.

The ^{13}C chemical shifts were indirectly calibrated through the high-frequency adamantane carbon signal (at 38.4 ppm relative to TMS).

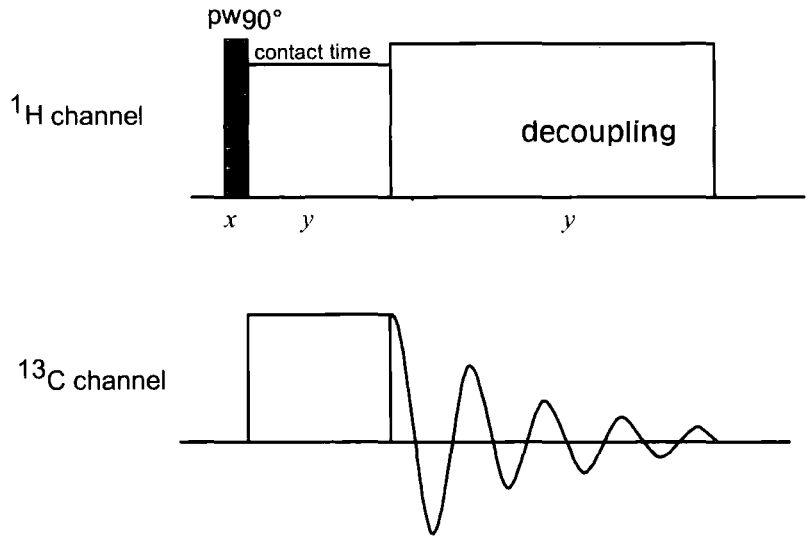

Figure 2.1. CP pulse sequence.

2.1.1.2 ^{13}C Direct Polarisation

Direct polarisation (i.e. simple pulse-and-acquire) was carried out on some finasteride samples (ethyl acetate and THF solvates) in order to distinguish the mobile ^{13}C peaks due to the solvent molecules, which can appear in the spectrum without having to have cross polarisation. The duration of the 90° pulse was 4.4 μs with a recycle delay of 11.0 s and 27 transients.

2.1.1.3 Dipolar Dephasing[2]

A Dipolar Dephasing pulse sequence (Figure 2.2) is normally performed to distinguish the quaternary and methyl carbons in a ^{13}C spectrum, hence aiding assignment of the spectrum. The pulse sequence is similar to a CP sequence but adding a window of time τ during which the carbons are allowed to relax before acquisition. The time is set to be sufficient for the signals from CH and CH_2 carbons to dephase, hence observing only methyl and quaternary carbons. The dipolar dephasing delay time (τ) was 40.0 μs.

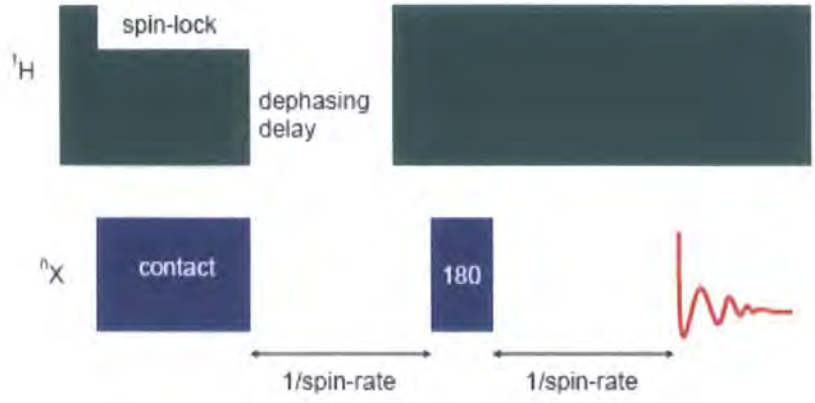

Figure 2.2. Dipolar Dephasing pulse sequence.

2.1.1.4 Selective Population Inversion[6]

This pulse sequence also simplifies the ^{13}C spectrum so that the CH_2 and CH peaks are distinguished. A phase inversion is applied to the CP sequence so that the inversion time τ is chosen to be appropriate for the inversion of the CH_2 carbons (Figure 2.3). Since the CH_2 peaks dephase faster, other carbon types will still appear in the spectrum though their intensities will decrease while the former will show up as base line or negative peaks. Very long inversion times will null or invert the CH peaks but the CH_2 peaks are inverted faster (approximately twice as fast). Typical inversion times were 25 and 50 μs for CH_2 and CH carbons respectively.

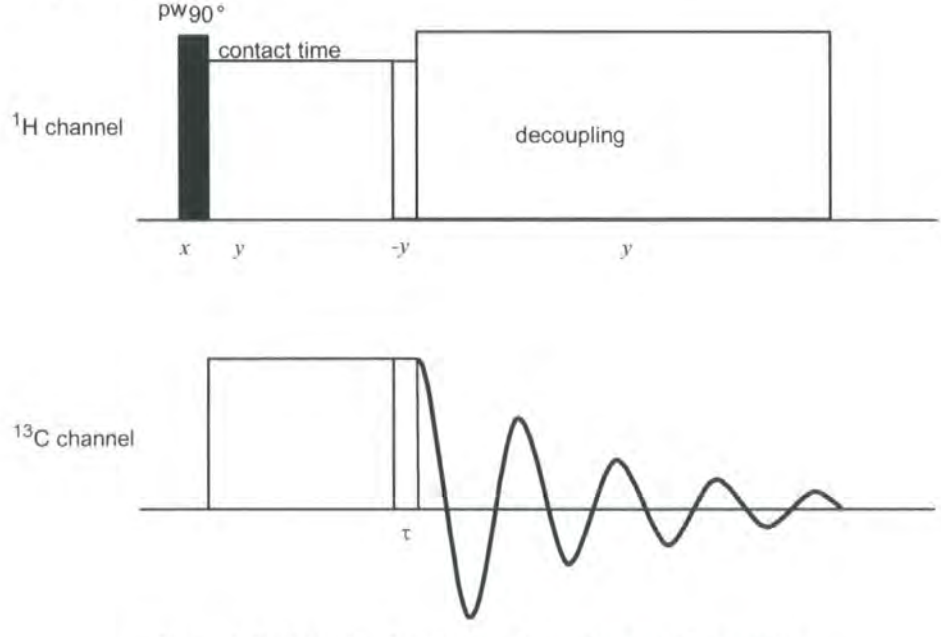

Figure 2.3. Selective Population Inversion pulse sequence

2.1.1.5 ^{1}H MAS NMR

Proton MAS spectra were obtained on a Varian InfinityPlus spectrometer, which operates at 499.70 MHz for ^{1}H using 5.0 or 2.5 mm rotors, spinning at 8.5 and 20.0 kHz respectively. Pulse angles of 90° were used, with recycle delays of 1 s and 5 s and numbers of transients of 4 and 10-20 for the two probes respectively. The ^{1}H chemical shifts were indirectly calibrated through the adamantane proton signal at 1.9 ppm (unresolved peak) relative to TMS. Empty rotor background was not recorded.

2.1.1.6 Saturation Recovery

Proton spin-lattice relaxation times (T_1) were obtained for various forms of finasteride by the saturation-recovery method at ambient temperature using the 5 mm probe under ^{1}H MAS conditions. Saturation was obtained by 100 90° pulses separated by 10μs. Plots were derived using between 10 to 20 points, with 1s recycle delays. The saturation recovery data were fitted using the following equation:

$$I(\tau) = I_0 \times \left[1 - \exp\left(\frac{-\tau}{T_1}\right)\right] \qquad \textbf{Equation 1}$$

where $I(\tau)$ is the intensity at the recovery time τ and I_0 is the maximum intensity at $\tau = \infty$.

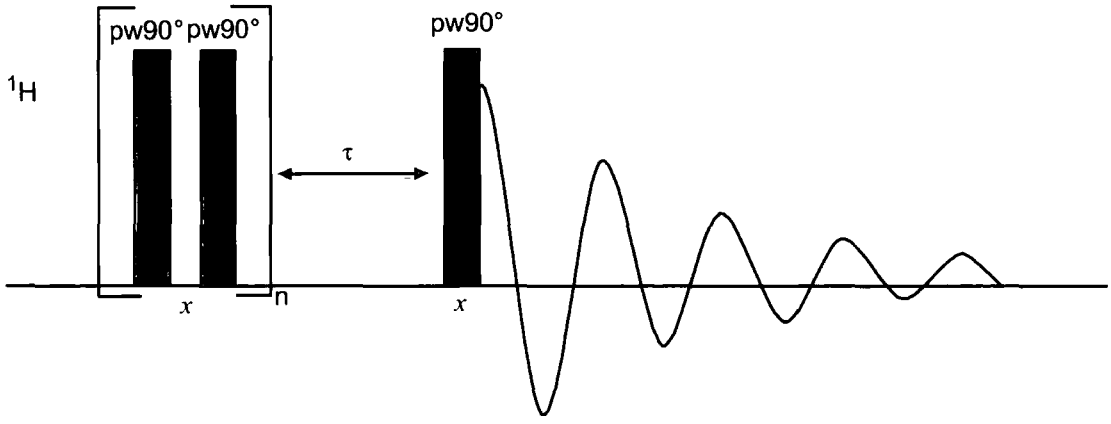

Figure 2.4. Saturation recovery pulse sequence

2.1.1.7 Variable Temperature NMR

A variable-temperature ^{13}C NMR experiment on finasteride dioxane solvate hydrate was carried out. The spectra were obtained at ten degree intervals from 50°C to 110°C and then at 115°C and 125°C, with *ca.* 45 minutes spent at each temperature. For each temperature set, the probe was left for 15 minutes for heat equilibrium and the total time to record each ^{13}C spectrum was 10 minutes. Saturation-recovery experiments were performed at each temperature to determine T_1 proton relaxation times under spinning and static conditions. A ^{13}C spectrum was checked towards the end at ambient temperature.

2.1.2 Solution-State NMR

2.1.2.1 1D NMR

A Varian Inova spectrometer was employed for solution-state NMR spectra of ^{13}C at 125.68 MHz. The spectra were obtained with recycle delays of 3 s, acquisition time of 1.4 s, pulse angles of 45° and 3000 and 5000 transients (for finasteride and androsterone, respectively). Proton decoupling for ^{13}C spectra was achieved by the WALTZ-16 pulse sequence.

The ^{1}H spectra were obtained with a Varian Inova spectrometer at 499.77 MHz .The parameters were as follows: 30 s recycle delays, 4.1 s acquisition times, 45° pulse angle and 32 transients.

2.1.2.2 Heteronuclear Single Quantum Correlation (HSQC)[7]

The 2D experiment shows one-bond correlation between dilute nuclei (^{13}C or ^{15}N) and protons. Hence, carbon or nitrogen atoms not attached (single bond) to any hydrogen atoms do not show any correlation. The pulse sequence is illustrated in Figure 2.5.

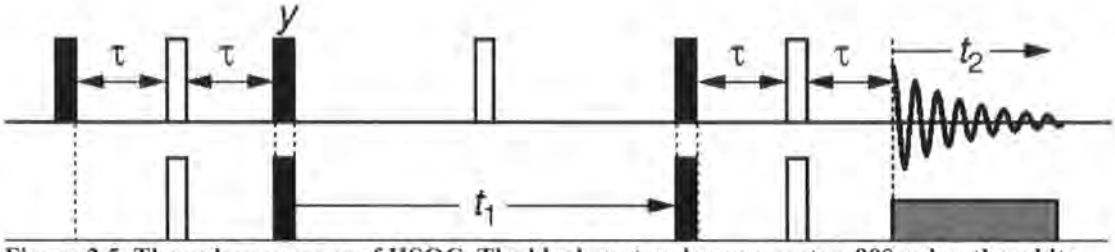

Figure 2.5. The pulse sequence of HSQC. The black rectangle represents a 90° pulse, the white rectangle represents a 180° pulse and the grey rectangle represents broadband decoupling.

2.1.2.3 Heteronuclear Multiple Bond Coherence (HMBC)[7]

HMBC is a long-range correlation experiment (Figure 2.6). Correlation between the dilute nuclei, say ^{13}C, and protons which are separated by 2-3 bonds are observed.

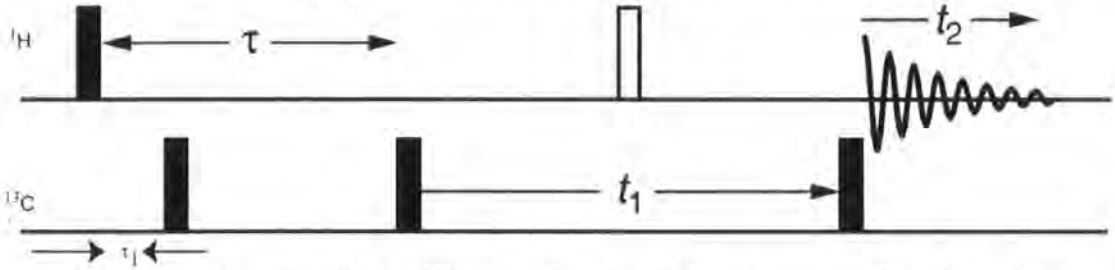

Figure 2.6. The pulse sequence of HMBC. The black rectangle represents a 90° pulse and the white rectangle represents a 180° pulse.

2.1.2.4 Nuclear Overhauser Effect SpectroscopY (NOESY)[7]

The NOE effect is shown between nuclei which exhibit cross relaxation. In order for the cross relaxation to happen, the nuclei have to be close in space. Hence, this experiment is different from the previous 2D NMR experiments where the correlations in this experiment are between nuclei which are correlated through space (not through bonds as in HMBC). See Figure 2.7 for illustration of the pulse sequence.

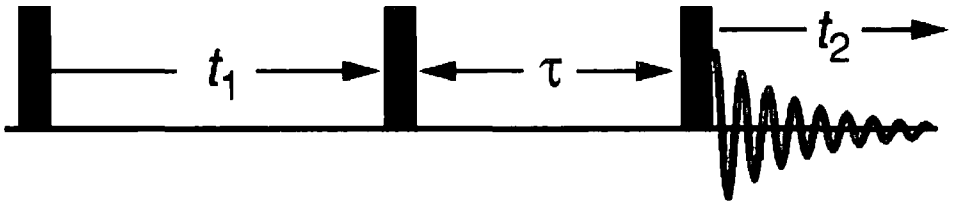

Figure 2.7. The pulse sequence of NOESY. The black rectangle represents a 90° pulse.

2.2 X-ray Diffraction

2.2.1 X-ray Powder Diffraction (XRPD)

Two diffractometers (Siemens D5000 and Bruker D8 Advance) were used for all routine work. They utilised $CuK_{\alpha 1,2}$ radiation. All sample scans were in the range of 5–70 or 5–50° 2θ, with a 20 mm variable-divergence slit and a time step of 1 s. Samples with large crystallites were ground under liquid nitrogen before examination in order to minimise preferred orientation effects. Samples were run on silicon slides except for androsterone form 1, which was run on a glass slide. The transformation of androsterone hemihydrate to form1 was monitored on the Bruker D8 Advance over 24 hours. The sample was examined on a silicon slide with 2θ range of 5–50, 10 mm variable-divergence slit and a time step of 0.3 s (each scan took ~14.7 minutes).

2.2.1.1 Rietveld Fitting[8]

The Rietveld method is reported as one of the fastest and most accurate quantitative phase analysis methods used in XRPD, especially because of the possibility to introduce a preferred orientation correction in addition to quantitative analysis with respect to all present phases. To carry out the quantitation, the atomic positions of each phase are needed[1] along with structural data. Scale factors for every phase present in the mixture are proportional to the fraction of the unit cells present in the irradiated volume of the sample. Hence, the scale factors can be converted into weight, molar or volume fractions.

[1] The CIF files were used in all fittings for this purpose, which were taken form the CSD.

The Rietveld[9] method is a crystal structure refinement method which refines the structural and instrumental parameters of a model to fit with the experimental pattern. The refinement is carried out by non-linear least square minimisation with the minimised function,Φ:

$$\Phi = \sum_{i=1}^{n} w_i (Y^{obs} - Y^{calc})^2 \qquad \textbf{Equation 2}$$

where n is the total number of points measured in the experimental pattern, w_i is the weight assigned to the i^{th} data point which often equals ($1/ Y^{obs}$), Y^{obs} is the observed intensity at point i and Y^{calc} the calculated intensity at point i.

The quality of the fitting is usually indicated by computing profile residual (R_p), weighted profile residual (R_{wp}), expected residual (R_{exp}) and goodness of the fit (χ^2); see the following equations.

$$R_p = \frac{\sum_{i=1}^{n} \left| Y_i^{obs} - Y_i^{calc} \right|}{\sum_{i=1}^{n} Y_i^{obs}} \times 100\% \qquad \textbf{Equation 3}$$

$$R_{wp} = \left[\frac{\sum_{i=1}^{n} w_i (Y^{obs} - Y^{calc})^2}{\sum_{i=1}^{n} w_i (Y_i^{obs})^2} \right]^{1/2} \times 100\% \qquad \textbf{Equation 4}$$

$$R_{exp} = \left[\frac{n-p}{\sum_{i=1}^{n} w_i (Y_i^{obs})^2} \right]^{1/2} \times 100\% \qquad \textbf{Equation 5}$$

$$\chi^2 = \frac{\sum_{i=1}^{n} w_i (Y^{obs} - Y^{calc})^2}{n-p} = \left[\frac{R_{wp}}{R_{exp}} \right]^2 \qquad \textbf{Equation 6}$$

where p is the number of free least squares parameters.

However, none of these parameters replace the importance of observing the difference plot between the observed and calculated patterns, which is shown at the bottom (grey colour) of each Rietveld fit. For the majority of the work reported here (where effects such as preferred orientation are often severe) we present graphical plots rather than quantitative agreement indices.

The plots of Rietveld fits used throughout the research show the percentage of the phase(s) in the solid examined at the right top, the data file name at the left top, the observed pattern in blue and the calculated pattern in red.

The parameters refined are: instrumental parameters, zero point, background, scale factor, unit cell parameters, temperature factors, peak shape and preferred orientation by spherical harmonic function. In the refinements which were carried out using finasteride ethyl acetate solvate model, the disordered atoms of the solvent (ethyl acetate) were excluded.

2.2.2 Single-crystal X-ray Diffraction (single-crystal XRD)

All single-crystal XRD data collections were performed on a Bruker SMART 6000 diffractometer, equipped with a CCD detector, Mo Kα source and an Oxford Cryosystems N_2 cooling system. In each case, a full sphere of data was collected and a multiscan absorption correction[10] was applied to the raw data. Frames were integrated using the program SAINT[11]. The crystal structure was solved by direct methods using the SIR92 software[12] and refined using the Oxford Crystals suite[13]. The positions and anisotropic atomic displacement parameters of all non-hydrogen atoms were refined. The same shifts in fractional coordinates obtained for hydrogen carrying C and N atoms were applied to the hydrogen atoms themselves (riding model) i.e. positions of hydrogen atoms were not refined independently. All crystallographic information, including experimental and structural details and the agreement factors obtained in the refinements, is given in Table 9 of chapter 2. All data collections and refinements were done by Dr I.R. Evans at the single crystal XRD service[2].

2.3 Thermal Analysis

2.3.1 Differential Scanning Calorimetry (DSC)

Thermal events in DSC appear as deviations from the baseline, in either an endothermic or exothermic direction, depending upon whether more or less energy has to be supplied to the sample relative to the reference material. The direction of the exothermic event is shown on the DSC thermogram (exo down). The thermal events shown in the thermogram represent phase transformations. The intercept between the tangent of the melting peak onset and the baseline provides the melting point. The difference in the enthalpy for each DSC event is shown in the plot[14].

The DSC analysis was carried out on a TA Instruments system. All samples were run from 25°C to 300 °C. Nitrogen was used as purge gas. The heating rate was kept constant at 1°C min^{-1}. Aluminium sample pans were used for all samples. A single point calibration was carried out using indium (melting point 156.60°C) as a standard sample.

[2] Chemistry Department, Durham University.

2.3.2 Thermal Gravimetric Analysis (TGA)

TGA is carried out to quantify the mass loss from a sample while being heated, here revealing information about the solvent included in the solid forms. The difference in the y-scale before and after the loss step represents the percentage mass loss (shown in the thermogram as "Delta Y"). A Perkin-Elmer Pyris 1 instrument was used for all TGA samples. Nitrogen was used as the purge gas and the heating rate was kept constant at 2°C min^{-1}.

2.4 References

1. Stejskal EO, Memory JD. 1994. High Resolution NMR in the Solid State. ed.: Oxford. p 66.
2. Harris RK. 1989. Nuclear Magnetic Resonance. ed.: Longman Scientific & Technical. p 157-159,170.
3. Duer MJ. 2004. Introduction to Solid-State NMR Spectroscopy. ed.: Blackwell. p 96.
4. Bennett AE, Rienstra CM, Auger M, Lakshmi KV, Griffin RG 1995. Heteronuclear decoupling in rotating solids. J Chem Phys 103:6951-6958.
5. Fung BM, Khitrin AK, Ermolaev K 2000. An improved broadband decoupling sequence for liquid crystals and solids. J Magn Reson 142:97-101.
6. Xiaoling W, Shanmin Z, Xuewen W 1988. Selective polarization inversion in solid state high-resolution CP MAS NMR. J Magn Res 77(2):347.
7. Keeler J. 2005. Understanding NMR Spectroscopy. ed.: Wiley. p 214-223,287.
8. Pecharsky VK, Zavalij PY. 2005. Fundamentals of Powder Diffraction and Structural Characterization of Materials. ed.: Springer. p 388, 608.
9. Rietveld H 1969. A profile refinement method for nuclear and magnetic structures. Journal of Applied Crystallography 2(2):65-71.
10. Sheldrick GM. 1998. SADABS. ed., University of Gottingen, Germany.
11. Systems BA. 1997-2001. SAINT+. Release 6.22 ed., Madison, Wisconsin.
12. Altomare A, Cascarano G, Giacovazzo A, Guagliardi A, Burla MC, Polidori G, Camalli M 1994. SIR92 – a program for automatic solution of crystal structures by direct methods. J Appl Cryst 27:435.
13. Betteridge PW, Carruthers JR, Cooper RI, Prout K, Watkin DJ 2003. CRYSTALS version 12: software for guided crystal structure analysis. J Appl Cryst 36:1487.
14. Brown ME. 1988. Introduction to Thermal Analysis: Thechniques and Applications. ed.: Chapman and Hall. p 24.

Chapter 3: Literature Review on Finasteride Solid Forms

3.1 Introduction

Finasteride (N-t-butyl-3-oxo-4-aza-5α-androst-1-ene-17β-carboxamide) is an azasteroid which is considered as the most potent 5α-reductase inhibitor[1]. A number of finasteride solid forms are reported; five (supposedly-different) polymorphs and three solvates are mentioned in the literature. Two of the polymorphs (form I and II) have been described in the patent literature[2-6] and also in the scientific literature[7-9]. The other three were only reported in the patent literature: novel form III claimed by Reddy *et al.*[5,6] in 2005 and another two forms (H1 and H2) claimed in the patent by Parthasaradhi *et al.*[10] in 2004. Two of the solvates were reported first in the scientific literature, with crystal structures, by Wawrzycka *et al.*[9] and later on they were reported in the patent literature[5,6] but prepared by different methods and characterised by XRPD. The solvates are an acetic acid solvate and an ethyl acetate solvate. A third solvate obtained from dioxane was characterized by Morzycki *et al.*[7] using FT-IR and solid–state NMR but the crystal structure was not confirmed.

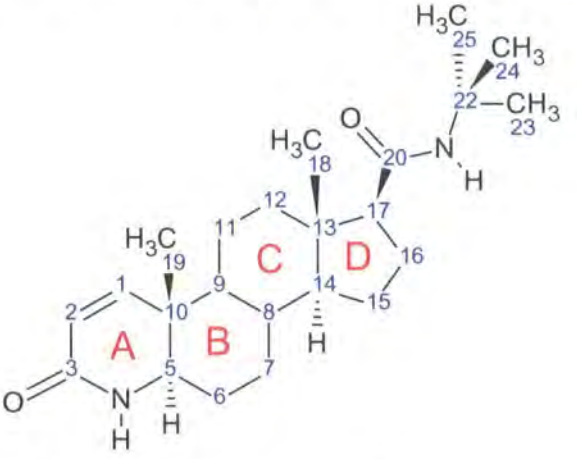

Molecular structure of finasteride

3.2 Finasteride Polymorphs Reported in The Scientific and Patent Literature

3.2.1 Form I

Finasteride form I was reported in both the scientific[7-9] and patent[2-6] literatures. The crystal structure of finasteride form I was reported by Wawrzycka *et al.*[9] and Wenslow *et al.*[8] with Cambridge Structural database (CSD) codes of WOLXOK01 and WOLXOK02, see Table 3.1. Finasteride form I crystallizes in the orthorhombic space group $P2_12_12_1$ (see Table 3.1 for unit cell parameters and Figure 3.1 for a view of the crystal structure).

Form I has strong intermolecular hydrogen bonds between ring A lactam groups where the lactam NH group is the donor and the carbonyl from another molecule is the acceptor. In the opposite part of the molecules C-H...O hydrogen bonds were observed between neighbouring methyl and peptide groups[9]. The lactam-to-lactam hydrogen bonding was reported to be strong, with the distance from the lactam nitrogen of one molecule to the lactam oxygen of its partner being 2.85 Å. The lactam-to-lactam chains produced are parallel to the crystallographic *a* axis. The tert-butylamide site of the molecule was found to be uninvolved in hydrogen bonding due to the steric effect of the tert-butyl group. This was confirmed from interatomic distances measured by XRD. It was also proved by IR spectroscopy where the NH stretch frequency in form I was similar to that of the solution state (in chloroform) frequency, indicating that it is behaving closely to the solution state in solvents where hydrogen bonding is not present[8].

Form I undergoes a solid-to-solid transformation to form II on heating, which then melts on further heating. This solid–solid phase transition temperature was found to be dependent on the heating rate (~230 to 200 °C as the heating rate is changed from 10 to 0.1 °C / min). The melting temperature (257 °C) varies by only two degrees over the same range of heating rates [6]. The system was characterised by McCauley *et al.*[4] to have a minor endotherm with a peak temperature of about 232°C, an extrapolated onset temperature of about 223°C with an associated heat of about 11 J/g and by a major melting endotherm with a peak temperature of about of 261°C, an extrapolated onset temperature of about 258°C and an associated heat of about 89 J/g.

Form I was characterised by ^{13}C CPMAS NMR and the chemical shifts were assigned[7,8]. The assignments were consistent with the crystallographic information provided by XRD.

Table 3.1. Crystallographic data on finasteride solid forms in the literature.

	Form I	Form II	Acetic acid solvate[9]	Ethyl acetate solvate[9]
Formula	$C_{23}H_{36}N_2O_2$	$C_{23}H_{36}N_2O_2$	finasteride. CH_3COOH	2finasteride. $H_2O.C_4H_8O_2$
FW	372.556	372.556	432.59	851.20
Lattice symmetry	orthorhombic	monoclinic	Monoclinic	orthorhombic
Space group	$P2_12_12_1$	$P2_1$	$P2_1$	$P2_12_12_1$
***a* (Å)**	6.437(1)	16.387(2)	12.170(l)	8.173(3)
***b* (Å)**	12.712(1)	7.958(2)	8.16521(7)	I8.364(6)
***c* (Å)**	25.929(1)	18.115(5)	13.577(l)	35.65(2)
α (°)	90	90	90	90
β (°)	90	107.25(2)	111.630(1)	90
γ (°)	90	90	90	90
Z	4	4	2	4
Z'	1	2	1	2
Unit cell volume (Å^3)	2121.7(6)	2256(2)	1254.1(2)	5350(4)
CSD code	WOLXOK02, WOLXOK01	WOLXOK03, WOLXOK	WOLXEA	WOLXIE
Melting point (°C)	253-256	253-256	255-257	252-255

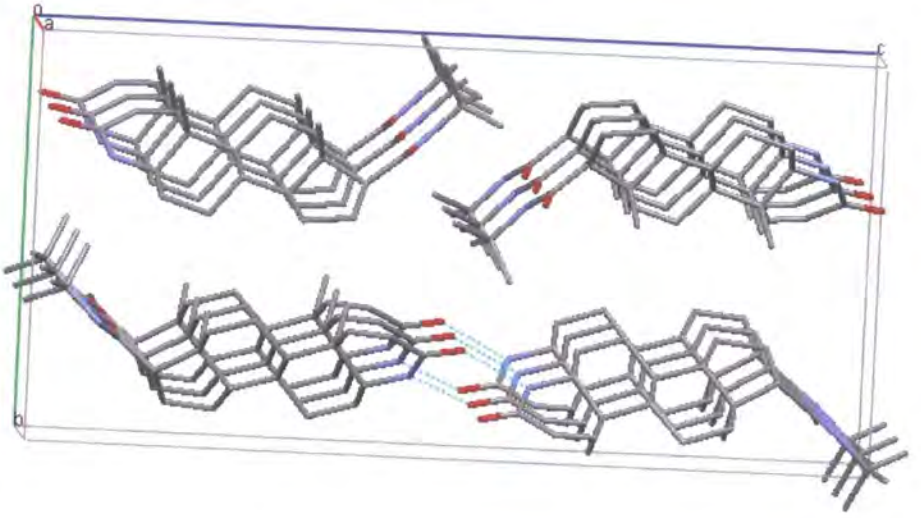

Figure 3.1. Form I crystal structure and packing inside the unit cell, viewed along the *a* crystallographic axis. Dotted lines represent hydrogen bonding.

3.2.1.1 Reported Methods of Preparation

The Following methods have been reported for the preparation of form I. Given the existence of solvates, some of these methods may be questionable particularly where the characterisation was very limited.

(i) Dissolving finasteride in glacial acetic acid (ca. 100 mg/mL) and adding water with stirring until the weight % of water equals or exceeds 84%. The resulting solid phase is collected by filtration and dried under vacuum and at about 50°C[4].

(i) Heating polymorphic form II of finasteride to about 25°C in water or an organic and recovering the resultant solid phase, e.g. by filtration. Additionally it was prepared by stirring form II overnight in dry toluene at ambient temperature, and recovering the resultant solid phase. Form I was also obtained by stirring form II overnight in dry acetonitrile at ambient temperature, and recovering the resultant solid phase[4].

(ii) Crystallisation from an ethanol / water (1:10) solution[9].

(iii) Crystallisation directly from dry ethyl or isopropyl acetate[4,8]. For example, to produce form I of finasteride from an ethyl acetate/ water mixture, the amount of water used is at most about 3.5 mg/mL, and from an isopropyl acetate/ water mixture, the amount of water used is at most about 1.6 mg/ mL, both at an ambient temperature of about 25°C. The isolated solids are dried under vacuum at about 50° C.

(iv) Recrystallisation from a binary solvent mixture (acetic acid and water). The exact concentration was not reported[7].

(v) Dissolving finasteride in a solvent, distilling off the solvent from the solution then adding a non-solvent and finally isolating the solid. The solvent can be methanol or dichloromethane and the non-solvent can be water, hexane, heptane, toluene, xylene, isobutyl acetate or isopropyl acetate3.

3.2.2 Form II

Form II is a monoclinic metastable form of finasteride, which is formed at higher temperatures (above 175 °C). Unit cell parameters of low reliability were determined by Wawrzycka *et al.*[9], the crystals having been prepared as illustrated in point (iv) under methods of preparation section 2.1.0[9]. Following that, the crystal structure was determined by Wenslow *et al.*[8]. Form II crystals have a $P2_1$ space group with two drug molecules in the asymmetric unit (see Table 3.1 for unit cell parameters). The conformations of the two molecules in the asymmetric unit were found to be similar. It was also reported that "the similarity in confirmation of the three molecules (one in form I and two in form II) suggests that the polymorphism between the forms is lattice rather than conformational"[8]. It was shown that strong hydrogen bonding due to the lactam group is present, which is in agreement with the case of form I where the measured hydrogen-bond distances from nitrogen to oxygen were 2.85 Å in form I and 2.85 and 2.80 Å for the two molecules in form II. The lactam-to-lactam chains caused by this hydrogen bonding are parallel to the crystallographic axis *b*. Also, as in the case of form I, the tert-butylamide substituents of the 5-membered ring are not involved in any hydrogen-bonding in the lattice; as the nearest contacts between the amide nitrogen, in any of the three molecules, and an acceptor atom were larger than 4.2 Å.

The lactam-to-lactam hydrogen-bonding interaction in form II was also proved by IR spectroscopy. The spectrum showed a broad and strong NH stretch at 3213 cm^{-1}, and the lactam carbonyl stretch at 1655 cm^{-1}. The tert-butylamide side chain NH stretch at 3440 cm^{-1} was found to be sharp, and its high frequency indicates that it does not participate in a hydrogen bond. The ^{13}C CPMAS spectrum of form II was reported and assigned The assignments were consistent with the crystallographic information provided by XRD[8].

Form II was also characterized by DSC at a heating rate of 20°C/ min and in a closed cup, exhibiting a single melting endotherm with a peak temperature of about 261°C and extrapolated onset temperature of about 258°C, with an associated heat of about 89 J/ g[4].

3.2.2.1 Reported methods of Preparation

The Following methods have been reported for the preparation of form II:

(i) Dissolving finasteride in glacial acetic acid (ca. 100 mg/mL) and adding water with stirring until the weight % of water equals about 75-80%. The resulting solid phase is collected by filtration and dried under vacuum at about 100 °C[4].

(ii) Heating form I up to about 150 °C, holding for a time sufficient to convert form I to form II, for example for about an hour, and cooling back to room temperature[4].

(iii) Recrystallisation from ethyl acetate containing from about 3.5 to 30 mg/mL of water, or from isopropyl acetate containing from about 1.6 to 15 mg/mL of water, at ambient temperature (about 25 °C); i.e. the amount of water used in the solvent mixture will be more than that used to produce form I from the same organic solvent. The isolated solids are dried under vacuum at about 80° C[4].

(iv) Obtained both by thermal decomposition of the acetic acid solvate (175 °C 30 min) and by sublimation of form I, acetic acid solvate or the ethyl acetate solvate (about 235 °C 30 min), using hot stage microscopy. In this case unit cell parameters of poor quality crystals were determined[9].

(v) A molten sample of the drug was held at 249 °C and seeded with a tiny crystal of the form II polymorph. Over a period of several hours, the sample was crystallized in the melting- point capillary[8].

(vi) Recrystallisation from a binary solvent mixture (acetic acid and water). The exact concentration was not reported[7].

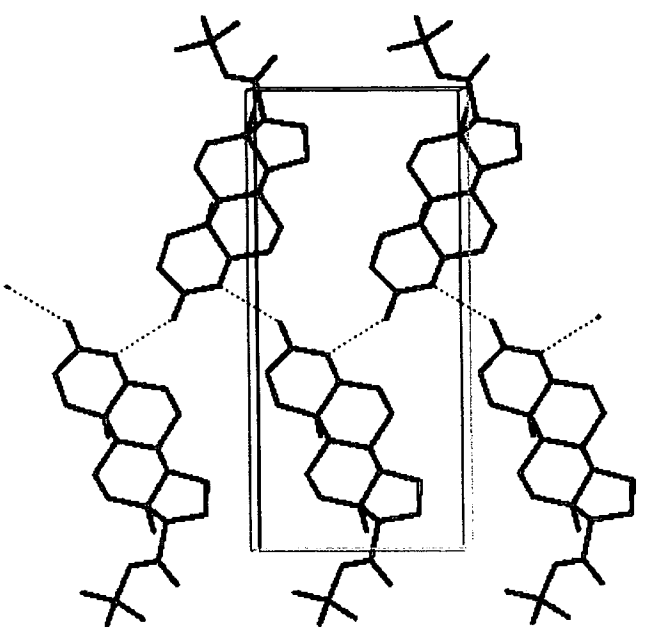

Figure 3.2. Form II crystal structure inside the unit cell with the view along the *a* crystallographic axis. Dotted lines represent hydrogen bonding.

3.3 Finasteride Polymorphs Reported in The Patent Literature

3.3.1 Form III[5,6]

Form III was isolated by Reddy *et al.* [5,6] while doing process development to optimize the yield and quality. The crystal structure was not determined for this form but it was characterised by DSC, FT-IR and powder XRD as follows:

(i) DSC melting endotherm with peak temperature of about 262°C proceeded by another minor endotherm at about 245°C and an exotherm at about 253°C (Figure 3.3).

(ii) The XRPD pattern and 2θ values were reported; see Figure 3.3 and Table 3.2, respectively.

(iii) Characteristic FT-IR wave numbers were reported as the following: 3427, 3233, 2931, 1679, 1600, 1501, 1451 and 820 cm^{-1}.

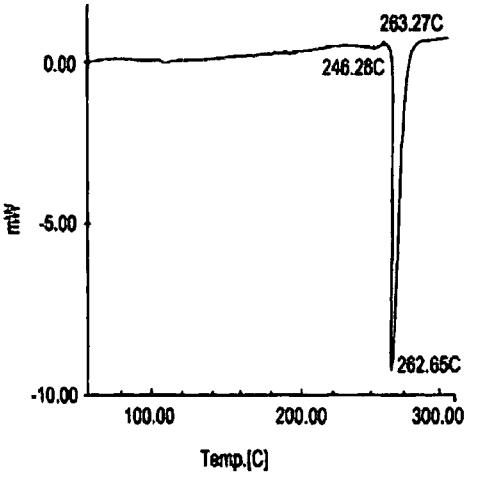

Figure 3.3. DSC thermogram data of the claimed form III[5,6]

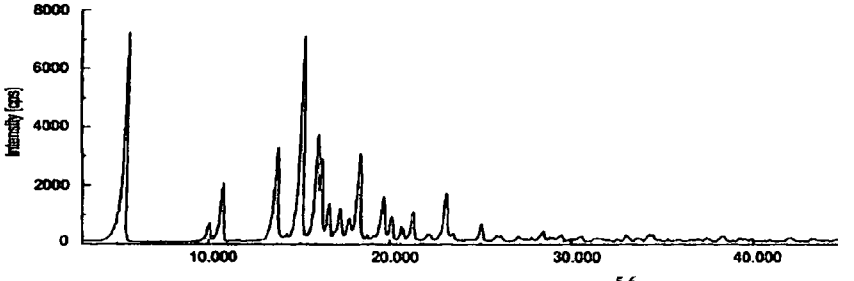

Figure 3.4. XRPD pattern for the claimed from III[5,6]

Table 3.2. The 2θ values for the patented finasteride polymorphs.

Form	2θ values
Form III	5.32, 10.70, 13.64, 14.96, 15.86, 16.12, 16.56, 17.20, 18.22, 19.60, 23.04
Form H1	5.3, 5. 8, 6.8, 7.3, 9.0, 9.4, 10.7, 13.9, 14.9, 15.9, 17.3, 18.2, 19.0, 20.1
From H2	5. 4, 9.9, 12.1, 14.5, 15.2, 16.2, 19.3, 29.0.

3.3.1.1 Reported methods of Preparation

Finasteride form III was reported to be prepared by the following general methods:

A- From Crude Finasteride:

(i) Dissolving crude finasteride in water-immiscible organic solvents such as halogenated (preferably "dichloromethane, chloroform" in the patent), aromatic hydrocarbon, "preferably toluene", or organic solvents from alkyl acetates, "preferably ethyl acetate".

(ii) Saturation of the solution with less polar solvent "aliphatic hydrocarbons, either straight chain or branched, preferably hexane or heptane or petroleum ether".

(iii) Concentrating the solution and isolating the form III by conventional methods.

B- From Finasteride Forms {form I, form II, ethyl acetate solvate and acetic solvate}

(i) Dissolving any of the solid forms (form I, form II, ethyl acetate solvate and acetic acid solvate) in water-immiscible organic solvents such as halogenated "preferably dichloromethane, chloroform", aromatic hydrocarbon "preferably toluene" or organic solvents from alkyl acetates "preferably ethyl acetate".

(ii) Distilling 60-70% of the solvent.

(iii) Saturating the remaining solution with less polar solvent "aliphatic hydrocarbons either straight chain or branched, preferably hexane or heptane or petroleum ether".

(iv) Concentrating the solution and isolating the form III by conventional methods.

The following are two specific examples of form III preparation mentioned in the patent:

3.3.1.2 Conversion of Crude Finasteride to Form III

(i) Crude Finasteride was dissolved in methylene chloride (3 mL) at 25-35°C.

(ii) The methylene chloride was saturated with petroleum ether (20 mL) at 25-30°C under stirring.

(iii) The separated solid, after removal of methylene chloride and petroleum ether under reduced pressure at 50-60°C, is isolated with petroleum ether (2 mL) at 10-15 °C.

(iv) The resultant solid was dried at ambient temperature (yield: 0.8 g).

3.3.1.3 Conversion of Finasteride Solid Forms to Form III

(i) 1 g of any finasteride solid form (form I, form II, ethyl acetate solvate or acetic solvate) was dissolved in 3 mL methylene chloride or chloroform.

(ii) 60-70 % of methylene chloride was distilled off at 40-45 °C; in the case of chloroform it was distilled off at 60-70 °C.

(iii) The resultant solution was saturated with petroleum ether (10 mL) at 40-60 °C under stirring.

(iv) The solution was concentrated at 60-65°C at atmospheric pressure

(v) The resultant residual solid was kept under vacuum at 60-65°C for about 30 minutes.

(vi) The solid obtained was isolated and dried in an oven at 70-90 °C for 8-12 hours, to yield form-III (yield: 0.8-0.9 g)

3.3.2 Form H1 and H2[10]

Parthasaradhi *et al.*[10] describe the preparation of two "novel crystalline" forms, H1 and H2, characterized only by XRPD. Table 3.2 shows the reported 2θ for each claimed form; see Figure 3.5 and Figure 3.6 for the corresponding XRPD patterns. The form H1 is obtained from alcohols (methanol, ethanol, IPA individually or from mixtures of these alcohols), whilst form H2 is prepared from a dioxane solution. It is worth mentioning here that a dioxane solvates has been reported by Morzycki *et al.*[7] though the XRPD of the solvate was not examined. Both forms, H1 and H2, are reported to be suitable for pharmaceutical formulation in the patent.

3.3.2.1 Preparation of form H1

The general method for the preparation of this form is by mixing finasteride and an alcohol, maintaining at about 40°C-60°C for about 10 minutes to 1 hour, then cooling slowly to about 0-5°C, maintaining for about 1-3 hours at this temperature and filtering the solid. The alcohol is methanol or ethanol or isopropyl alcohol or mixtures. The author reported that this procedure can be repeated using form H2 instead of finasteride to give form H1 of finasteride.

The following is a specific preparation example:

(i) Finasteride (10 g) is dissolved in methanol (25 mL), heated to 55°C and maintained at this temperature for 15 minutes. The solution is slowly cooled to 0°C in 3 hours and maintained at 0°C for 1.5 hours. The separated crystals are filtered at 0°C to give 8.5 g of form H1 of finasteride.

(ii) Finasteride (10 g) is dissolved in isopropyl alcohol (40 mL), heated to 55°C and maintained at this temperature for 15 minutes. The solution is slowly cooled to 0°C in 3 hours and maintained at 0°C for 1.5 hours. The separated crystals are filtered at 0°C to give 8.5 g of form H1 of finasteride.

3.3.2.2 Preparation of form H2

The general method for the preparation of this form is by dissolving finasteride in dioxane, maintaining at about 70°C-80°C for about 10 minutes to 30 minutes, then cooling the solution slowly to about 20°C-25°C maintaining at about 20°C-25°C for about 2 hours to 4 hours and filtering the solid separated. The author reported that this procedure can be repeated using form H1 instead of finasteride to give form H2 of finasteride. The following is a specific preparation example:

Finasteride (10 g) is dissolved in dioxane (50 mL), heated the solution to 80°C and maintained at 80°C for 15 minutes. The solution is slowly cooled to 25°C, maintained for 3 hours at 25°C and the solid separated is filtered to give 9 g of form H2 of finasteride.

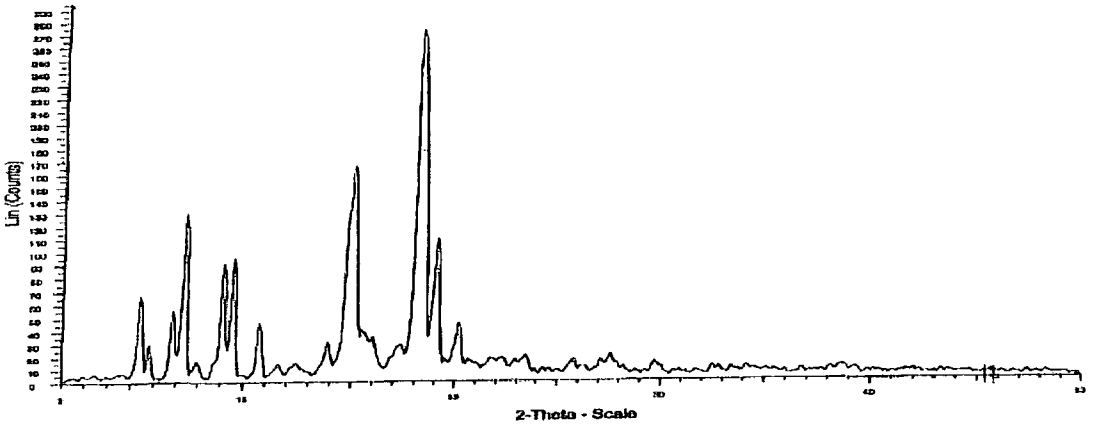

Figure 3.5. XRPD pattern for the claimed H1 from[10].

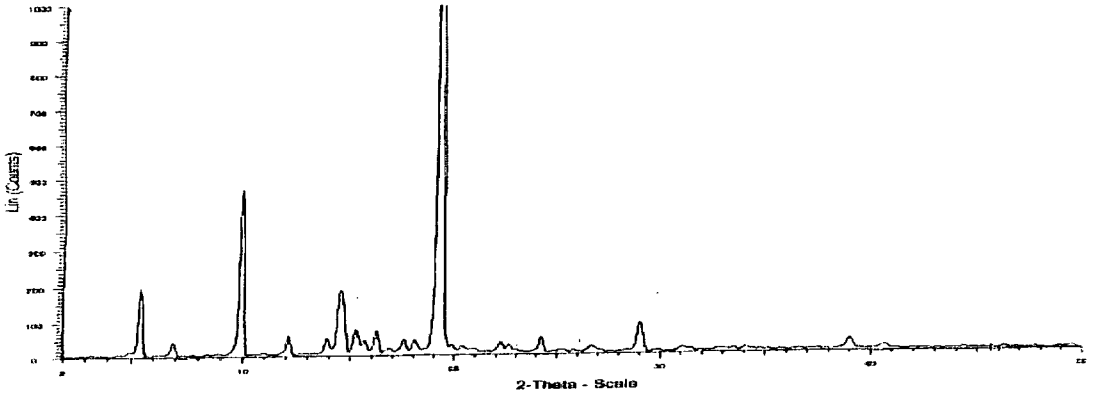

Figure 3.6. XRPD pattern for the claimed H2 from[10].

3.4 Finasteride solvates

Three solvates have been reported in the literature; only two of them have crystal structures established in the scientific literature[9] (the acetic acid and the ethyl acetate solvates) but no solid-state NMR published. In contrast, the dioxane solvate, was characterised by NMR and FT-IR[7] but neither crystal structure determined nor XRPD reported. The first two solvates were also reported in the patent literature[5,6] to be prepared with different methodologies and were claimed to be in agreement with XRPD data in the scientific literature.

3.4.1 Acetic acid solvate (Finasteride-Acetic Acid Complex[9])

Finasteride acetic acid crystallises in the monoclinic space group $P2_1$ containing two molecules in the unit cell; see Table 3.1 for the unit cell parameters. The lattice contains one molecule of acetic acid. It decomposes, losing acetic acid, and recrystallises in the range 170-174°C (melting point. 255-257°C)[9]. The complex was found to be with a 1:1 molar ratio. The methyl groups of the host and solvent molecules were found to be in a nearly parallel orientation. Molecules of co-crystallizing acetic acid are parallel to the two-fold screw axis.

The finasteride lactam fragment and the carboxyl group of acetic acid are responsible for strong inter-molecular hydrogen bond formation. As in the case of forms I and II, hydrogen bonding from the tert-butylamide group is absent; the distance between the finasteride peptide group and the acetic acid carboxyl group was measured to be 3.447(6) Å, which was suggested to be outside the range for such hydrogen bonding11. Additionally, two weak intramolecular hydrogen bonding interactions of C-H...O (methyl... carbonyl) type were reported. One of them comes from the interaction of the C19 methyl and the peptide group oxygen of finasteride, and the second one comes from the methyl and carboxyl group atoms of acetic acid.

3.4.1.1 Methods of preparation

The following methods of preparation were reported:

(i) Dissolving finasteride in an aqueous acetic acid of the ratio 4:6 (acetic acid: water) such that the amount of acetic acid is 5-15 v/w of finasteride, heating the resultant mixture to 70-80°C then cooling to 10-20°C, filtering the resulting material and isolating by conventional methods[5,6].

(ii) Crystallising finasteride from an acetic acid/ water mixture (about 2:1) by slow evaporation of the solvent[9].

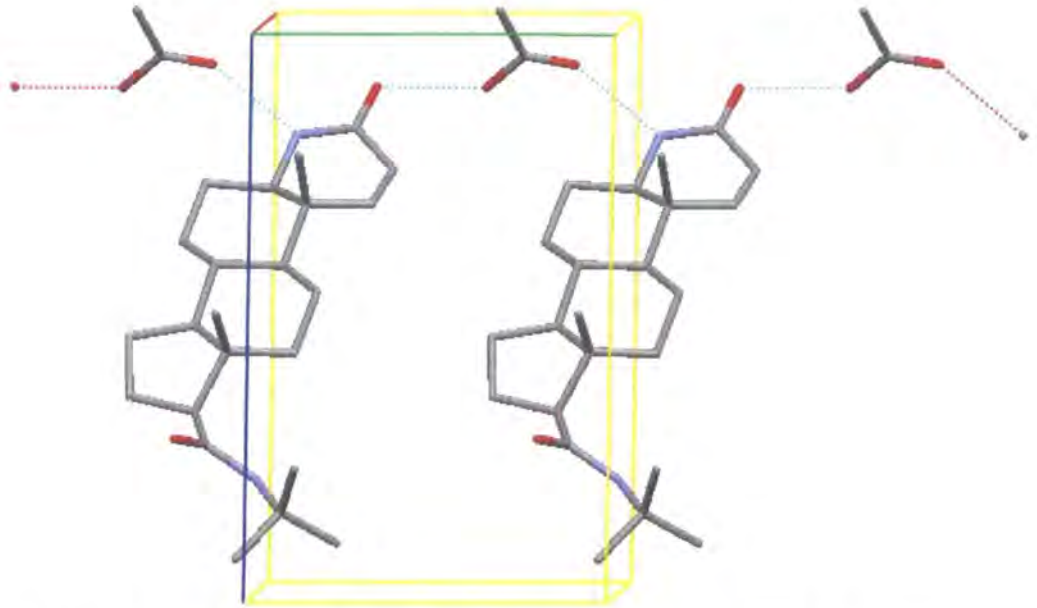

Figure 3.7. The acetic acid solvate crystal structure, with the view along the *a* crystallographic axis. Dotted lines represent hydrogen bonding.

3.4.2 Ethyl acetate solvate (Bis-finasteride Monohydrate Ethyl Acetate Clathrate)[9]

The unit cell of this solvate contains one molecule of ethyl acetate for two molecules of finasteride. It crystallises in the orthorhombic space group $P2_12_12_1$ and contains four molecules in the unit cell; see Table 3.1 for the unit cell parameters. Two molecules of finasteride in the asymmetric unit form dimers. This alignment is stabilized by two N-H ...O hydrogen bonds between the lactam groups of ring A (Figure 3.8), and the hydrogen-bonded water molecule was shown to be a bridging unit connecting three finasteride dimers. The water molecule is a double donor of H atoms to the lactam O atoms, and an acceptor from the N atom of the tert-butyl side of finasteride. Hence, this solvate is the only finasteride solid form in the literature which has the tert-butyl side of finasteride involved with hydrogen bonding. The double-layer arrangement of the complexed host molecules was found to be the reason behind the formation of channels along the crystal *a* axis (Figure 3.9). The ethyl acetate molecules were found to be disordered, filling the channel of the clathrate crystal[9]. The stoichiometric ratio is reported to be finasteride: water: ethyl acetate = 2:1:1. The ratios were presumably concluded from the XRD analysis of the disordered solvent molecules, as the author did not present evidence from any other analytical technique.

3.4.2.1 Methods of preparation

The following methods of preparation were reported:

(i) preparing a slurry of finasteride in an ethyl acetate, THF and water mixture such that the ratio ethyl acetate: THF: water is 1:1:~0.1 and the ratio of this solvent mixture used is 1-3 v/w of finasteride, heating the resultant slurry to a temperature of 50 to 60°C, then cooling the slurry to -5 to 5 °C, recovering the resultant solid by filtration and washing with a chilled mixture of ethyl acetate, THF and petroleum ether[5,6].

(ii) Evaporating a solution of finasteride in ethyl acetate (containing traces of water); in this case unstable crystals are formed[9].

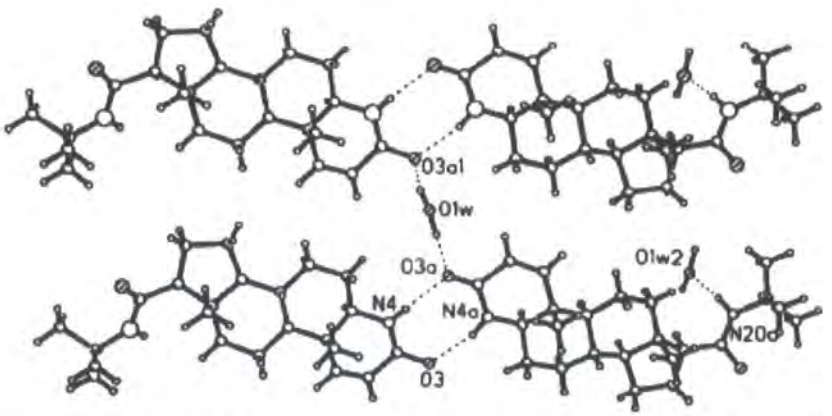

Figure 3.8. Hydrogen bonding pattern in the ethyl acetate solvate shown by Wawrzycka *et al.*[9]

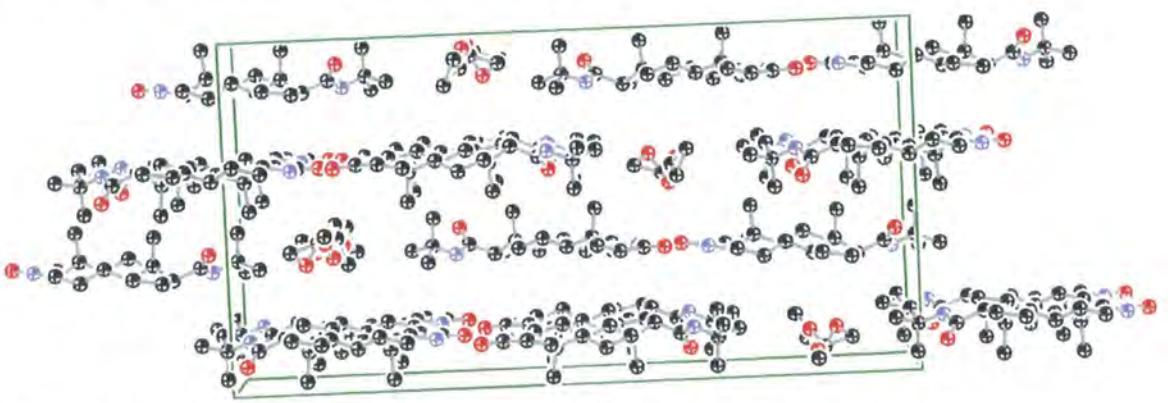

Figure 3.9. Crystal structure packing for the ethyl acetate solvate with the view along the *a* crystallographic axis. Atoms inside the clathrate channel represent the disordered ethyl acetate molecule.

3.4.3 Dioxane solvate[7]

This form was obtained by recrystallisation from dioxane. The presence of dioxane was confirmed by solid-state NMR. The dioxane signal appeared at 67 ppm in the ^{13}C CPMAS NMR spectrum. The stoichiometry of finasteride: dioxane was found to be 1:1 by integration of the peaks in the ^{1}H-NMR spectrum of the sample dissolved in $CDCl_3$[7]. The ratio was mentioned without showing the ^{1}H-NMR spectrum or actual values of integrals. As mentioned earlier, no X-ray examination of this solvate was carried out. However, the solvate was additionally characterised by FT-IR spectroscopy. The reported FT-IR frequency does not readily distinguish between forms I and II and the prepared dioxane solvate (Table 3.3).

Table 3.3. Selected infrared frequencies for examined finasteride solid forms by Morzycki *et al.*[7].

	Infrared wavenumber (cm^{-1})		
Functional Group	**Form I**	**Form I**	**Dioxane solvate**
NH	3429	3439	3429
NH	3241	3221	3240
C=O	1689	1689	1689
C=O	1669	1678	1668

3.5 Experimental Overview

The next chapter will be dealing with the preparation and characterisation of the solid forms (polymorphs and solvates) mentioned herein by XRPD, solid-state NMR and thermal analysis where applicable. Other newly prepared solvates will also be presented.

3.6 References

1. Dolling UH, McCauley JA, Varsalona RJ. 1994. A process for the production of finasteride. European Patent Office (EPO), ed., EU: Merck & Co Inc.
2. Dolling UH, McCauley JA, Varsalona RJ. 1999. Finasteride processes. United States Patent and Trade Mark Office, ed., USA.
3. Kankan RN, Rao DR. 2005. Process for the preparation of finasteride Form I. World Intellectual Property Organization (WIPO), ed.
4. McCauley JA, Varsolona RJ. 1997. Process for the production of finasteride. United States Patent and Trade Mark Office, ed., US: Merck & Co., Inc.
5. Reddy MS, Rajan ST, Rao MVNB, Vyas K, Reddy SV, Rekha KS. 2002. Novel polymorphic form of 17-beta-(N-ter. butyl carbamoyl)-4-aza-5-alpha-a- ndrost-1-en-3-one and a process for preparing it. World Intellectual Property Organization (WIPO), ed.
6. Reddy MS, Rajan ST, Rao MVNB, Vyas K, Reddy SV, Rekha KS. 2005. Novel polymorphic form of 17-beta-(N-ter. butyl carbamoyl)-4-aza-5-alpha-a- ndrost-1-en-3-one and a process for preparing it. United States Patent and Trade Mark Office, ed., US: Dr. Reddy's Laboratories Ltd.
7. Morzycki JW, Wawer I, Gryszkiewicz A, Maj J, Siergiejczyk L, Zaworska A 2002. C-13-NMR study of 4-azasteroids in solution and solid state. Steroids 67(7):621-626.
8. Wenslow RM, Baum MW, Ball RG, McCauley JA, Varsolona RJ 2000. A spectroscopic and crystallographic study of polymorphism in an aza-steroid. J Pharm Sci 89(10):1271-1285.
9. Wawrzycka I, Stepniak K, Matyjaszczyk S, Koziol AE, Lis T, Abboud KA 1999. Structural characterization of polymorphs and molecular complexes of finasteride. J Mol Structure 474:157-166.
10. Parthasaradhi R, Bandi, Rathnakar R, Kura , Raji R, Rapolu, Muralidhara R, Dasari, Subash Chander R, Kesireddy. 2004. Novel Crystalline Forms of Finasteride. World Intellectual Property Organization (WIPO), ed.
11. Jeffrey GA, Saenger W. 1991. Hydrogen Bonding in Biological Structures. ed.: Springer Verlag.

Chapter 4: Finasteride Solid Forms

4.1 Finasteride Polymorphs Reported in the Scientific Literature

In this section, characterisation of polymorphs reported in the scientific literature will be presented.

4.1.1 Form I

The sample was sent by Hikma Pharmaceuticals-Jordan (B#060102) and manufactured by Hunan Steroids Chemicals Co Ltd, China.

The obtained XRPD pattern (Figure 4.1) fits with the powder pattern of form I calculated from the reported structure. The DSC thermogram (Figure 4.2) shows an endothermic event at about 217°C corresponding to the transformation of form I to the metastable form II. Form II then melts at 257.9°C. The DSC data are consistent with literature results reported by Wenslow *et al.*[1].

The ^{13}C CPMAS spectrum (Figure 4.3) is in agreement with the published spectra by Wenslow *et al.*1 and Morzycki *et al.*[2] Each non-equivalent carbon in the spectrum corresponds to one peak which agrees with the crystal structure of form I having one molecule in the asymmetric unit (Z'=1). The assignments of the chemical shifts for the obtained spectrum were adopted from the Morzycki et al. publication since the author found that the older assignments by Wenslow *et al.* for C3 and C20 were swapped (Table 4.1).This statement was a result of the assumption that C3 in both form I and II should have a closely similar chemical shift since the hydrogen bond lengths of the lactam group in the two forms are the same (2.85 Å). The assumption was further supported by the fact that the lactam carbonyl in both forms is more involved in the hydrogen bonding than the amide carbonyl, which was confirmed by the hydrogen bond lengths. Hence C3 has to be in the higher frequency part of the spectrum compared to C20[2]. The obtained spectrum is of a better quality than the ones in the literature since it was acquired on a 500 MHz (proton frequency) spectrometer while the spectra in the literature were acquired on 300[2] and 400[1] MHz (proton frequency) spectrometers. Better resolution was obtained, especially in the CH_2 region. Although our spectrum looks better resolved, the best line widths obtained were in the range of 15-20 Hz, while Wenslow *et al.* reported having some peaks with line widths of 5Hz[1]. The quadrupolar effect of ^{14}N nuclei on resonances of neighbouring ^{13}C nuclei was less pronounced than the literature case since the sample was acquired at a higher magnetic field. Nitrogen-bonded carbons showed split ^{13}C resonances in the literature data while in our case the peaks were only broadened, showing shoulders sometimes.

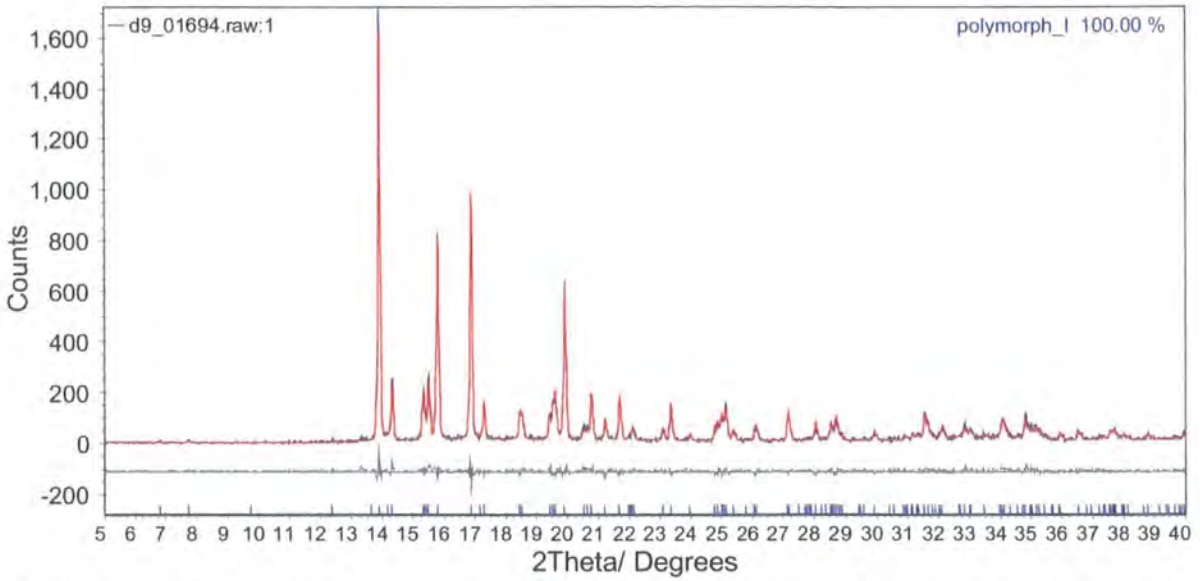

Figure 4.1. Rietveld fitting of the observed diffractogram with the calculated powder pattern of form I.

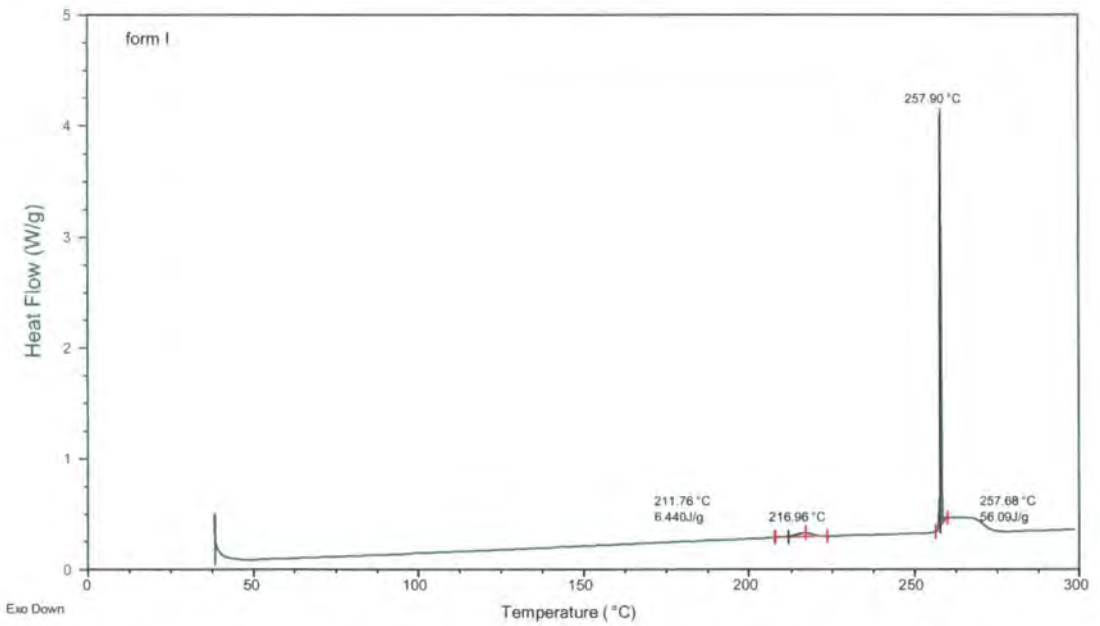

Figure 4.2. DSC thermogram obtained for form I at a heating rate of 1°C/ min.

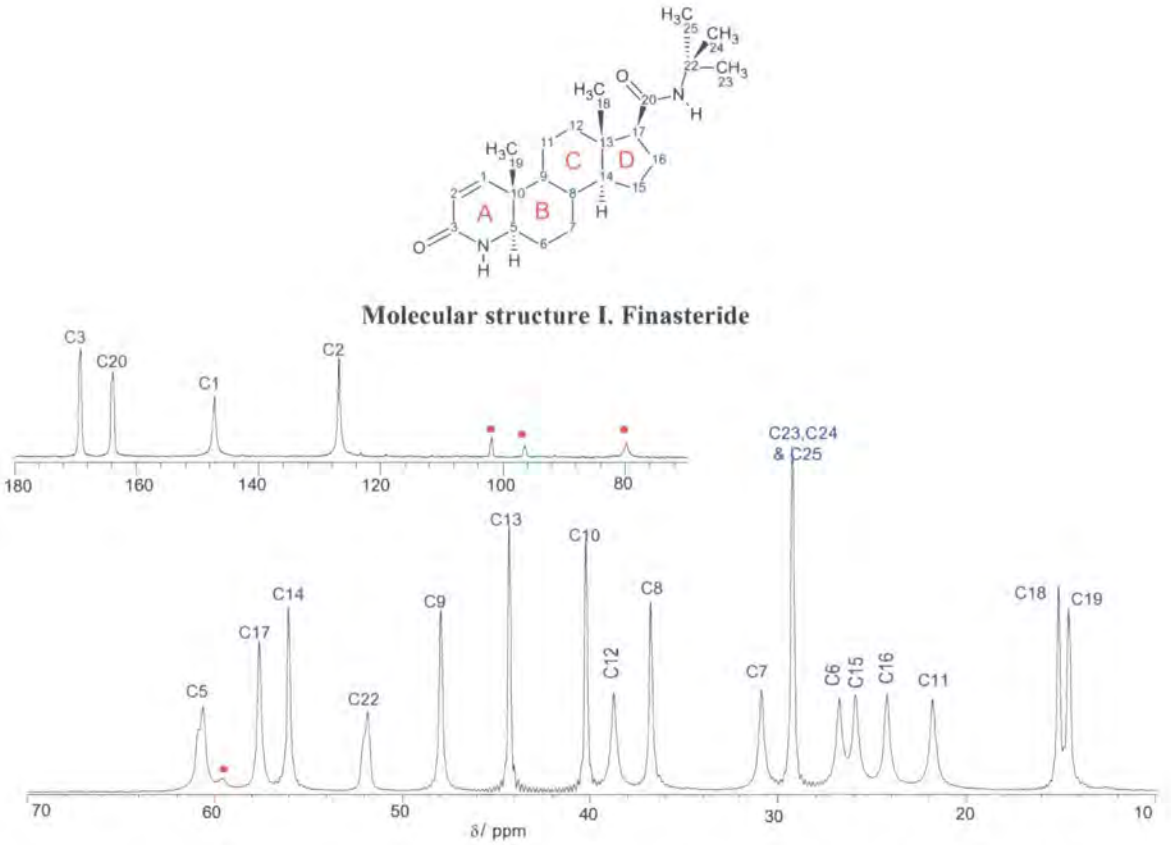

Molecular structure I. Finasteride

Figure 4.3. Obtained ^{13}C CPMAS spectrum for form I. Asterisks represent spinning side bands. The spectrum was acquired for 40 ms with proton decoupling power of 63 kHz.

Table 4.1. Chemical shifts (δ_C/ppm) and their assignments for form I in the literature and in the obtained spectrum.

Carbon Number	Wenslow *et al.*[1]	Morzycki *et al.*[2]	Obtained spectrum
1	146.9	146.7	146.9
2	126.6	126.4	126.9
3*	163.3	168.8	169.3
5*	60.1	59.9	60.6
6	26.5	25.9	26.8
7	30.6	30.5	30.6
8	36.5	36.2	36.8
9	47.6	47.4	48.0
10	39.0	39.6	40.2
11	21.5	21.5	21.9
12	38.4	38.3	38.8
13	43.9	43.7	44.3
14	55.7	55.5	56.1
15	25.6	25.5	26.0
16	24.0	23.8	24.3
17	57.3	57.1	57.6
18	14.9	14.6	15.2
19	14.3	14.1	14.7
20*	168.8	163.5	164.3
22*	51.5	51.5	51.9
23,24 and 25	28.9	28.6	29.3

*Showing quadrupolar effect due to bonding with nitrogen.

4.1.2 Form II

The sample was prepared (B# LB1/ 26) by dissolving about 1 g of form I in a solution of ethyl acetate containing water with a concentration of 24 mg/ mL. The solution was then maintained at ambient temperature with stirring for an hour. The solution was left to evaporate overnight and then the solid was dried in a vacuum oven for 6 hours at 80 °C. This methodology is an implementation of the method described in the patent by McCauley *et al.*[3].

The solid was characterised by XRPD (Figure 4.4), ^{13}C CPMAS (Figure 4.6) and DSC (Figure 4.5); all data agree with the reported results in the literature. The XRPD pattern fits with the calculated powder pattern of form II but shows small differences due to preferred orientation of the microcrystallites. The DSC thermogram shows only one endothermic event at 257.8 °C, corresponding to the melting point of form II.

The ^{13}C CPMAS spectrum obtained indicates that there are two molecules in the asymmetric unit as most carbons sites show split peaks. Again better resolution was obvious in the CH_2 region presumably due to better dipolar decoupling. For example, carbons C16, C15 and C6 were reported[1,2] (Table 4.2) to each have a single peak, but in the obtained spectrum four resolved peaks are seen. The extra peaks most likely correspond to splitting of the peak of C16 (Figure 4.6). Also, as in the case of form I, the quadrupolar effect on carbons bonded to nitrogen is less pronounced than in the literature spectra.

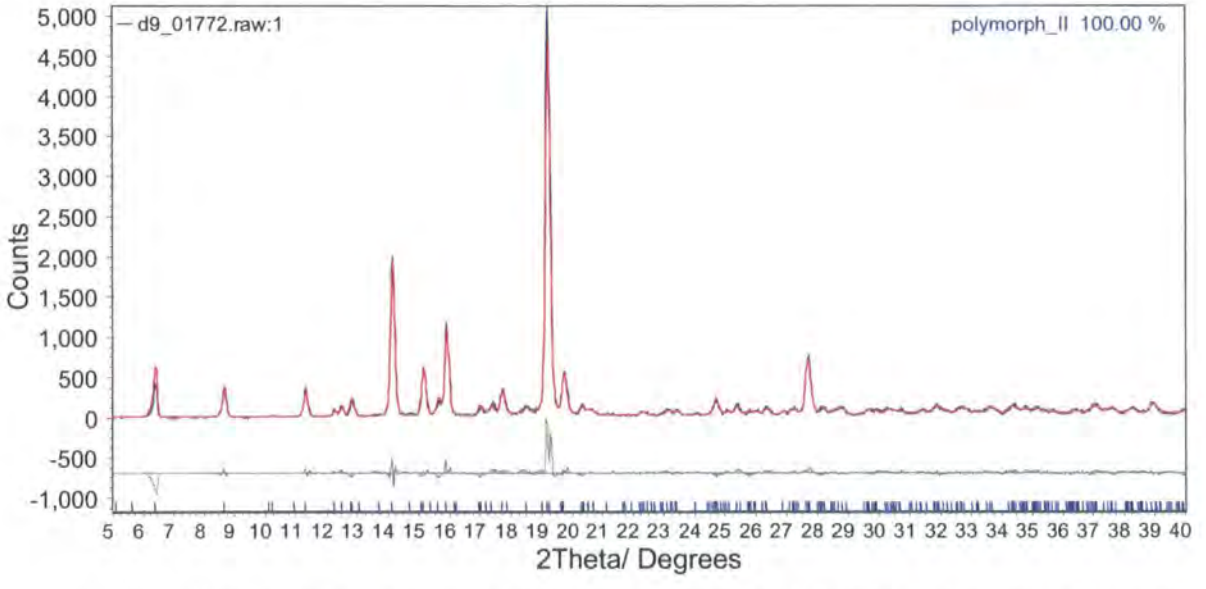

Figure 4.4. Rietveld fitting for the observed diffractogram with the calculated powder pattern of form II.

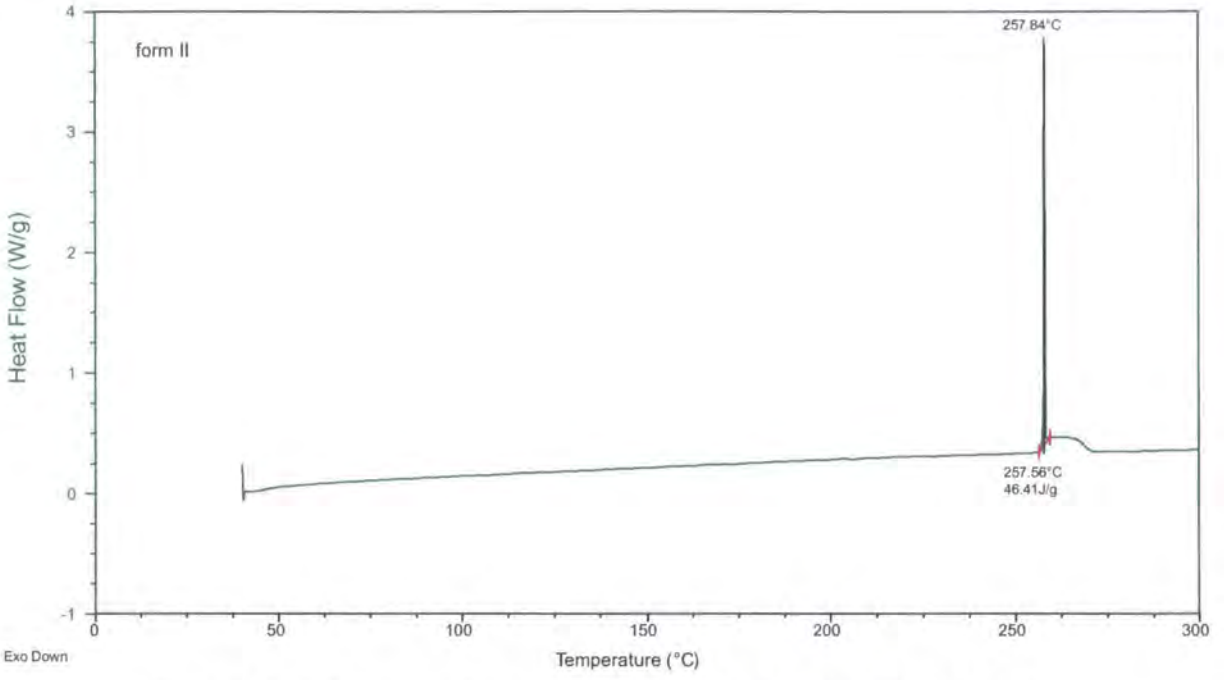

Figure 4.5. DSC thermogram obtained for form II at a heating rate of 1°C/ min.

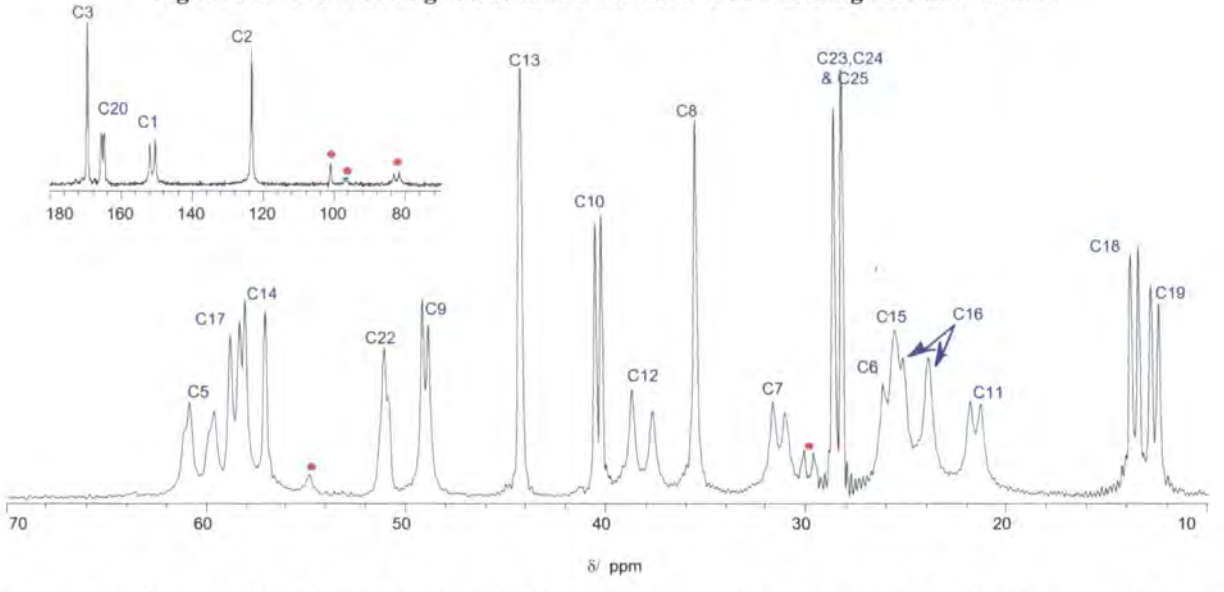

Figure 4.6. Obtained ^{13}C CPMAS for form II. Asterisks represent spinning side bands. The spectrum was acquired for 40 ms with proton decoupling power of 63 kHz.

Table 4.2. Chemical shifts (δ_C/ppm) and their assignments for form II in the literature and in the obtained spectrum.

Carbon Number	Wenslow *et al.*[1]	Morzycki *et al.*[2]	Current work
1	150.1/151.6	149.9/151.4	150.4/151.9
2	123.0	122.8	123.3
3	169.4	169.2	169.7
5	59.2/60.4	59.8	59.6/60.9
6	25.9	25.3	26.6
7	30.8/31.4	30.8	31.1/31.7
8	35.3	35.0	35.6
9	48.5/48.8	48.6	48.9/49.2
10	39.9/40.3	39.7/40.0	40.3/40.6
11	21.0/21.5	22.6	21.3/21.9
12	37.4/38.4	38.3	37.7/38.7
13	44.0	43.8	44.3
14	56.7/57.8	56.5	57.1/58.1
15	24.8	25.0	25.6
16	23.6	24.0	24.0/25.2
17	58/58.5	57.9	58.3/58.8
18	13.1/13.6	13.3/12.9	13.5/13.9
19	12.1/12.59	12.3/11.9	12.5/12.9
20	165.1/164.4	164.8	164.9/165.7
22	50.8	50.7	50.9
23,24 and 25	27.9/28.2	27.7/28.1	28.3/28.7

4.2 Finasteride Polymorphs Reported in the Patent Literature

In this section, characterisation of polymorphs and crystalline forms reported in the patent literature will be presented.

4.2.1 Form III

The patent for this claimed form is published in the US patent and trademark office[4] and in the World Intellectual Property Organisation(WIPO)[5]. A number of trials were carried out to prepare this form. The trials varied because of the number of solvent combinations listed in the patent. The general method used for the preparation of this form was as follows; 1 g of finasteride form I was dissolved in 3 mL of dichloromethane. 60-70% of the dichloromethane was evaporated at 40-45°C. The resulting solution was then saturated with about 10 mL of petroleum ether at 40-60 °C under stirring. The solution was concentrated at 60-65 °C for about 15 minutes. The solid was kept over night to dry. The resulting solid was then kept under vacuum at 65 °C for 30 minutes. Further drying was done in the oven at 80 °C for 12 hours.

4.2.1.1 Synthesis

(i) Trial#1(B# LB1/26)

1 g of finasteride form I was dissolved in 3 mL of dichloromethane. 60-70% of the dichloromethane was evaporated at 40-45°C. The resulting solution was then saturated with about 10 mL of petroleum ether at 40-60 °C under stirring. The solution was concentrated at 60-65 °C for about 15 minutes. The solid was kept over night to dry. The resulting solid was then kept under vacuum at 65 °C for 30 minutes. Further drying was done in the oven at 80 °C for 12 hours.

(ii) Trial#2(B# LB1/32)

0.5 g of finasteride form I was dissolved in 1.5 mL of chloroform. 60-70% of the chloroform was distilled off at 60-70°C.The resulting solution was saturated with about 5 mL of petroleum ether at 60-65 °C under stirring. The solution was concentrated at 60-65 °C for about 15 minutes. The solid was kept over night to dry. The resulting solid was then kept under vacuum at 65 °C for 30 minutes. Further drying was done in the oven at 80 °C for 12 hours.

(iii) Trial#3(B# LB1/34)

The sample was prepared by mixing form I and a 1:1 solution of diethyl ether (replacing petroleum ether) and chloroform at 60°C. The resultant slurry solution was evaporated to dryness under ambient conditions overnight. A portion of the sample was taken for XRPD examination and the rest of the sample was subjected to drying under vacuum at 65 °C for 30 minutes. In both cases the sample was a microcrystalline powder, i.e. no big crystals were observed.

(iv) Trial#4(B# LB1/35)

The same methodology as in trial#2 was repeated to confirm the results.

(v) Trial#5(B# LB1/36)

0.5 g of form I was dissolved in 1.5 mL of chloroform and maintained for 10 minutes at about 65-70 °C. The resulting mixture was left at ambient conditions over night to dry. The sticky solid produced was put in the vacuum oven for 30 minutes at 60 °C. A sample was taken at this step for XRPD examination (portion#1). Further drying was done in the oven at 80 °C for 12 hours (portion #2).

(vi) Trial#6(B# LB1/36)

The method in Trial #2 was repeated but with checking of the sample before and after the drying steps. The sample was left to dry overnight at ambient temperature and then the sample was characterised before being put in the vacuum oven.

4.2.1.2 Characterisation

(i) Trial#1

The examined XRPD pattern for trial #1(Figure 4.7) showed a mixture of forms I and II. Rietveld fitting was used to approximate the percentage of each phase in the powder (see the right top of Figure 4.7). Preferred orientation was observed at peaks of 2θ values (13.9° and 19.0°), where the observed peaks (blue) are more intense than the calculated peaks (red).

(ii) Trial#2

Trial #2 was a repetition of trial #1 replacing dichloromethane with chloroform. The XRPD pattern (Figure 4.8) showed the sample to be a mixture of three forms. Peaks due to forms I and II fit with the calculated powder pattern (red trace Figure 4.8). Unfitted peaks correspond to the 2θ values reported for form III in the patent (Table 4.3).

The ^{13}C CPMAS spectrum (Figure 4.9) was run to confirm the XRPD results and to extract the characteristic peak positions for form III. Peaks apart from those of the two known forms were labelled (Figure 4.9) and the chemical shifts were tabulated (Table 4.5). Looking at the carbonyl region in the spectrum, it may be concluded that this form has three molecules in the asymmetric unit. The peak at 63.7 ppm (green arrow in Figure 4.9) is not a finasteride peak, i.e. the peak is due to a certain solvent. The solution-state ^{13}C NMR was run in order to check this observation. Since petroleum ether is not miscible with chloroform, another solvent was used to run solution-state NMR. THF was found to be miscible with petroleum ether, hence deuterated THF was used. As expected, the corresponding ^{13}C spectrum (Figure 4.10) showed a peak at 62.8 (labelled as solvent in Figure 4.10). Solution-state ^{1}H NMR (Figure 4.11) of the sample dissolved with solvents THF-d_8 was run to check for extraneous peaks. The spectrum showed a moderately different spectrum than that of finasteride alone with some peak differences of impurities level. The presence of solvent(s) in the sample might be further concluded from the TGA loss (Figure 4.12) of 2.2 % observed at 64.3 °C though one cannot be sure from this evidence what the "solvate "is. The DSC (Figure 4.13) analysis for this sample did not show any special feature compared to that of form II.

(iii) Trial#3

As a consequence of the previous trial (trial #2), the solvate which is producing peaks corresponding to "form III" can be either a chloroform solvate or a petroleum ether solvate. To continue the investigation it was attempted to prepare a diethyl ether solvate. Diethyl ether was chosen because the extraneous peak found in both solid and solution states ^{13}C NMR at about 63 ppm is close to the CH_2 of diethyl ether, which should appear according to the tables at 65.9 ppm.

The XRPD pattern (Figure 4.14) of a first portion fits with the calculated powder pattern of the known ethyl acetate solvate. The XRPD pattern (Figure 4.16) of the other portion (the dried one) fits with the calculated powder pattern of form II. These results suggest that portion #1 of the sample represents a solvate. This was further confirmed by TGA. The TGA thermogram of portion#1 showed

a mass loss of 17.9 % at 72.6°C (loss expected due to diethyl ether is 16.6%) observed (Figure 4.15). This experiment suggests that diethyl ether is not the solvent included in trial #2.The dried solid (portion #2) was shown to be form II by XRPD (Figure 4.16), indicating that the solvate converts to the form II by heating the solid for 30 minutes at 65 °C.

(iv) Trial#4

The same methodology as in trial#2 was repeated to confirm the results. However, different results were obtained as the solid was found to be a mixture of forms I and II by XRPD (Figure 4.17). Peaks at 2θ values corresponding to the patented form III were not seen; hence, the methodology is non-reproducible, at least in my hands.

(v) Trial#5

This sample was prepared to check the probability of having a chloroform solvate (rather than another solvate) which could be the claimed form III. 0.5 g of form I was dissolved in 1.5 mL of chloroform and maintained for 10 minutes at about 65-70 °C. The resulting solution was evaporated at ambient conditions over night. The sticky solid produced was put in the vacuum oven for 30 minutes at 60 °C. A sample was taken at this step for XRPD examination (portion#1). Further drying was done in the oven at 80 °C for 12 hours (portion #2).

The first portion was showed to be a mixture of forms I and II by XRPD (Figure 4.18). The solid stayed as a mixture (Figure 4.19) of the two forms after the final drying step with increase in the percentage of the metastable form II (Figure 4.19) from 70.9 % to 84.6%.

Neither a chloroform solvate was produced nor was the produced solid the claimed form III.

(vi) Trial#6

A solvate was produced giving an XRPD pattern which (Figure 4.20) fits with the ethyl acetate solvate (as in the diethyl ether case). Drying in the vacuum oven produced 51.4 % of form II (Figure 4.21). Also as in the case of trial #5, further heating in the last step produces form II (metastable), this time producing pure form II at the end (Figure 4.22).

Table 4.3. 2θ values of form III trial #2 compared with the reported values

Peak number	2θ values/ d-spacings of numbered peaks	Corresponding 2θ values/ d-spacings of form III[4,5]
1	5.4/16.36	5.3/ 16.67
2	10.7/ 8.29	10.7/ 8.29
3	13.7/ 6.50	13.6/ 6.55
4	16.2/ 5.52	16.1/ 5.56
5	18.3/ 4.90	18.2/ 4.93

4.2.1.3 Summary

A summary of the trials carried out and results is shown in Table 4.4.

Table 4.4. summary of the trials carried out following "form III"

Sample ID	Method of preparation	Characterization	Conclusion
Trial#1 (B# LB1/26)	Using dichloromethane as the halogenated solvent	XRPD show a mixture of form I and II	Preparation of form III was not achieved.
Trial#2 (B# LB1/32)	Using chloroform as the halogenated solvent	XRPD and ^{13}C CPMAS show that the sample is a mixture of three forms (I,II, and III)	Form III was identified with 2θ values as reported in the patent
Trial#3 (B# LB1/34)	From diethyl ether and isolating samples from before and after drying	Form XRPD, the sample before drying is apparently a diethyl ether solvate and after the drying procedure the sample transformed into the metastable form II	Diethyl ether solvate was prepared (only small portion) and characterized by XRPD and TGA.
Trial#4 (B# LB1/35)	Same methodology used for trial #2 was repeated	XRPD show a mixture of form I and II	The results for trial#2 were not reproduced.
Trial#5 (B# LB1/36)	From Chloroform alone	XRPD show a mixture of form I and II	It is not possible to have a chloroform solvate (the sample was shown to be sticky and after drying it was shown to be a mixture of form I and II).
Trial#6 (B# LB1/36)	From petroleum ether without drying the sample in the oven (portion #1) and after drying in the oven (portion#2)	From XRPD, portion #1 is a solvate and portion#2 is a mixture of form I and form II	A petroleum ether solvate can be prepared

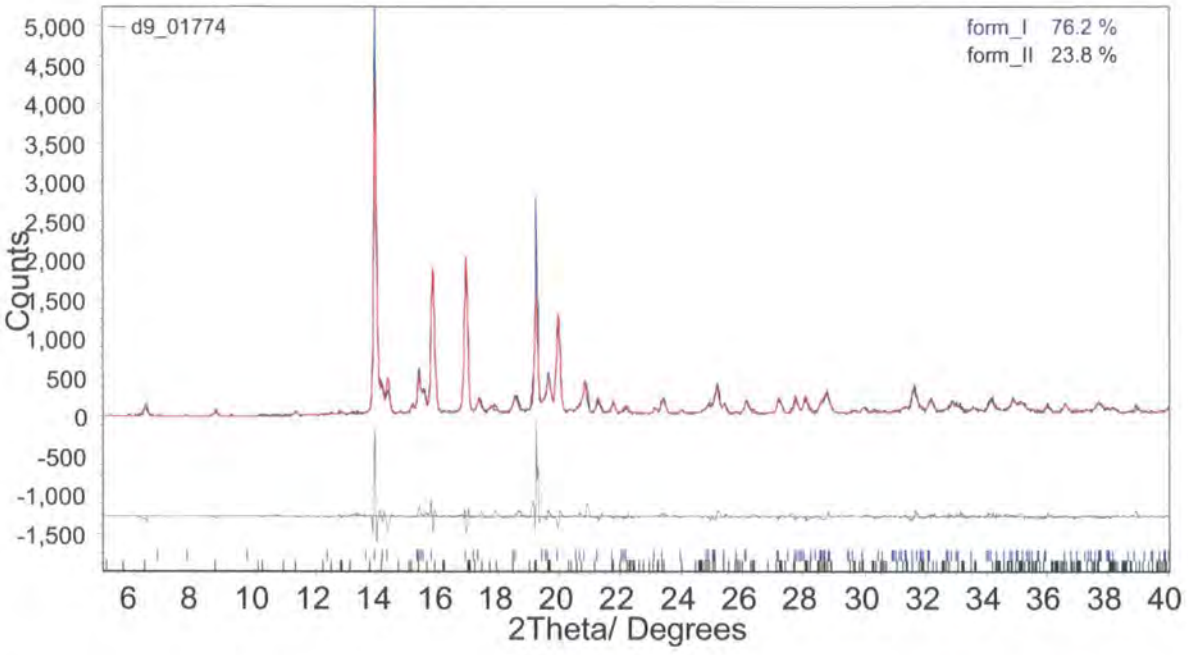

Figure 4.7. Rietveld fitting for the observed diffractogram of trial#1 with the calculated powder pattern of forms I and II.

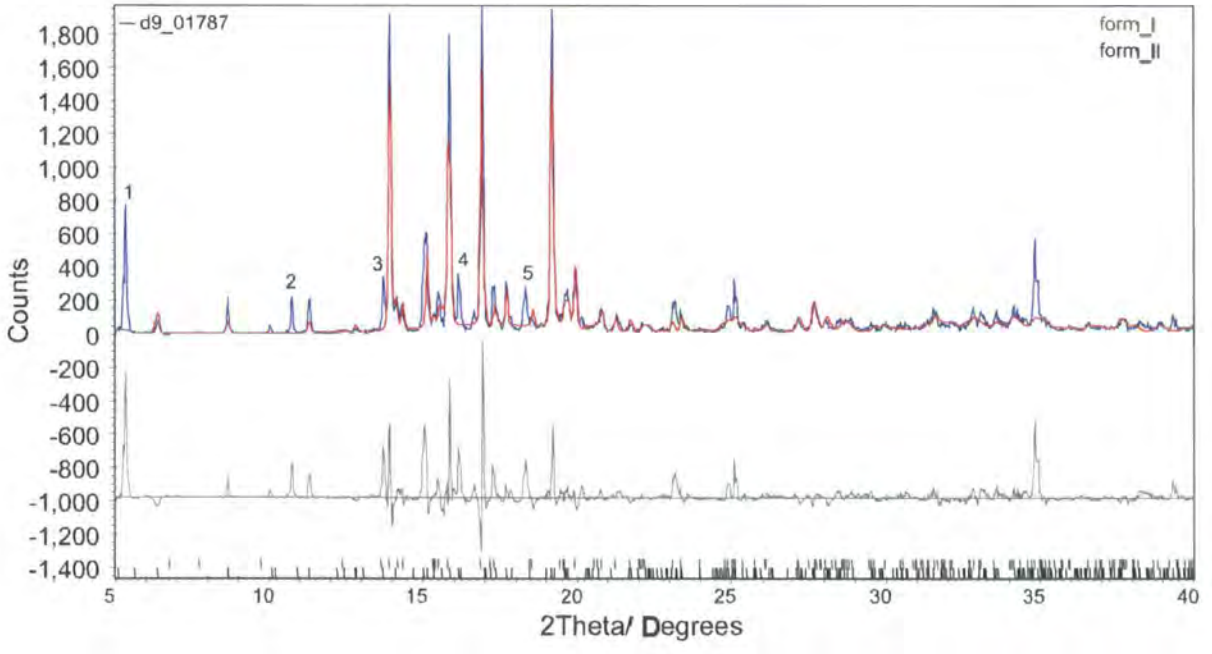

Figure 4.8. Diffractogram of form III trial#2 sample (blue trace). The red trace is the calculated powder pattern for forms I and II. Numbered peaks do not correspond to those of any of the two forms.

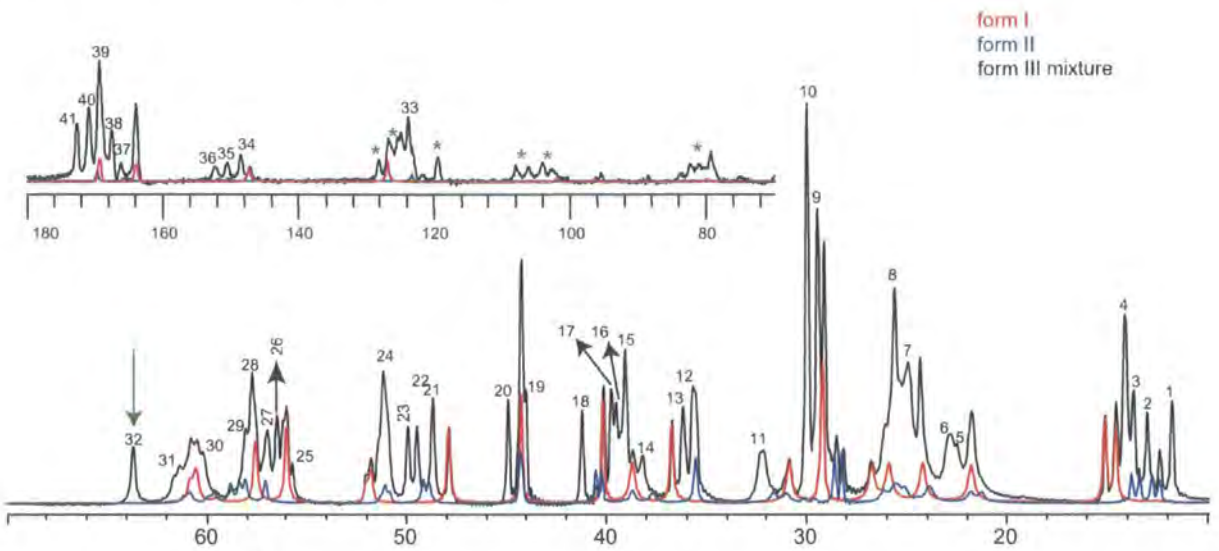

Figure 4.9. Obtained ^{13}C CPMAS for form III trial #2(black trace). Red and blue traces correspond to the spectra of forms I and II, respectively, in the mixture. Asterisks represent spinning side bands. The spectrum was acquired for 40 ms with proton decoupling power of 58 kHz.

Table 4.5. Chemical shifts for the distinct peaks in the spectrum of form III trial #2

Number	Chemical shift/ ppm		Number	Chemical shift/ ppm	
1	11.8	methyl groups	21	48.7	C9
2	13.0		22	49.5	
3	13.7		23	50.0	
4	14.1		24	51.2	C22
5	22.6	C6,C11,C15 and C16	25	55.7	C14
6	22.9		26	56.5	
7	25.0		27	57.0	
8	25.6		28	57.7	C17
9	29.5	t-butyl group	29	58.1	
10	29.9		30	60.3	C5
11	32.2	C7	31	61.4	
12	35.7	C8	32	63.7	Solvent
13	36.2		33	124.0	C2
14	38.2	C10, C12 and C13	34	148.6	C1
15	39.1		35	150.6	
16	39.5		36	152.5	
17	39.8		37	166.3	C3 and C20
18	41.2		38	167.4	
19	44.0	C13	39	169.4	
20	44.9		40	171.0	
			41	172.6	

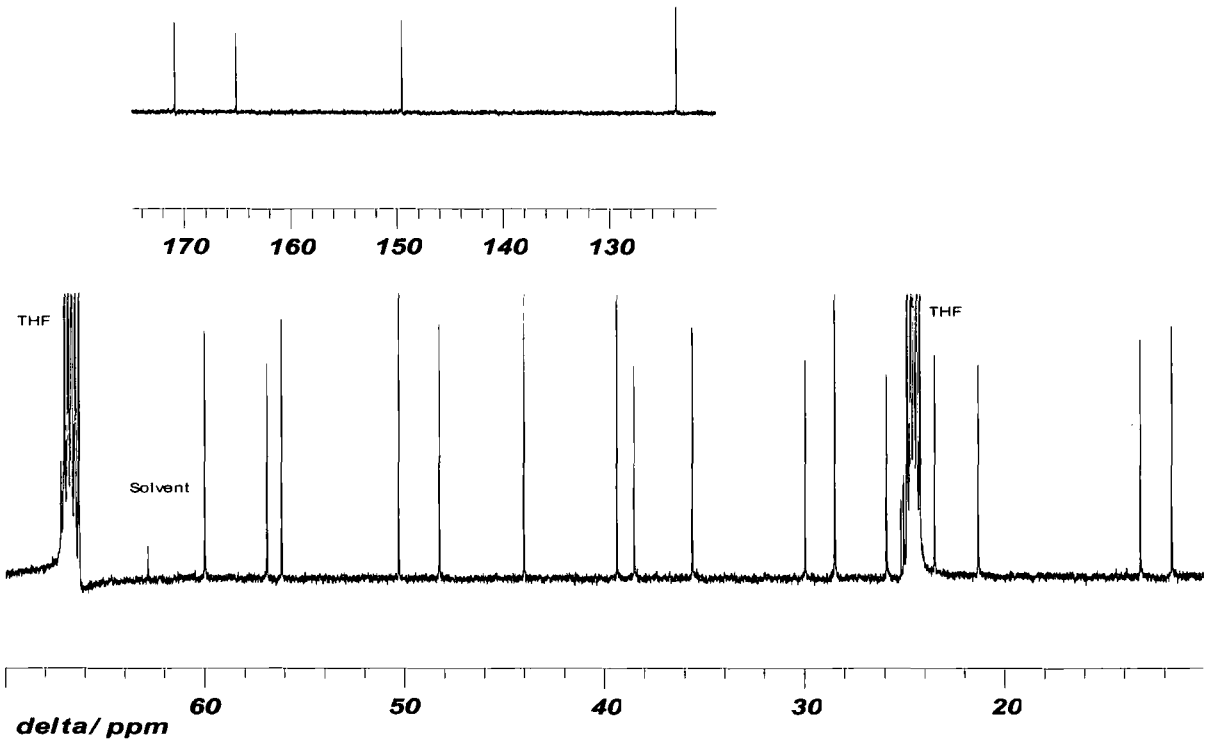

Figure 4.10. Obtained ^{13}C NMR of finasteride form III trial #2 sample dissolved in THF-D8. The peak due to the included solvent is labelled as "solvent".

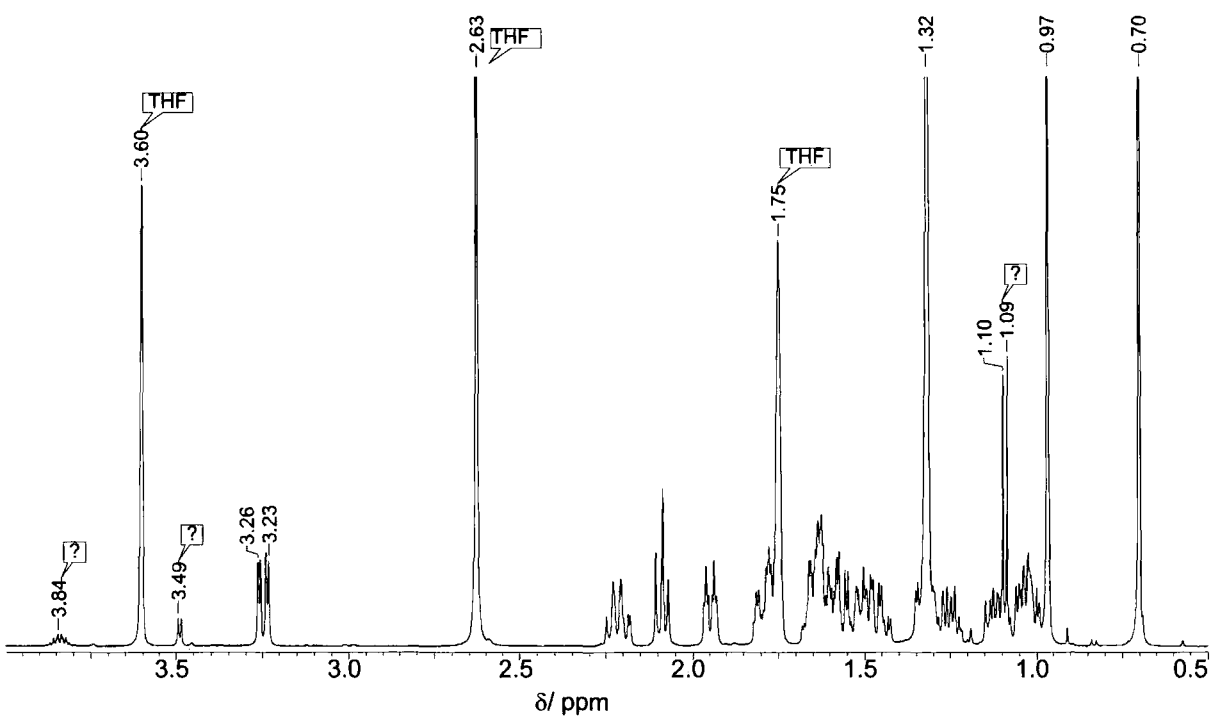

Figure 4.11. Obtained ^{1}H NMR of finasteride form III trial #2 sample dissolved in THF-D8. Peaks apart from THF or finasteride are labelled by a question mark "?".

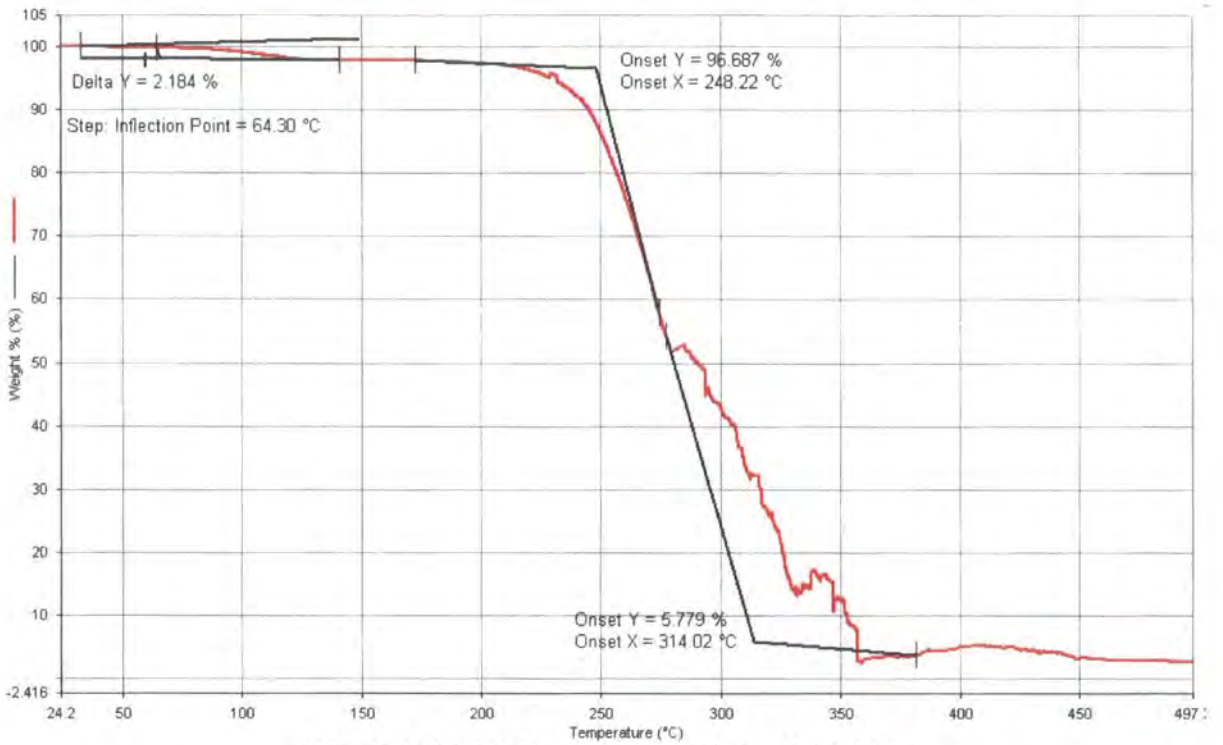

Figure 4.12. TGA thermogram for form III trial #2.

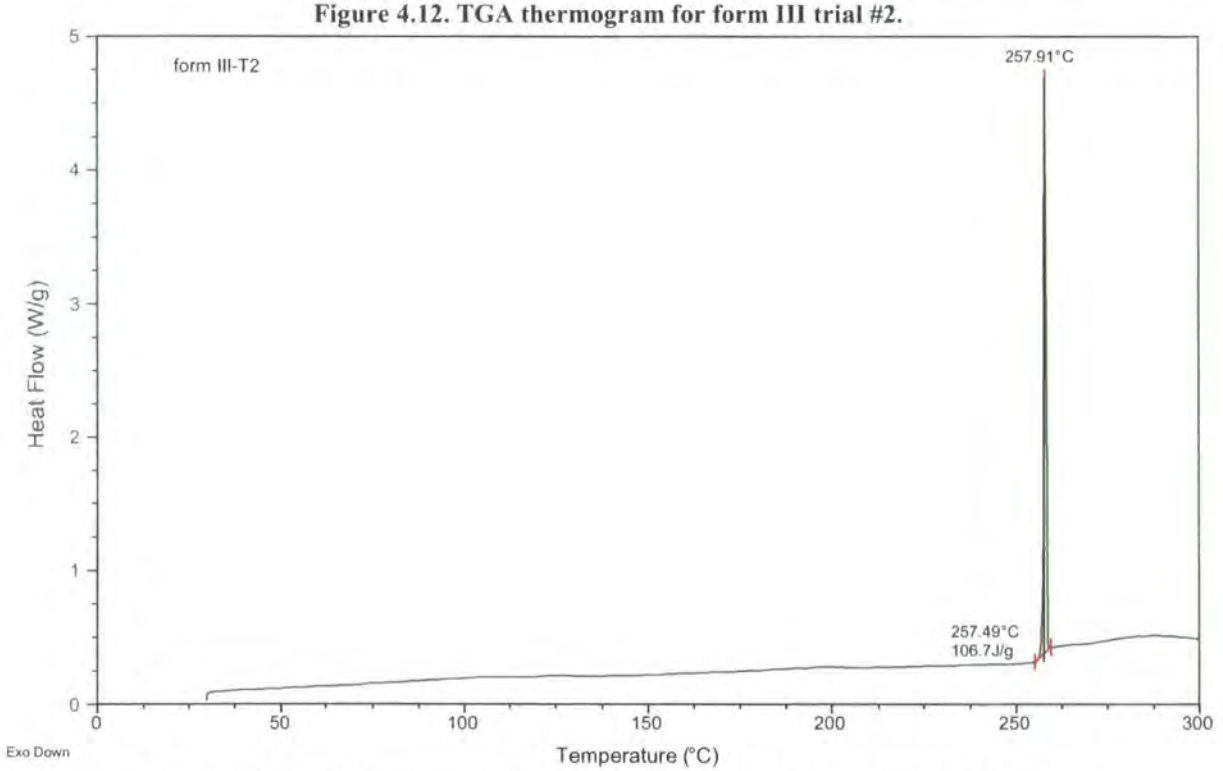

Figure 4.13. DSC thermogram for form III trial #2 at a heating rate of 1°C/ min.

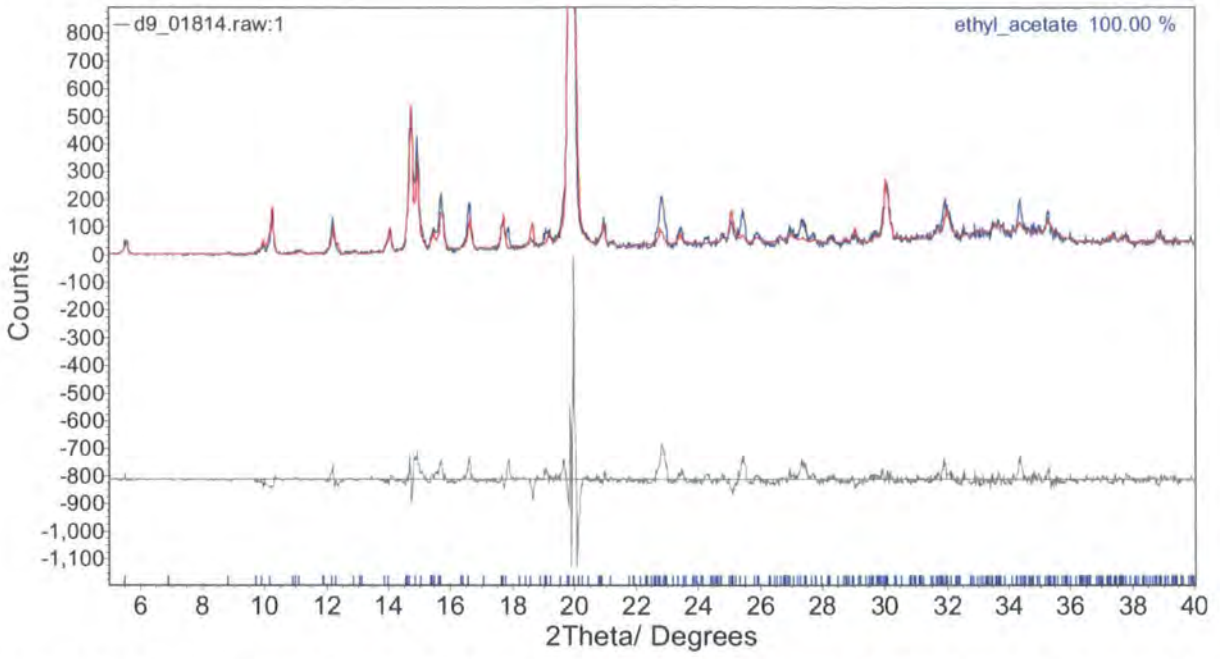

Figure 4.14. Diffractogram for form III trial#3 portion one (blue trace). The red trace is the calculated powder pattern for the ethyl acetate solvate.

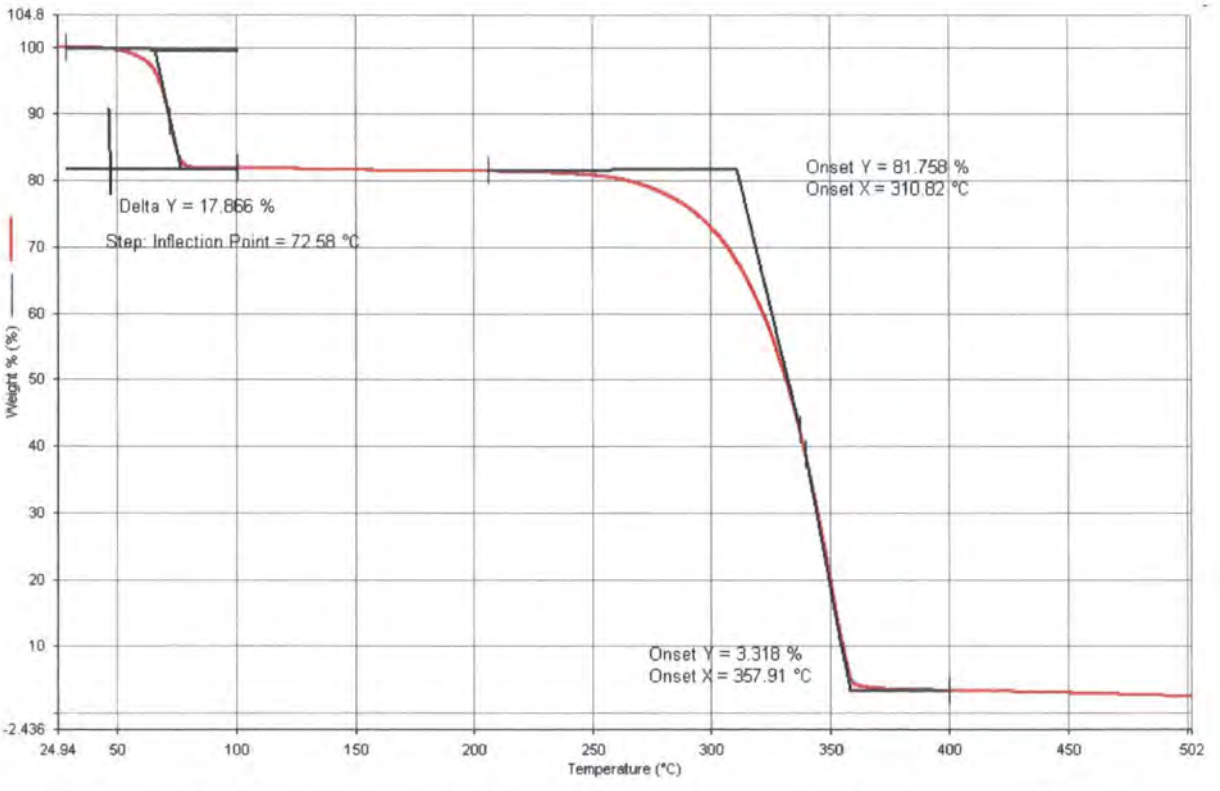

Figure 4.15. TGA thermogram for form III trial #3- portion #1 at a heating rate of 2°C/ min

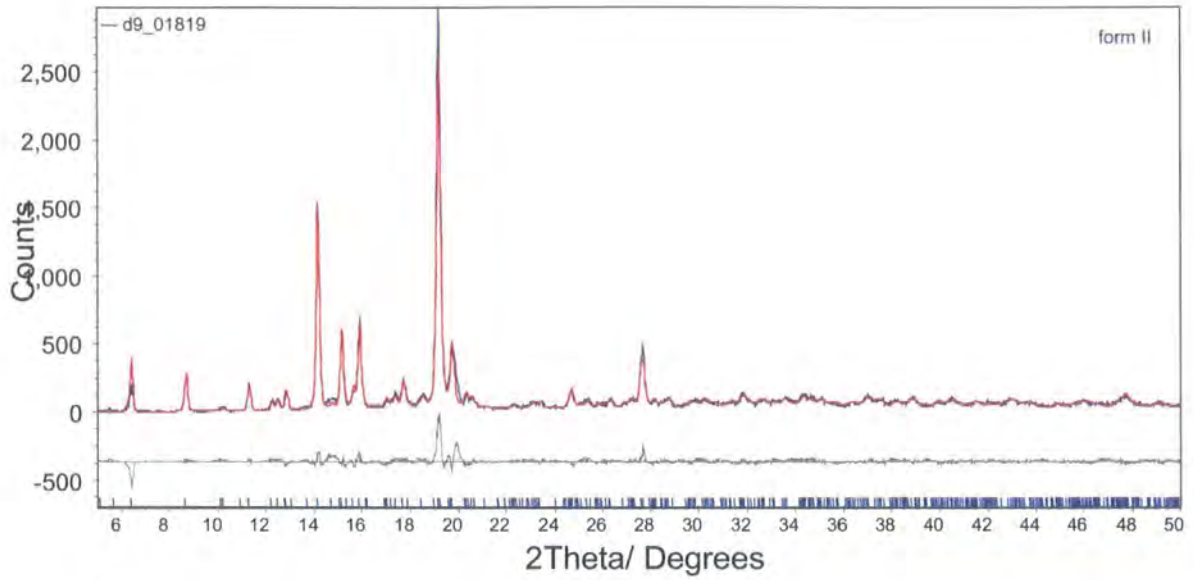

Figure 4.16. Diffractogram for form III trial#3 portion two (blue trace). The red trace is the calculated powder pattern for form II.

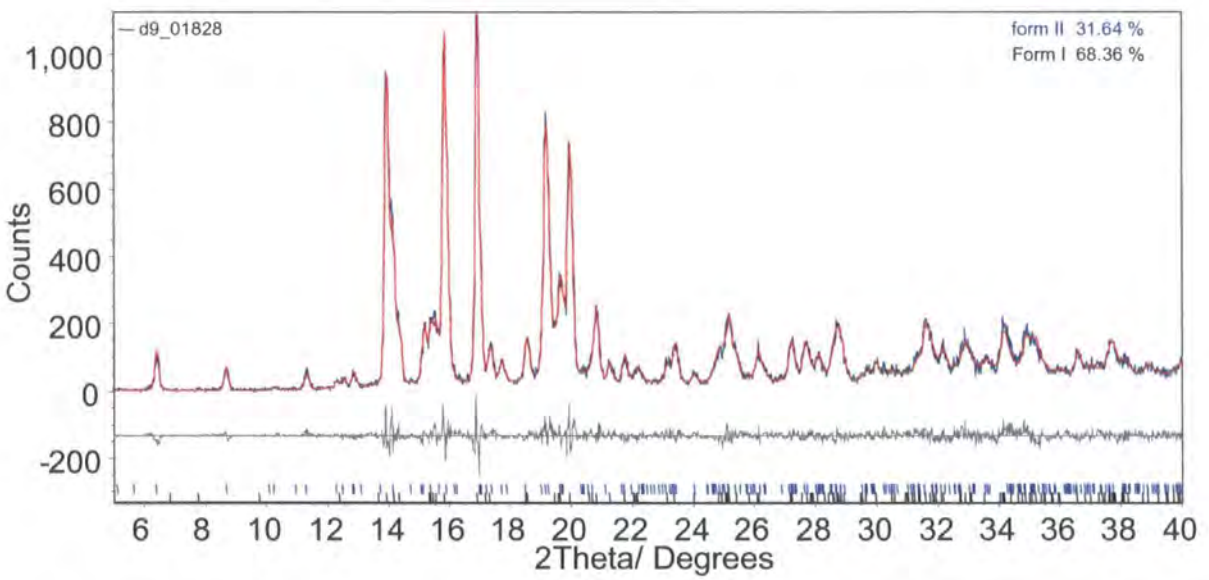

Figure 4.17. Diffractogram for form III trial#4 (blue trace). The red trace is the calculated powder pattern for forms I and II.

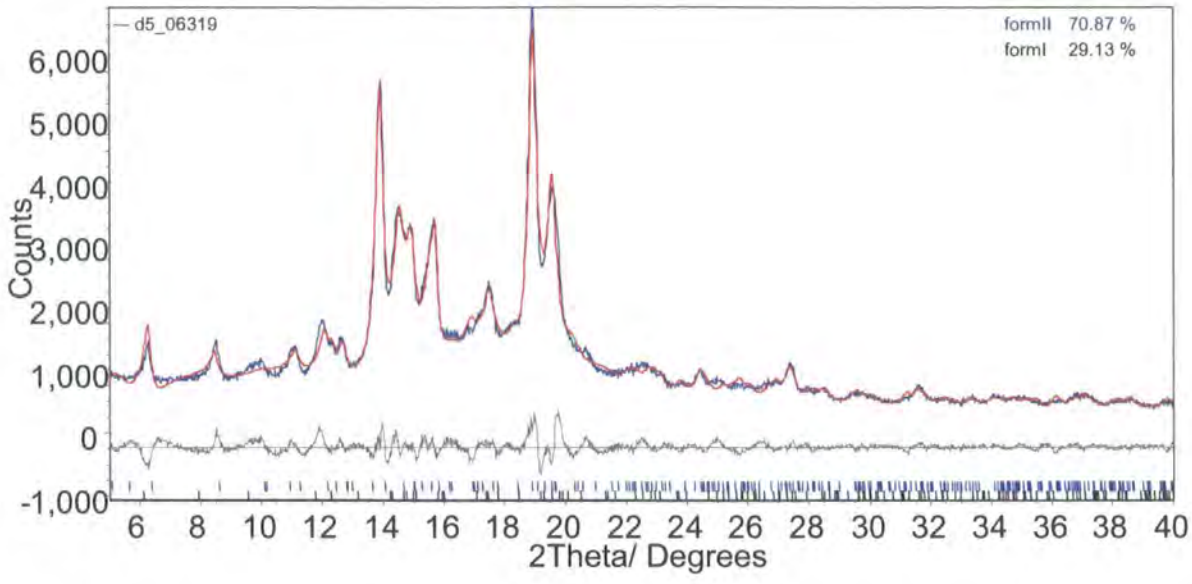

Figure 4.18. Diffractogram for form III trial#5-portion#1 (blue trace). The red trace is the calculated powder pattern for form I and II.

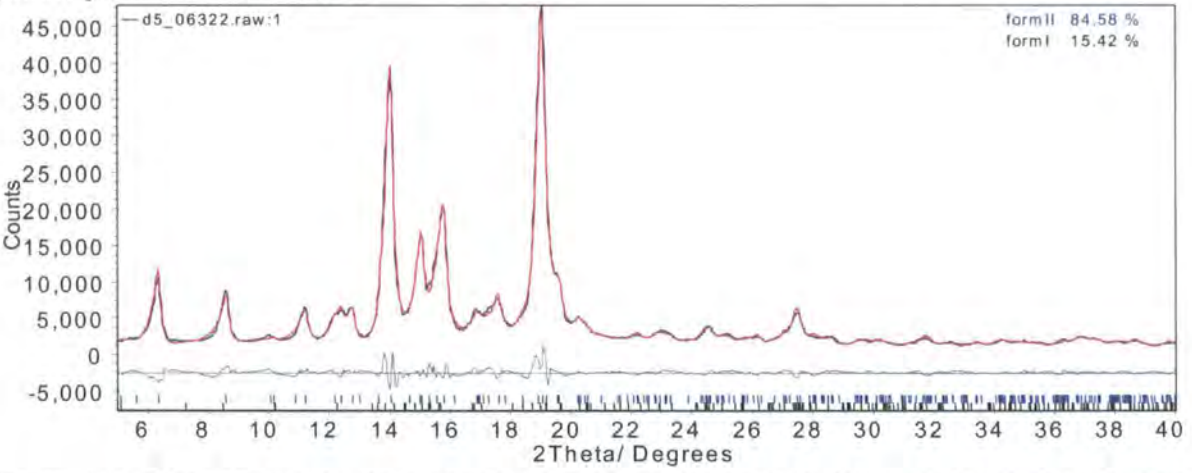

Figure 4.19. Diffractogram for form III trial#5-portion#2 (blue trace). The red trace is the calculated powder pattern for form I and II.

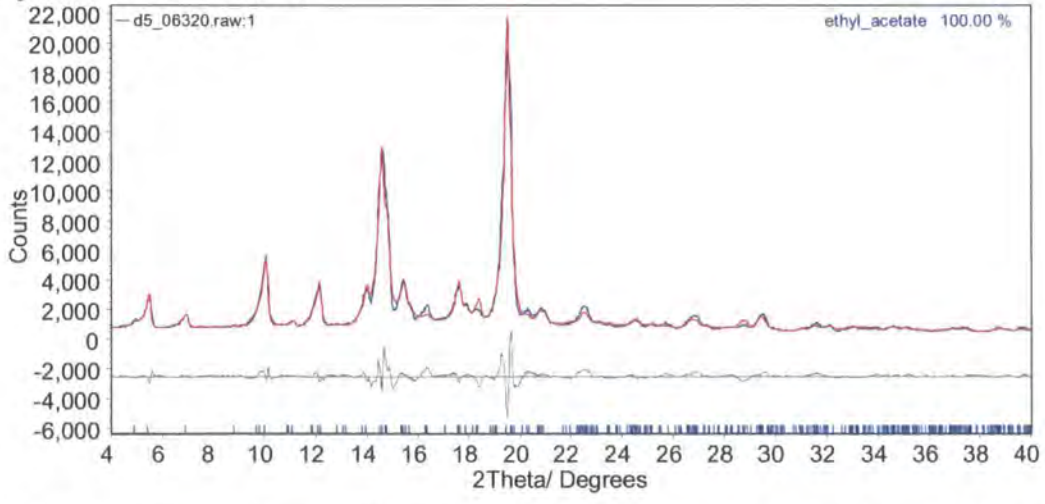

Figure 4.20. Diffractogram for form III trial#6-portion#1 (blue trace). The red trace is the calculated powder pattern for the ethyl acetate solvate.

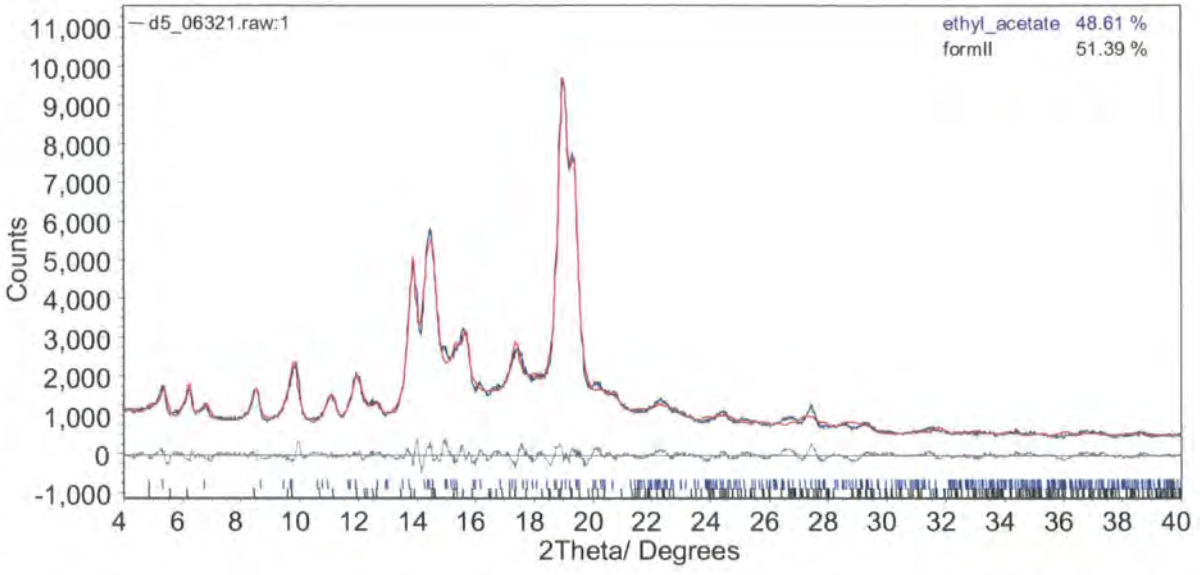

Figure 4.21. Diffractogram for form III trial#6-portion#2 (blue trace). The red trace is the calculated powder pattern for the ethyl acetate and form II.

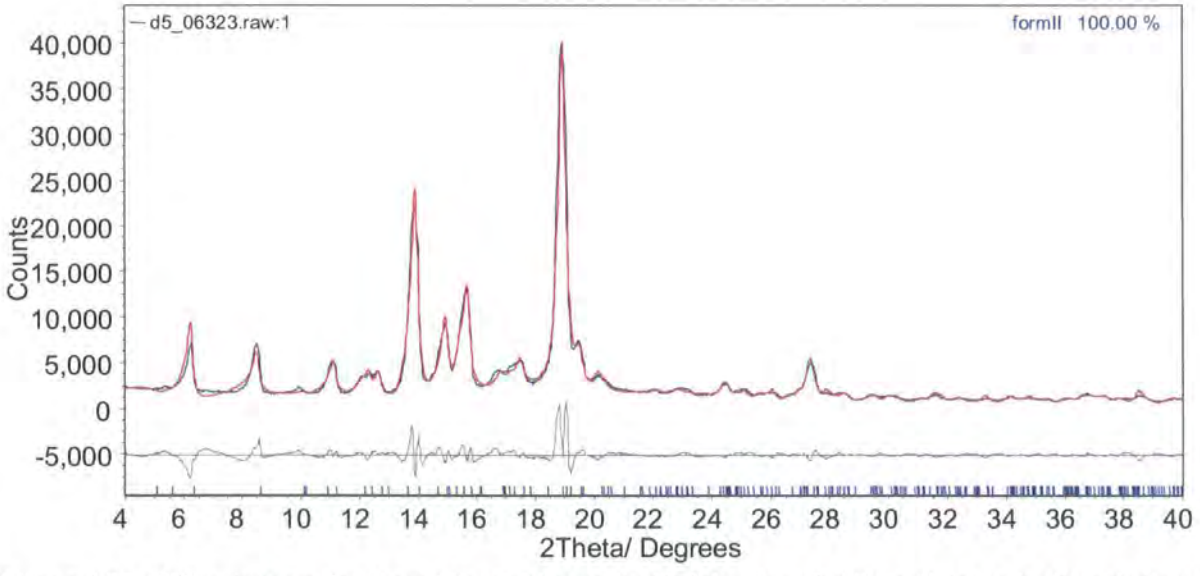

Figure 4.22. Diffractogram for form III trial#6-portion#3 (blue trace). The red trace is the calculated powder pattern for the ethyl acetate solvate.

4.2.2 Form H1

This form is reported in the patent[6] to be prepared from different alcohols. Each alcohol mentioned was tried individually in this research in order to reproduce the H1 form. The form was only characterised by XRPD in the patent.

4.2.2.1 Synthesis

(i) **Trial#1(B# LB1/30)**

0.5 g of finasteride form I was dissolved in 2 mL of ethanol, heated to 55°C and maintained at this temperature for 15 minutes. The solution was left to evaporate over night.

(ii) **Trial#2(B# LB1/34)**

0.5 g of Finasteride form I was dissolved in 2 mL methanol, heated to 55°C and maintained at this temperature for 15 minutes. The solution was cooled to RT and then left to evaporate at RT overnight.

(iii) **Trial#3(B# LB1/37){IPA solvate}**

0.5 g of finasteride form I was dissolved in 2 mL IPA, heated to 60°C and maintained at this temperature for 1 hour. The solution was cooled in the fridge overnight. The solution was then left to evaporate at RT for 24 hours. A highly crystalline sample was produced (sufficient for single crystal XRD studies).

4.2.2.2 Characterisation

(i) **Trial#1**

The XRPD (Figure 4.23) shows clearly that the sample is of form I.

(ii) Trial#2

This time the XRPD pattern obtained (Figure 4.24) shows that the sample is of form II.

(iii) Trial#3{IPA solvate}

Although the obtained XRPD pattern (Figure 4.25) is different to that of forms I and II, it is not in agreement with the pattern of the claimed H1 form. The observed XRPD is closely similar to the calculated powder pattern of the ethyl acetate solvate, with some differences due to preferred orientation. At this stage and with only the XRPD examination, the identity of the solid is not known. The ^{13}C CPMAS NMR spectrum of this sample (Figure 4.51) is different from those of any of the known forms, including that of the ethyl acetate solvate. In fact the sample was found to be an IPA monohydrate solvate (see section 4.4). A distinct DSC thermogram (Figure 4.61) was observed for this solid form. The TGA thermogram shows a loss of 9.8% in two stages between 40°C and 100°C, indicating the presence of the solvent in the solid. Further structural characterisation of the solvate is included later in sections 4.4.2 and 4.4.3.

4.2.2.3 Summary

A summary of the trials carried out and results is shown in Table 4.6.

Table 4.6. Summary of the of the trials carried out following the claimed "H1 form"

Sample ID	Method of preparation	Characterization	conclusion
Trial#1 (B# LB1/30)	From ethanol	From XRPD form I was produced	None of the trials match with the produced form in the patent
Trial#2 (B# LB1/32)	From methanol	From XRPD form II was produced	
Trial#3 (B# LB1/34)	From IPA	From solid-state NMR and single crystal XRD and IPA solvate was prepared	

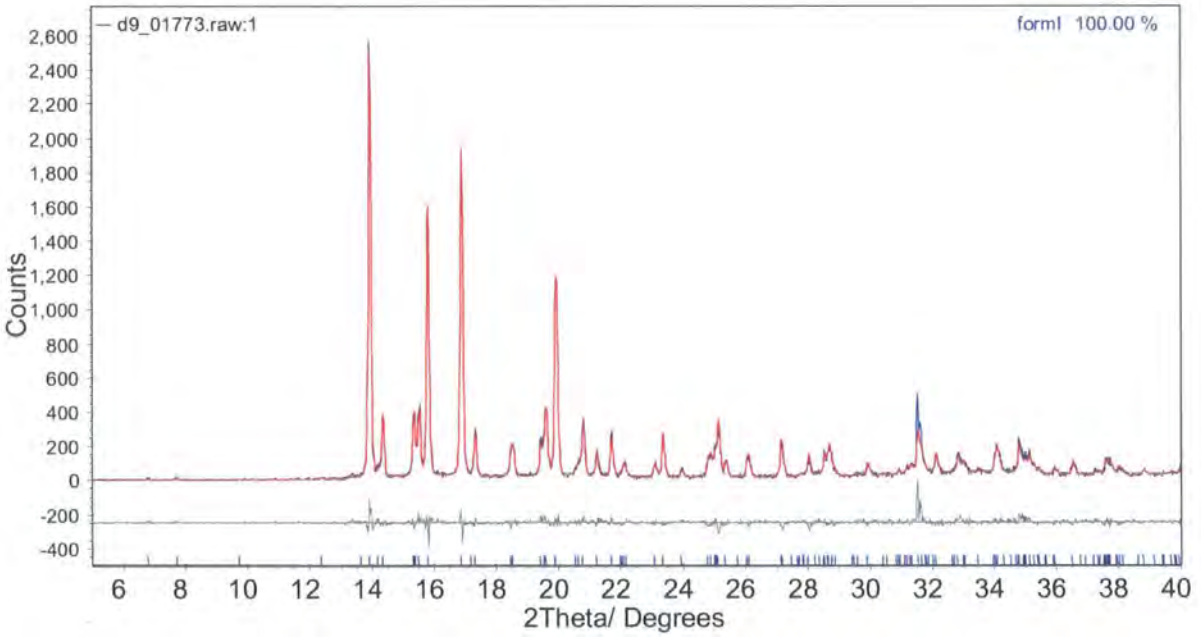

Figure 4.23. Diffractogram for form H1 trial#1 (blue trace). The red trace is the calculated powder pattern for form I.

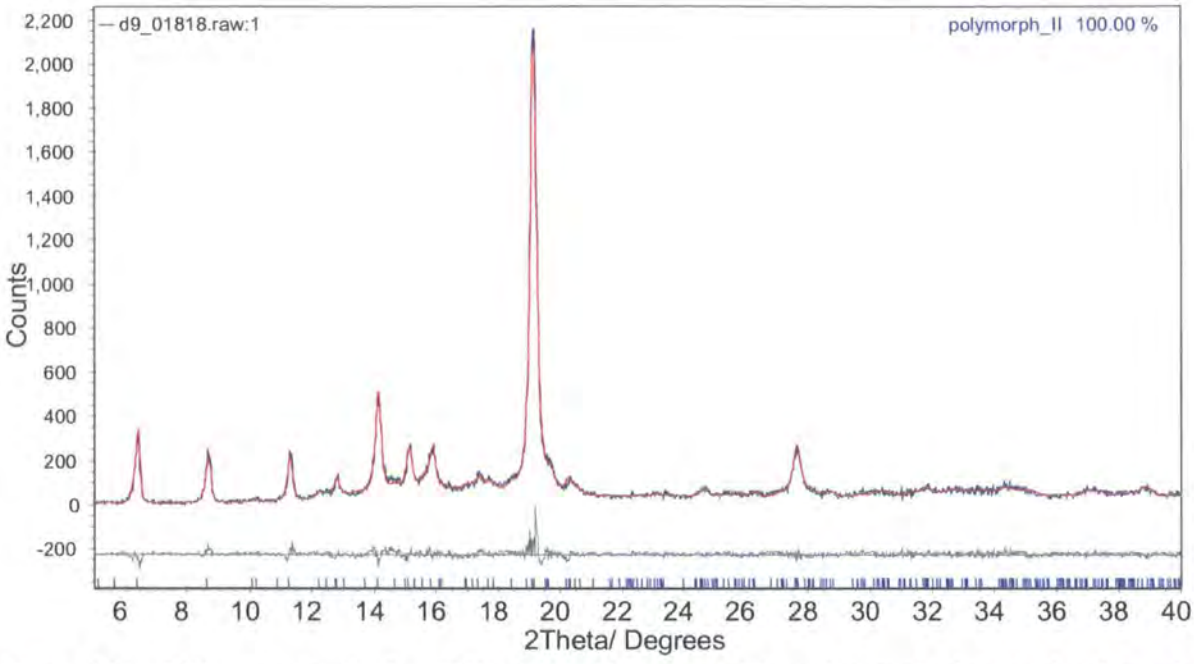

Figure 4.24. Diffractogram for form H1 trial#2 (blue trace). The red trace is the calculated powder pattern for form II.

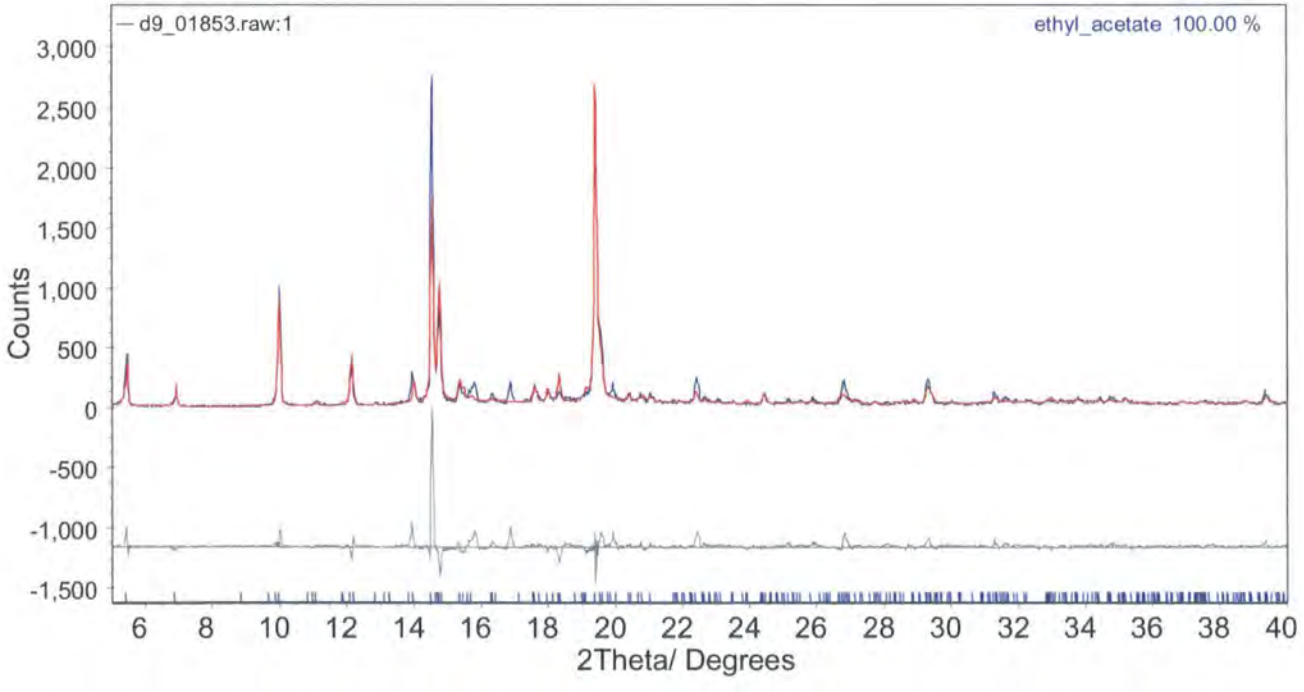

Figure 4.25. Diffractogram for the IPA solvate (blue trace). The red trace is the calculated powder pattern for the ethyl acetate solvate.

4.2.3 Form H2

This form was reported in the patent to be prepared from a solution in dioxane by Parthasaradhi *et al.*[6] in 2004 (the same patent as the H1 form). It was claimed to be a new polymorph suitable for pharmaceutical formulation. The form was characterised only by XRPD. Since a dioxane solvate was already reported in 2002 by Morzycki *et al.*[2], the form was suspected not to be a true polymorph. The form was prepared as per the patent to be checked by full characterisation (solid-state NMR, thermal analysis and XRD).

0.5 g of finasteride of form I was dissolved in 2.5 mL of dioxane, heated to 80°C and maintained at this temperature for 15 minutes. The solution was cooled to 25 °C within 3 hours. The resulting solution was maintained at ambient temperature over night to evaporate. A highly crystalline sample was produced.

The XRPD pattern obtained (Figure 4.26) matches the one reported in the patent, with relative different intensities due to preferred orientation. The pattern is different than those of forms I and II but fits closely with the ethyl acetate solvate calculated powder pattern. Hence, Parthasaradhi *et al.*[6] seem to have erroneously considered this form as a new one because its XRPD pattern was not compared with those of the published ethyl acetate solvate[7]. As in the case of the IPA solvate, the XRPD examination is not enough to determine the identity of the solid.

The ^{13}C CPMAS NMR spectrum of this sample (Figure 4.52) is different to those of the known forms, including the ethyl acetate solvate. The peaks due to dioxane were assigned in the ^{13}C CPMAS (Figure 4.52) according to the ^{13}C solution-state NMR spectrum. Peaks due to dioxane were also assigned in the ^{1}H MAS NMR spectrum (Figure 4.56). A distinct DSC thermogram (Figure 4.62) was observed for this solid form. The TGA thermogram shows a loss of 13.2% at about 60 °C, indicating the presence of the solvent in the solid. Further structural characterisation of the solvate is included later in sections (4.4.2 and 4.4.3).

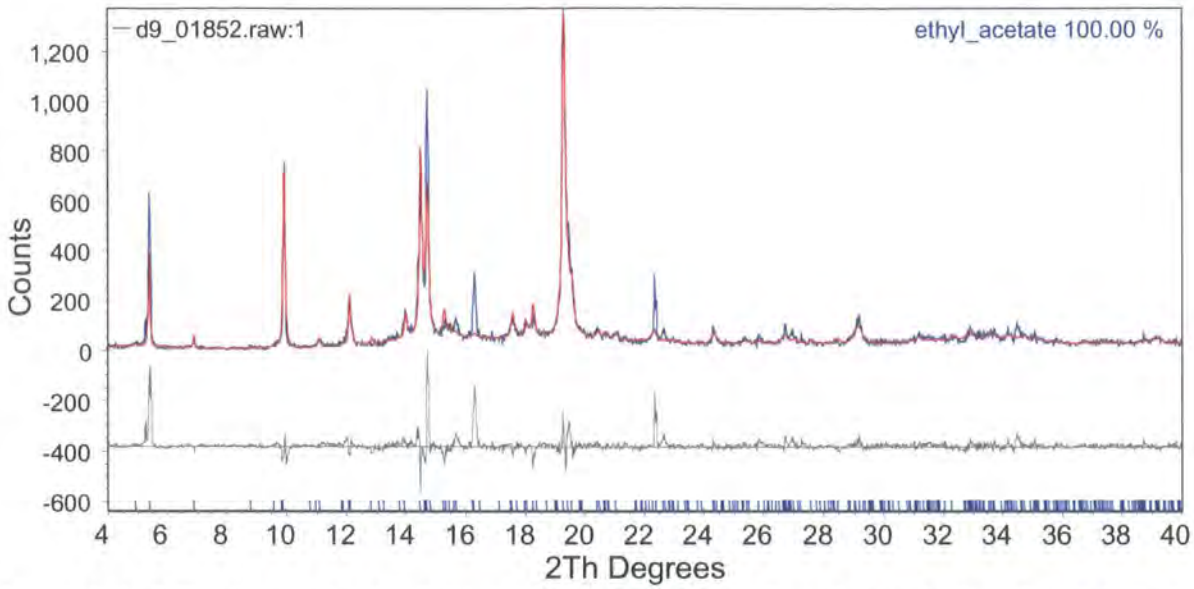

Figure 4.26. Diffractogram for the dioxane solvate (blue trace). The red trace is the calculated powder pattern for the ethyl acetate solvate. Some differences appear due to preferred orientation.

4.3 Finasteride Solvates Reported In the Scientific Literature

4.3.1 Acetic Acid Solvate(Finasteride-Acetic Acid Complex[7])

The solid was prepared as per the methods published in the scientific[7] and patent[4,5] literature. In both cases a gluey solid was produced, but this matter was not discussed in the literature. Further drying of the product in the vacuum oven at 50 °C for an hour produced a highly crystalline solid which then became examinable.

The crystals were crushed under liquid nitrogen for XRPD examination. The observed pattern (Figure 4.27) shows that the bulk sample is of the acetic acid solvate in the literature. The ^{13}C CPMAS spectrum observed (Figure 4.28) agrees with the crystal structure of this form as it shows there is one molecule in the asymmetric unit. Chemical shift assignments were made according to the assignments for form I, which also has one molecule in the asymmetric unit. Peaks due to acetic acid were assigned according to the known solution-state shifts. The ^{1}H MAS NMR spectrum (Figure 4.29) shows a characteristic peak due to the acetic OH proton (compared with solution state) while there is some uncertainty about the acetic acid methyl group. The peak at -0.1 ppm is still not identified. It may be due to the acetic acid methyl group although the expected chemical shift in the solution state is 2.0 ppm.

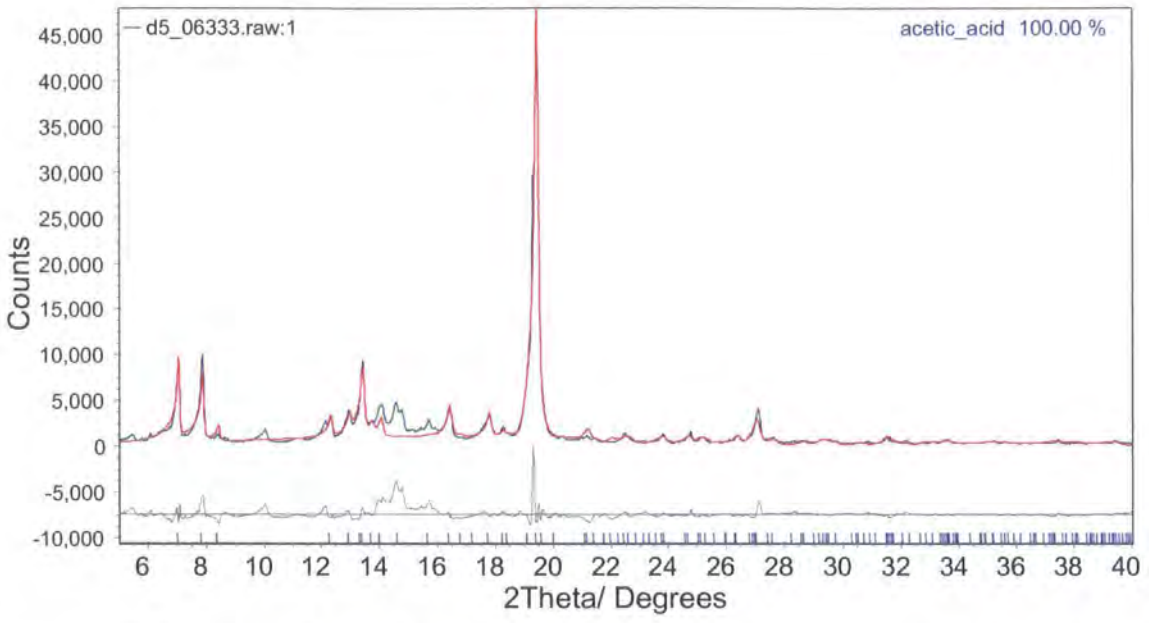

Figure 4.27. Diffractogram for the dioxane solvate (blue trace). The red trace is the calculated powder pattern for the acetic acid solvate.

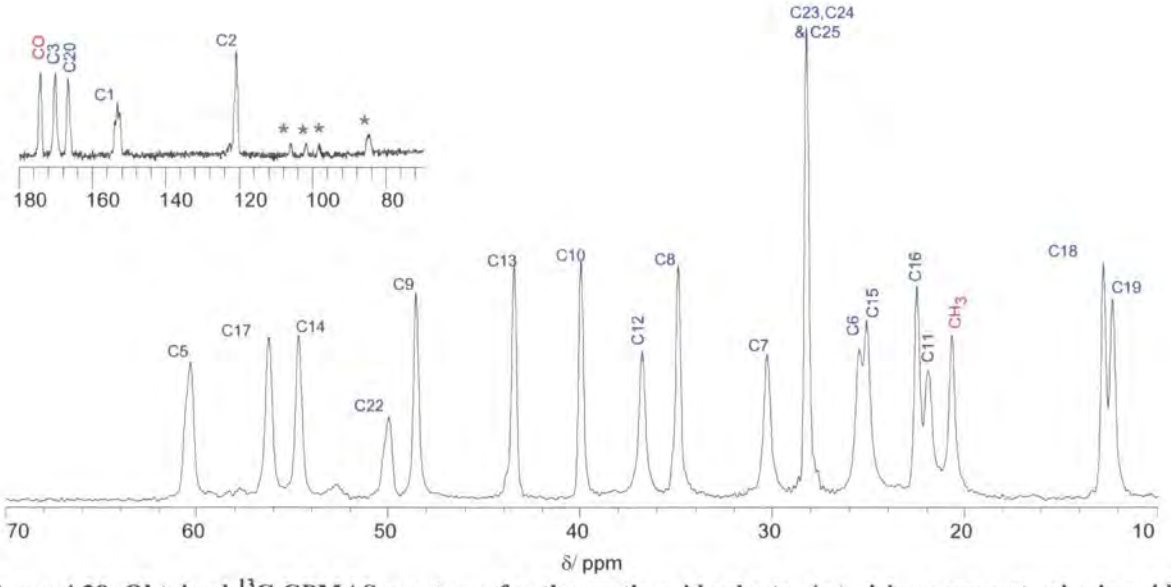

Figure 4.28. Obtained ^{13}C CPMAS spectrum for the acetic acid solvate. Asterisks represent spinning side bands. The spectrum was acquired for 40 ms with proton decoupling power of 100 kHz.

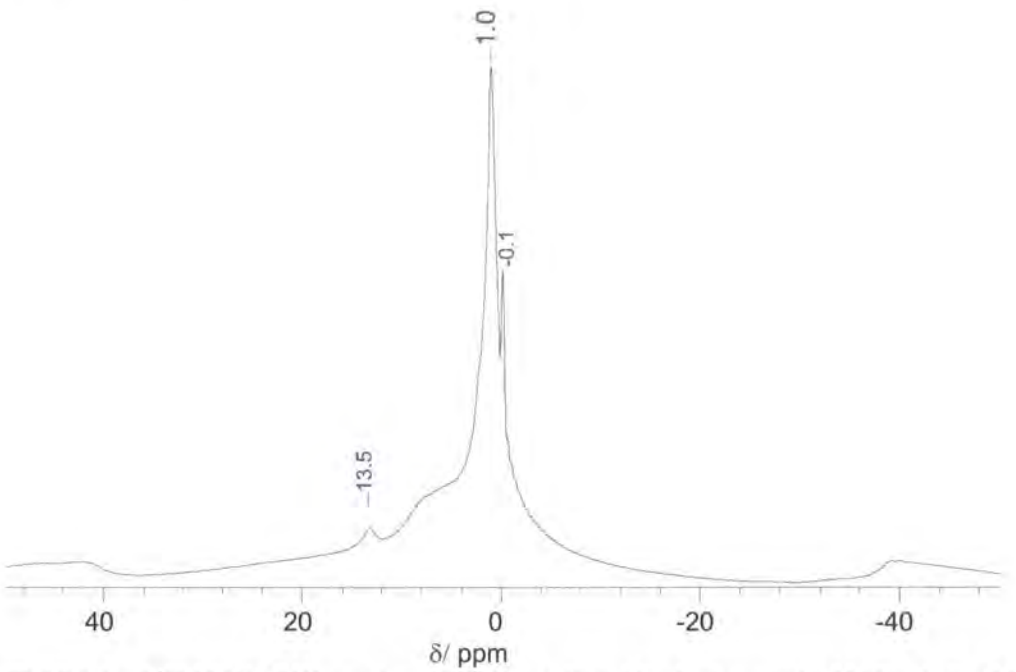

Figure 4.29. Obtained ^{1}H MAS NMR spectrum for the acetic acid solvate sample. MAS rate is 20 kHz.

4.3.2 Ethyl Acetate Solvate(Bis-Finasteride Monohydrate Ethyl Acetate Clathrate[7])

This solid was reported by Wawrzycka *et al.*[7] in 1999. Later it was reported to be prepared by a different methodology in the patent literature[4,5].

Firstly, the patent methodology was tried (B# LB1/35) by preparing a slurry of a 0.5 g of finasteride form I in 1.5 mL of an ethyl acetate, THF and water mixture such that the ratio of ethyl acetate: THF: water is 1:1:~0.1, then heating the resultant slurry to a temperature of 60°C for about 20 minutes. The slurry was then cooled in the fridge over night. The solid was left to dry at RT.

The observed XRPD pattern (Figure 4.30) fits closely with the calculated powder pattern of the ethyl acetate solvate. To help assigning the ^{13}C CPMAS spectrum (Figure 4.31), the solution-state ^{13}C NMR (Figure 4.32) was obtained. Peaks other than those of finasteride were found to be characteristic for ethyl acetate and, unexpectedly, THF. The ^{13}C CPMAS spectrum was then found to be a mixture of two spectra corresponding to the ethyl acetate and a THF solvate (see section 4.3.24.4.3) but it is not known whether the THF and ethyl acetate are in the same crystals or if the sample is a mixture of crystals. There were no big crystals in the sample enough to check with single crystal XRD.

The DSC (Figure 4.33) shows a different thermogram from those of any of the anhydrous forms. The TGA thermogram (Figure 4.34) showed a loss of 10.8% at about 55ºC, thus confirming the presence of solvents. Quantitative solution-state ^{1}H NMR was done to calculate water and solvent molar ratios in the sample. First the ^{1}H NMR spectrum was run for the sample (Figure 4.35) and then for a sample spiked with small drops of water (Figure 4.36) in order to determine the water peak position. Integrals of solvent peaks were tabulated (Table 4.7) and the molar ratios were calculated.

The water peak was shifted (to around 1.9 ppm) after spiking indicating its presence. The molar ratios agree with the ^{13}C CPMAS spectrum as the THF solvate spectrum was the major component in the mixture. Only traces (impurity) of ethyl acetate were detected. The ratio of the ethyl acetate was calculated based on the CH_3O (4.12 ppm) since it is resolved, unlike other resonances (1.25 and 2.04 ppm). In the case of THF, the resonances gave a ratio of 0.4. The water peak showed a ratio of 0.6, which is close to the ethyl acetate case, where it is expected to be 0.5 from the crystal structure. The theoretical TGA loss expected from a ratio of 0.5 of each of water and THF (without counting the traces of ethyl acetate) is 10.8% which is in agreement with the observed value (10.8%).

Table 4.7. Quantitative analysis obtained from solution-state ^1H NMR for the "ethyl acetate" solvate sample prepared according to the patent recipe.

Chemical shift/ δ_H	Solvent/ assignment	Integral	Molar ratio/ finasteride
3.7	THF/ CH_2O(multiplet)	1.56	0.4
1.85	THF/ CH_2(multiplet)	1.73	0.4
4.12	Ethyl acetate/ CH_2O(quartet)	0.09	0.05
1.9	water	1.19	0.6

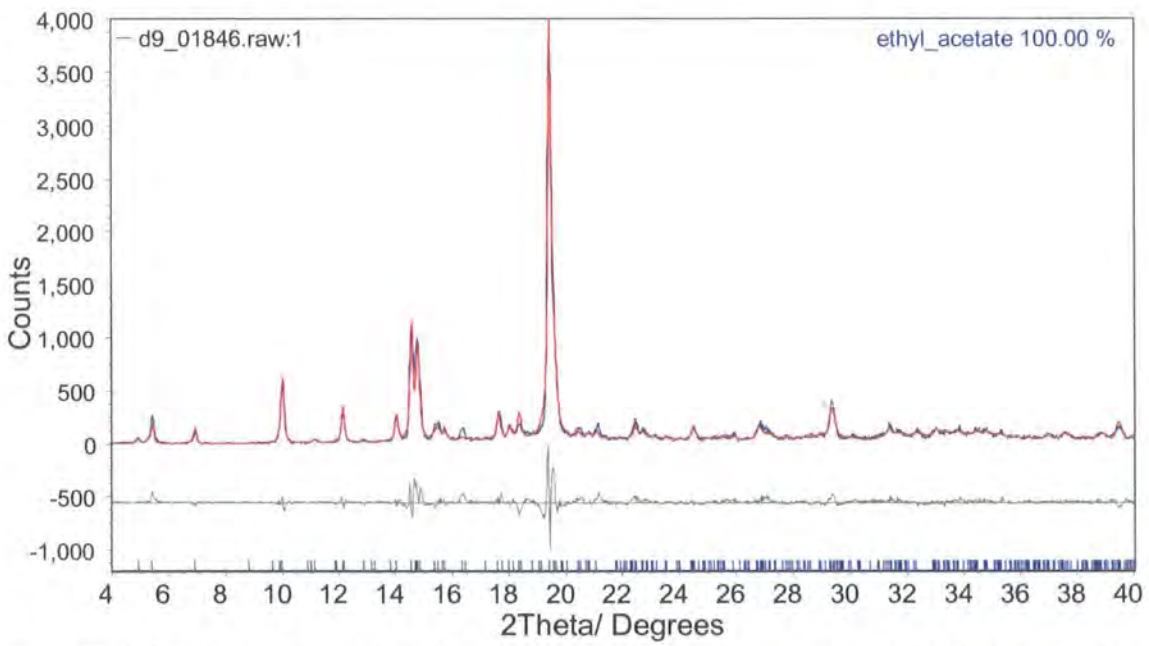

Figure 4.30. Diffractogram for the "ethyl acetate" solvate sample prepared according to the patent recipe. The red trace is the calculated powder pattern for the ethyl acetate solvate.

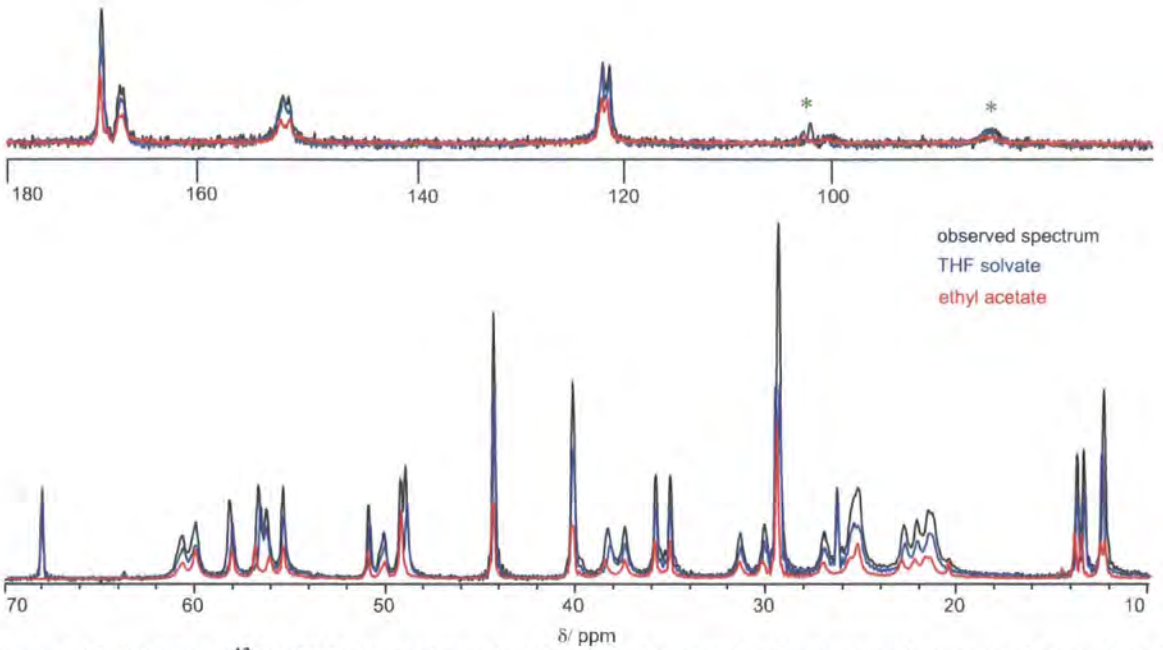

Figure 4.31. Obtained ^{13}C CPMAS spectrum for the "ethyl acetate" solvate sample prepared according to the patent recipe. Asterisks represent spinning side bands. The spectrum was acquired for 40 ms with proton decoupling power of 55 kHz.

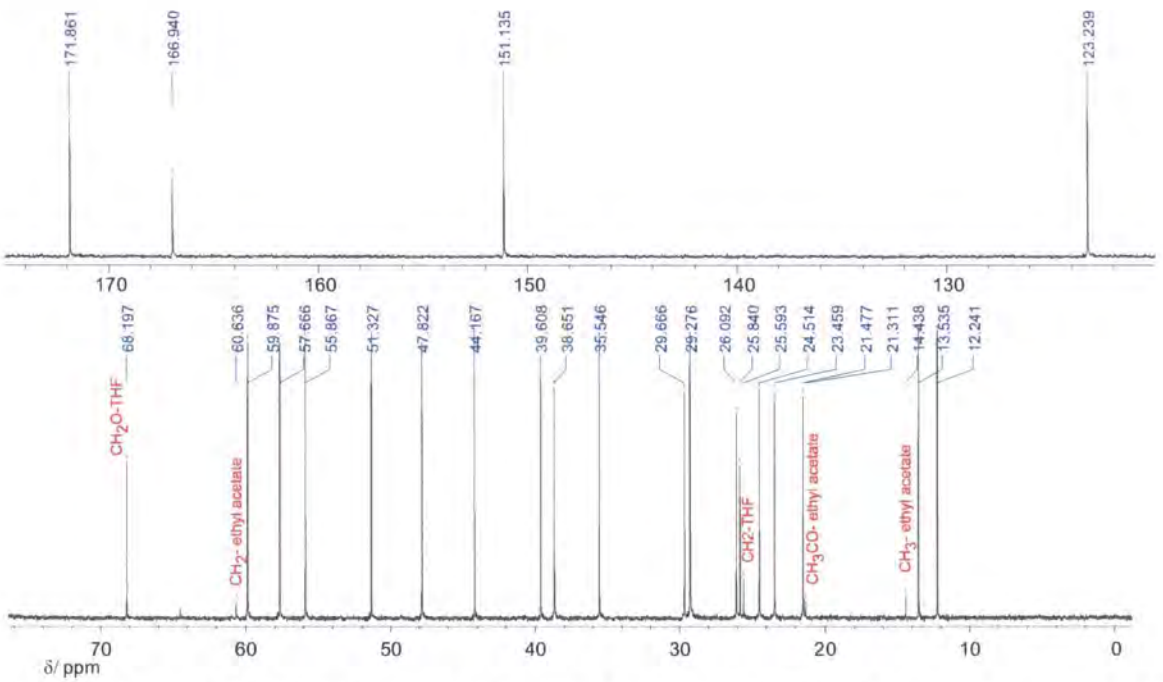

Figure 4.32. Obtained ^{13}C NMR spectrum of the "ethyl acetate" solvate sample prepared according to the patent recipe and dissolved in $CDCl_3$.

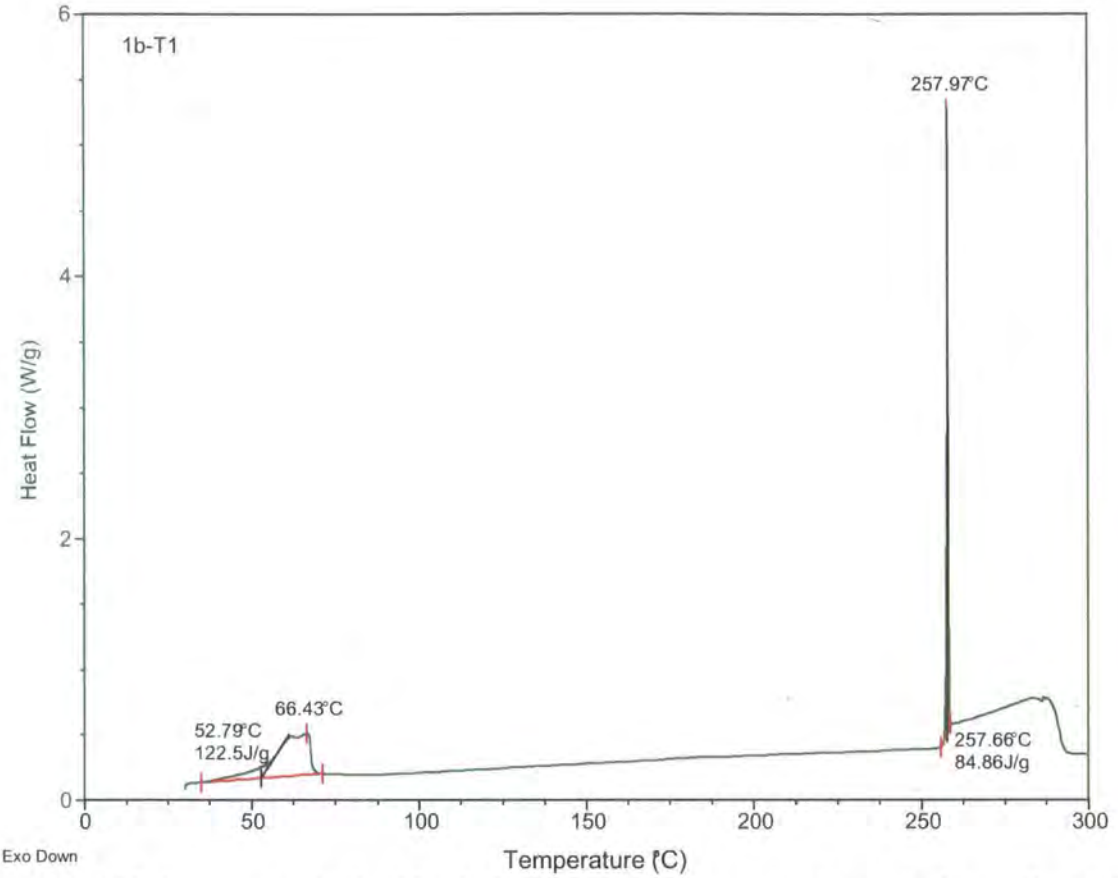

Figure 4.33. DSC thermogram obtained for the "ethyl acetate" solvate sample prepared according to the patent recipe.

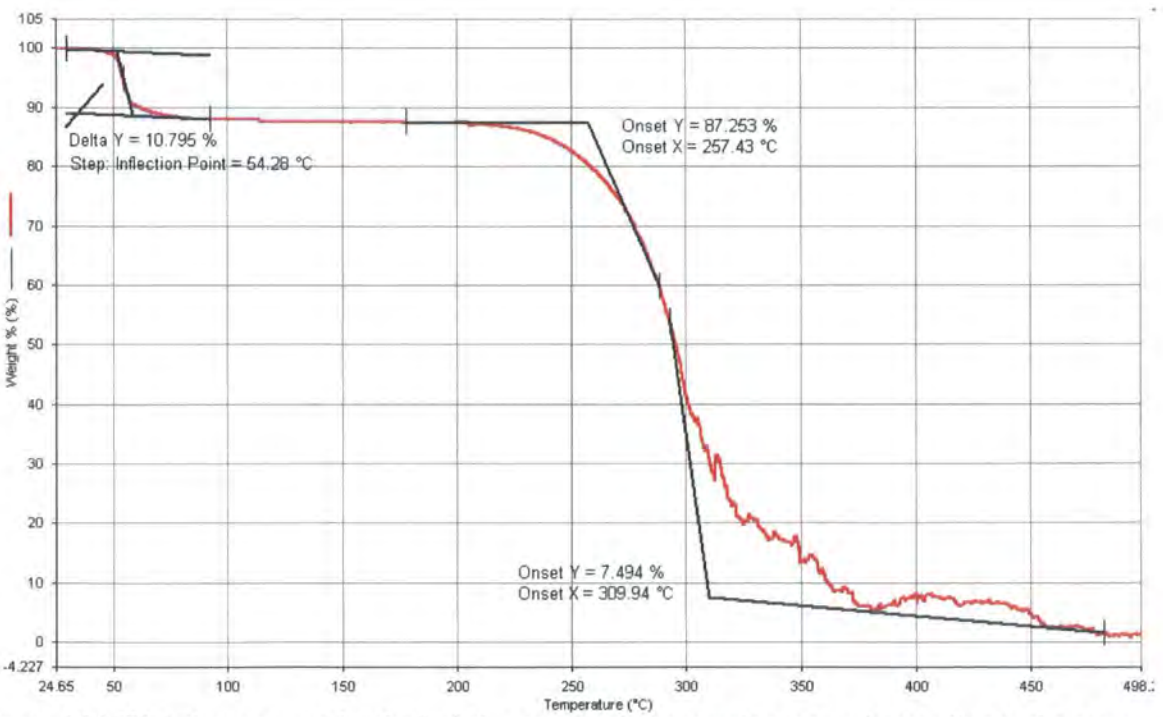

Figure 4.34. TGA thermogram for the "ethyl acetate" solvate sample prepared according to the patent recipe.

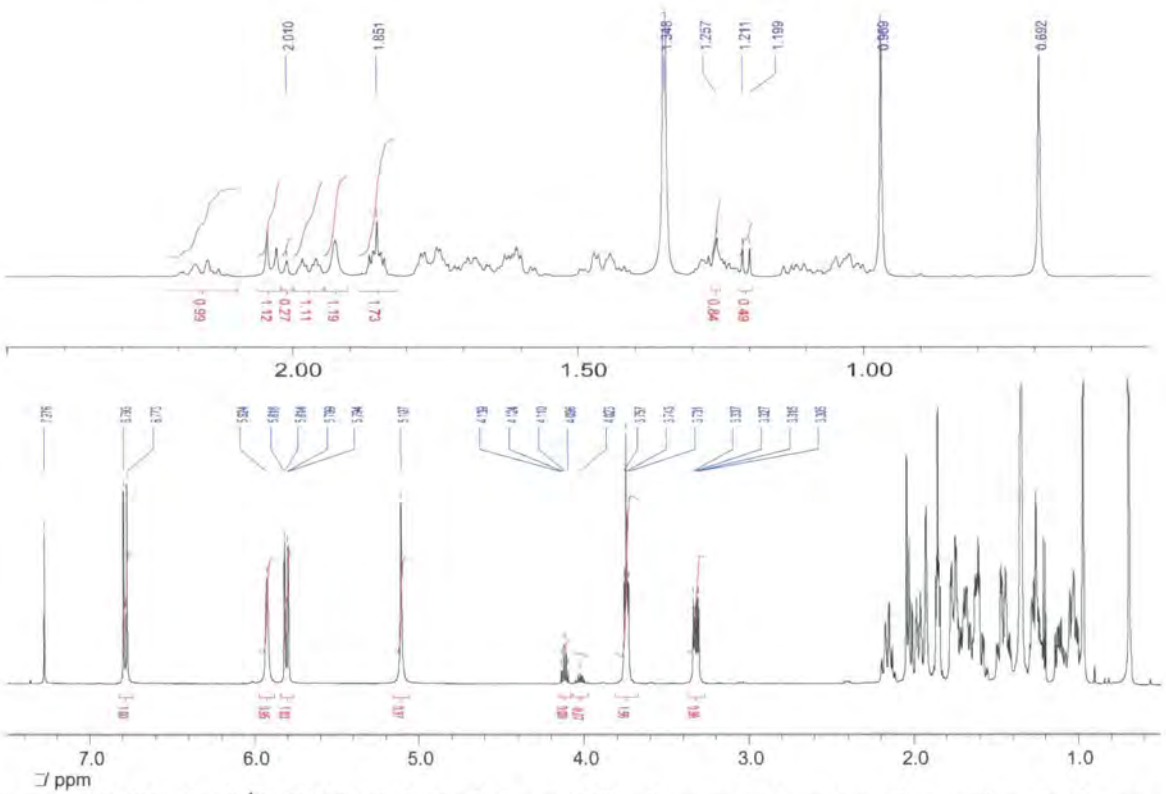

Figure 4.35. Obtained ^{1}H NMR of the "ethyl acetate" solvate sample prepared according to the patent recipe and dissolved in $CDCl_3$.

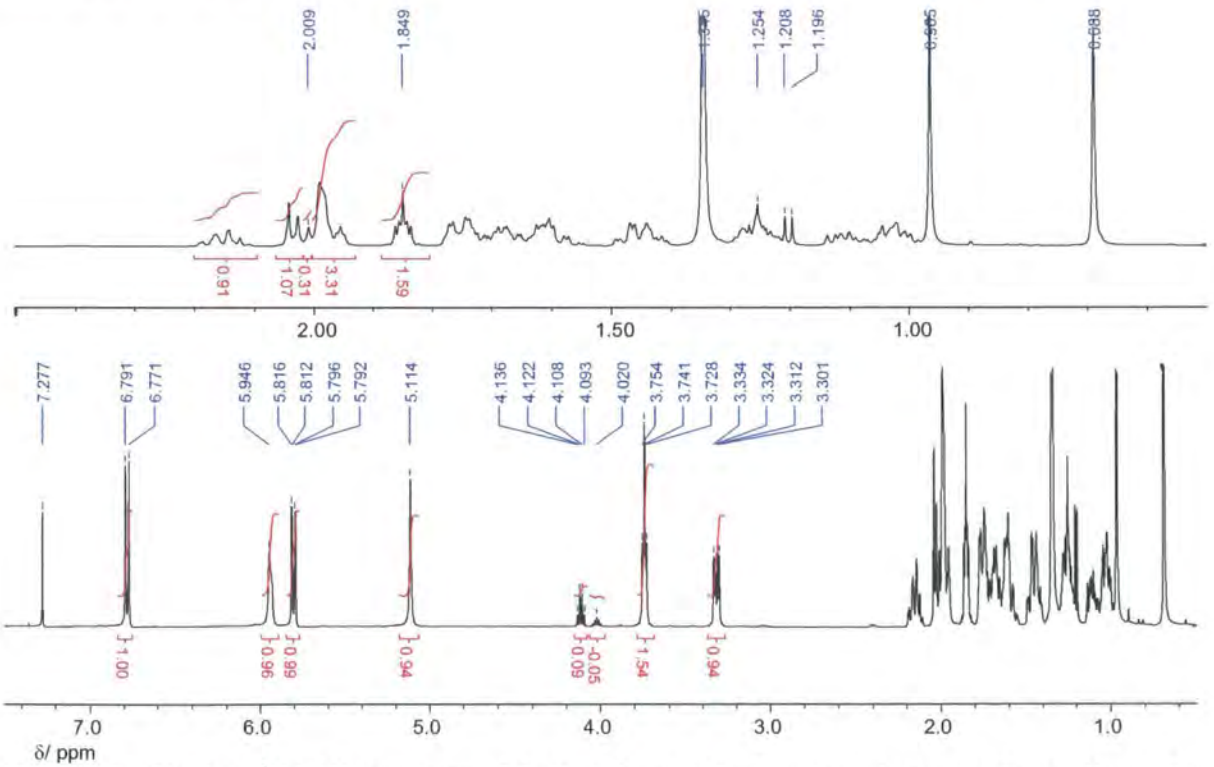

Figure 4.36. Obtained ^{1}H NMR spectrum of the "ethyl acetate" solvate sample prepared according to the patent recipe solvate, dissolved in $CDCl_3$ and spiked with water. The shift of the water peak after spiking helped identifying the chemical shift of water.

Because the results for the first sample, prepared according to the patent method, were anomalous, another sample was prepared (B# LB1/39) according to the scientific literature reference[7]. 0.5 g finasteride form I was dissolved in ethyl acetate and a few drops of water. The resulting mixture was heated to a temperature of 55°C for about 20 minutes. The mixture was then cooled to RT and left to evaporate over night.

The observed XRPD pattern (Figure 4.37) fits with the ethyl acetate calculated powder pattern, as in the case of the first trial, but this time showing a 13C CPMAS spectrum (Figure 4.38) which corresponds to that of a pure ethyl acetate solvate. As expected from the crystal structure of the ethyl acetate in the literature, the spectrum indicates that there are two molecules in the asymmetric unit. Chemical shift assignments were based on the solution-state assignments. The ethyl acetate peaks in the 13C CPMAS spectrum were distinguished by direct pulse (DP) 13C NMR (Figure 4.39). The most prominent peaks in the DP spectrum arise form the mobile methyl carbons, which have relatively short relaxation times. Somewhat unusually, signals from some quaternary carbons appear weakly, presumably because their relaxation times are shortened by their proximity to the methyl groups.The ^{1}H MAS NMR spectrum (Figure 4.40) shows peaks due to the solvent.

Quantitative solution-state ^{1}H NMR shows that there is a molar ratio of 0.4 and 0.5 of ethyl acetate and water, respectively, to finasteride (Table 4.8). Theoretically, from the crystal structure, the ratios should be 0.5 for each. The theoretical TGA % loss expected is 10.6% (based on 0.4 and 0.5 ratios) which is similar to the result obtained (10.3%) within experimental error (Figure 4.41). The obtained DSC thermogram (Figure 4.42) is somewhat different from that of the first trial (THF and ethyl acetate mixture). The DSC and TGA data have not been reported in the literature.

Table 4.8. Quantitative analysis obtained from solution-state ^{1}H NMR for the ethyl acetate solvate.

Chemical shift/ δ_H	Solvent/ assignment	Integral	Molar ratio/ finasteride
4.12	Ethyl acetate/ CH_2O(quartet)	0.86	0.4
1.9	water	2.05-1.10= 0.95	0.5

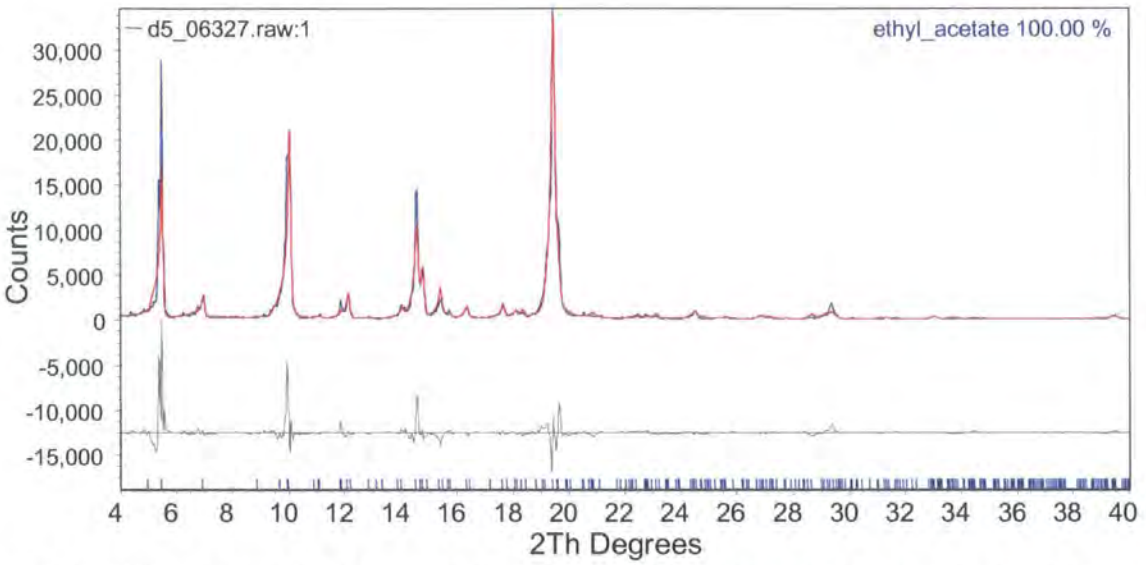

Figure 4.37. Diffractogram for the ethyl acetate solvate sample. The red trace is the calculated powder pattern for the ethyl acetate solvate.

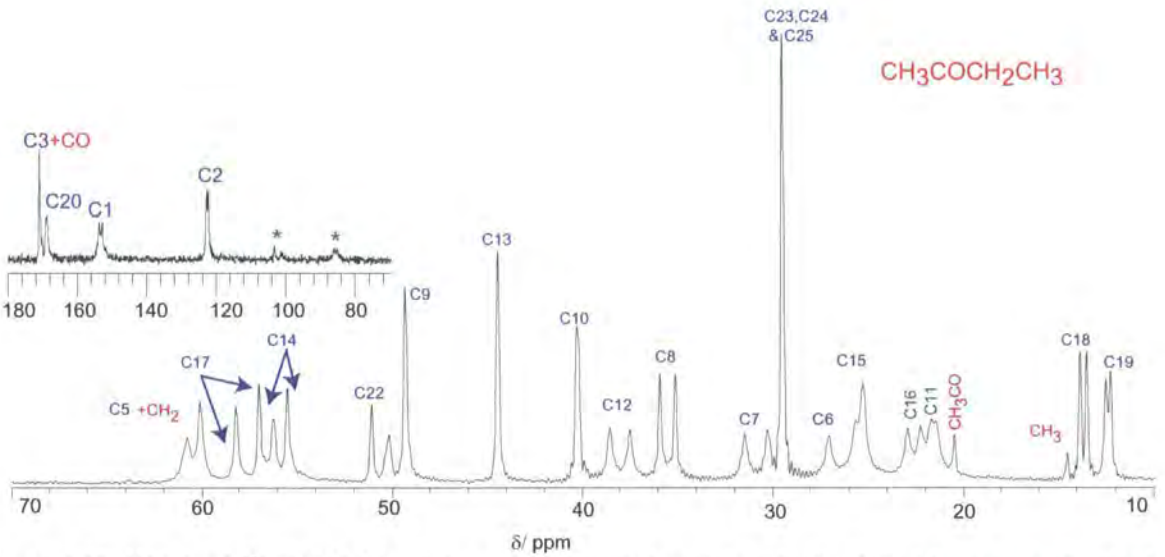

Figure 4.38. Obtained ^{13}C CPMAS spectrum for the ethyl acetate solvate. Asterisks represent spinning side bands. The spectrum was acquired for 40 ms with proton decoupling power of 55 kHz.

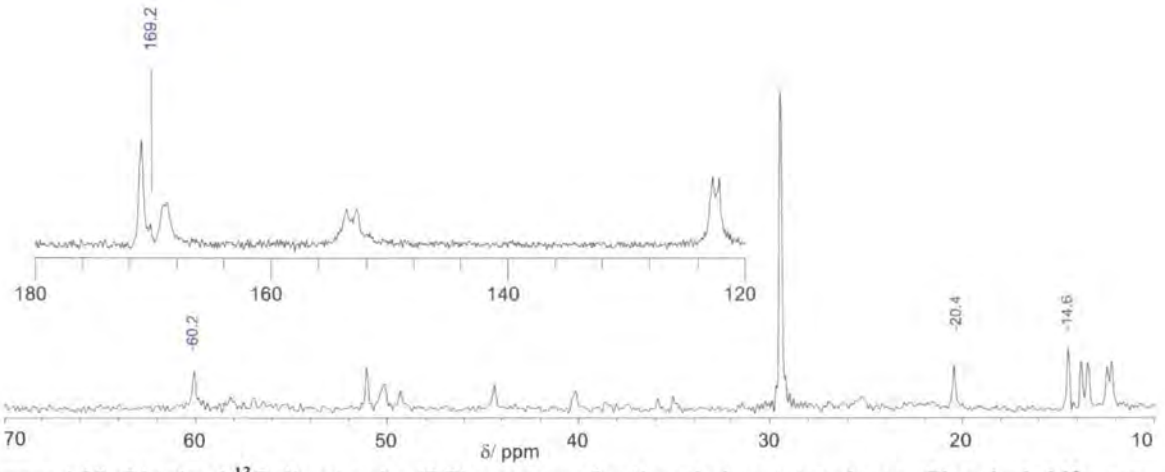

Figure 4.39. Obtained ^{13}C direct pulse (DP) spectrum for the ethyl acetate solvate. Chemical shifts are shown for peaks due to the ethyl acetate solvent.

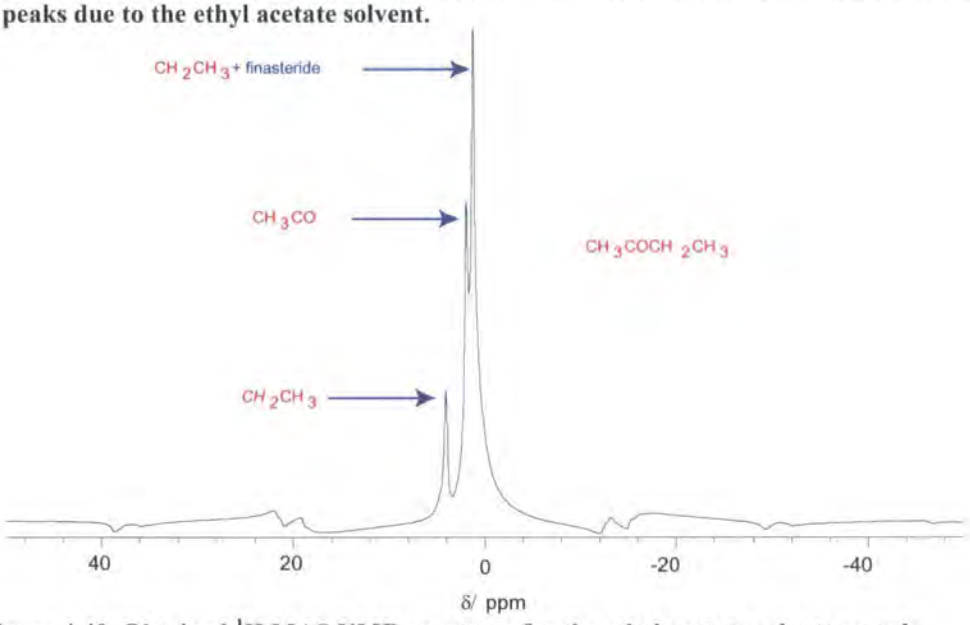

Figure 4.40. Obtained ^{1}H MAS NMR spectrum for the ethyl acetate solvate sample.

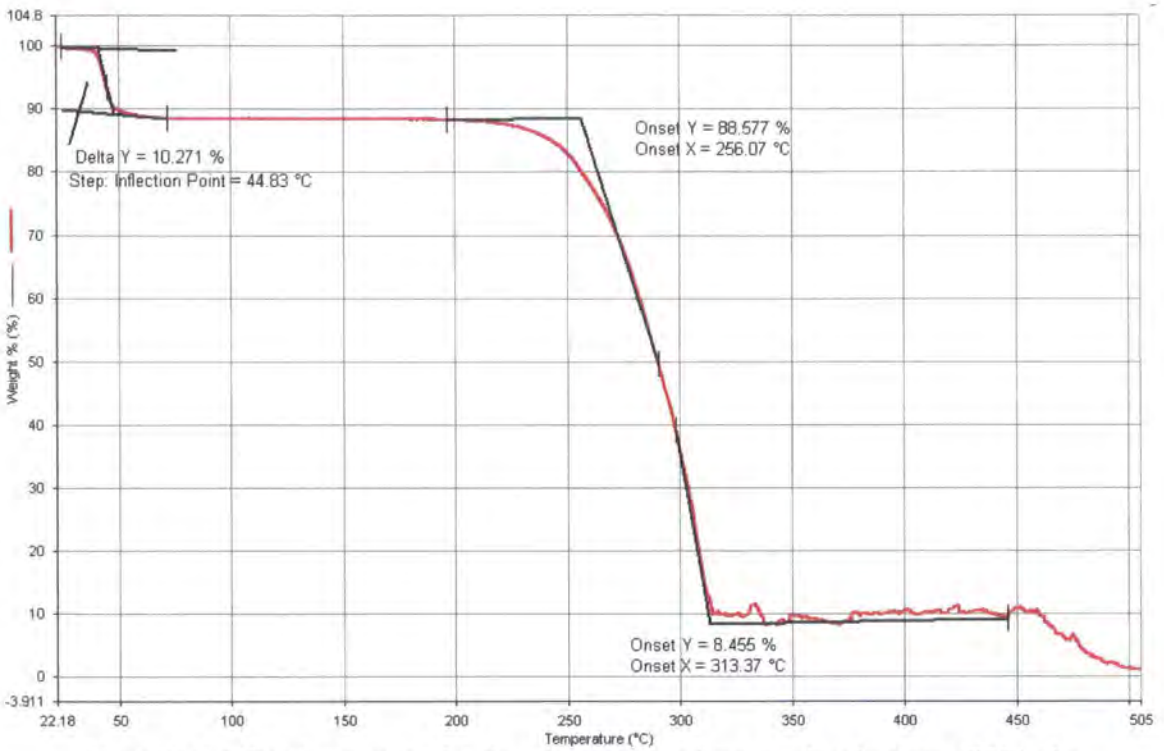

Figure 4.41. TGA thermogram for the ethyl acetate solvate at a heating rate of2°C/ min.

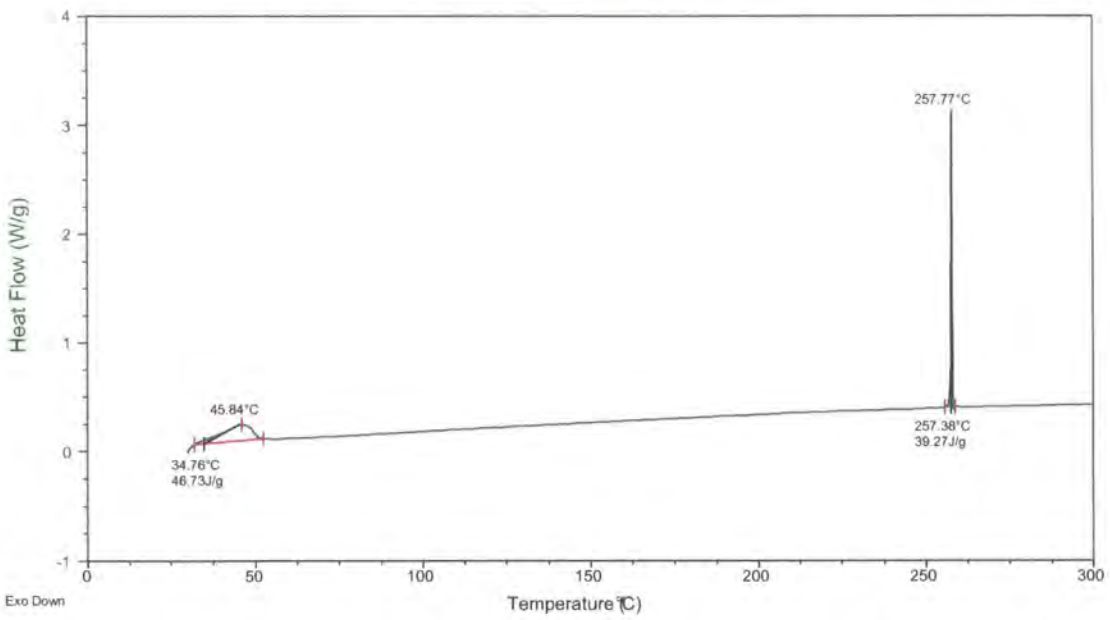

Figure 4.42. DSC thermogram obtained for the ethyl acetate solvate at a heating rate of 1°C/ min.

The idea of having an ethyl acetate solvate without the existence of water was checked by preparing a sample like the ethyl acetate sample but without adding water (B# LB1/39). 0.5 g of finasteride form I was dissolved in ethyl acetate. The resulting mixture was heated to a temperature of 55°C for about 20 minutes then cooled to RT and kept to evaporate over night.

The XRPD pattern (Figure 4.43) shows that the sample is a mixture of three forms; ethyl acetate solvate, form I and form II. The results were also confirmed in the ^{13}C CPMAS spectrum (Figure 4.44). It can be concluded that water stabilises the ethyl acetate solvate (including water) and

decreasing the concentration of water in the sample initiates the formation of the other anhydrous forms (I and II).

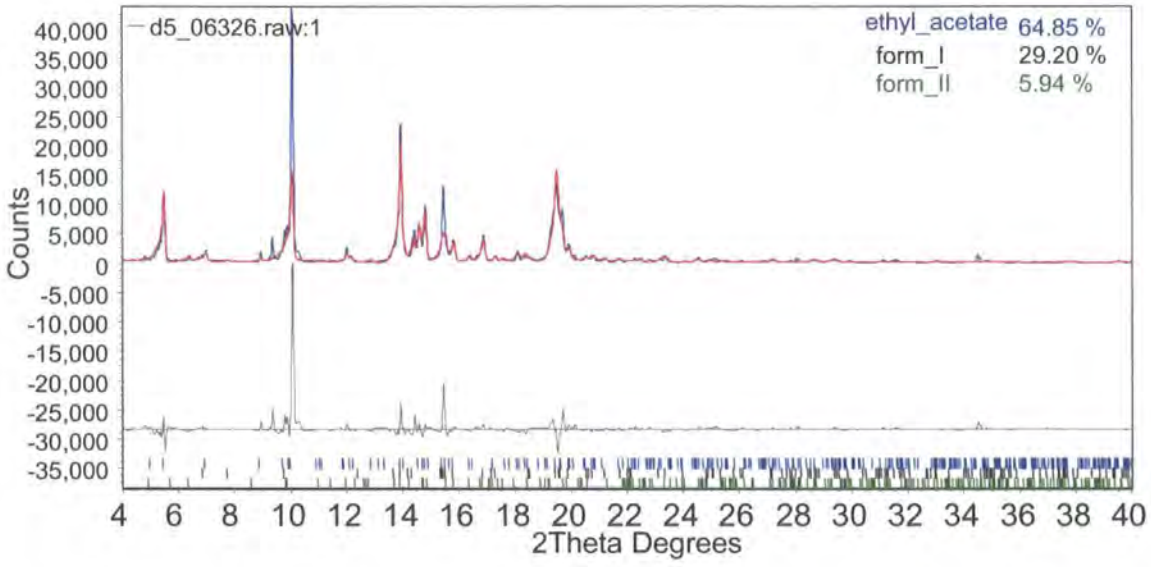

Figure 4.43. Diffractogram for the "ethyl acetate solvate" sample prepared without water. The red trace is the calculated powder pattern for the ethyl acetate solvate, form and form II.

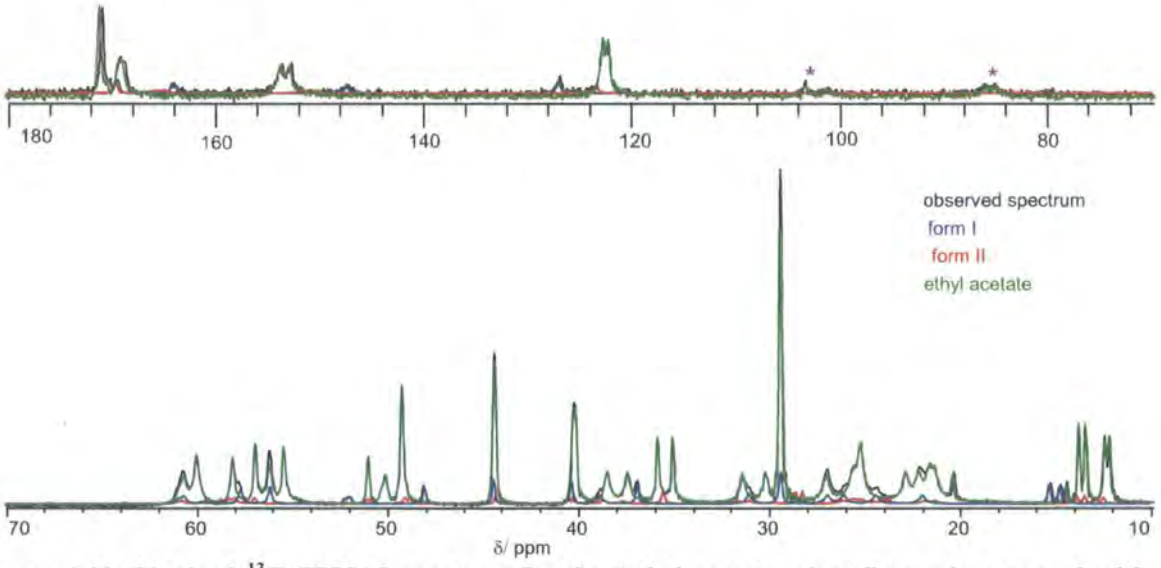

Figure 4.44. Obtained ^{13}C CPMAS spectrum for the "ethyl acetate solvate" sample prepared without water. Asterisks represent spinning side bands. The spectrum was acquired for 5 ms with proton decoupling power of 55 kHz.

4.4 Newly prepared Finasteride Solvates

The synthesis and characterisation of a newly prepared solvates are included in the section.

4.4.1 Synthesis

4.4.1.1 Finasteride THF Hydrate Solvate {Bis-Finasteride Mono-Tetrahydrofuran Monohydrate}

0.5 g of finasteride form I was dissolved in THF. The resulting solution was heated to a temperature of 55 °C for about 20 minutes, then was cooled to RT and kept to dry overnight (B# LB1/39). Large colourless crystals of prismatic shape suitable for single crystal XRD examination were produced.

Another sample (sample#2) was prepared to investigate the effect of adding water (not excluding it as in the ethyl acetate case) on the preparation of the THF solvate (B# LB1/39). 0.5 g finasteride form I was dissolved in THF and a few drops of water. The resulting solution was heated to a temperature of 55 °C for about 20 minutes, then cooled to RT and kept to evaporate overnight. Finer crystals were produced compared to the first trial.

4.4.1.2 Finasteride IPA Hydrate Solvate { Bis-Finasteride Mono-Isopropanol Monohydrate}

0.5 g of finasteride form I was dissolved in 2 mL IPA, heated to 60 °C and maintained at this temperature for 1 hour. The solution was cooled in the fridge overnight. The solution was then left to evaporate at RT for 24 hours. Large colourless crystals of prismatic shape suitable for single crystal XRD examination were produced.

4.4.1.3 Finasteride Dioxane Hydrate Solvate {Bis-Finasteride Mono-Dioxane Monohydrate}

0.5 g of finasteride of form I was dissolved in 2.5 mL of dioxane heated to 80 °C and maintained at this temperature for 15 minutes. The solution was cooled to 25 °C within 3 hours. The resulting solution was maintained at ambient temperature over night to evaporate. Large colourless crystals of prismatic shape crystals suitable for single crystal XRD examination were produced.

4.4.2 X-ray Characterisation

4.4.2.1 XRPD characterisation

Samples of the IPA and dioxane solvates were ground prior XRPD examination to minimise the preferred orientation effect. The grinding was done under liquid nitrogen, except for the THF solvate sample, to prevent phase transformation. The crystals of the THF solvate sample were crushed smoothly (not ground). The corresponding XRPD patterns for the IPA and dioxane solvates were shown previously (Figure 4.25 and Figure 4.26 in sections 4.2.2 and 4.2.3 respectively). The XRPD

pattern for the THF solvate and THF solvate sample #2 (with additional water) are shown below (Figure 4.45 and Figure 4.53 respectively).

All prepared samples have XRPD patterns which fit reasonably with the calculated powder pattern for the ethyl acetate solvate. The differences due to preferred orientation between the observed and the calculated powder patterns for all prepared samples varied from one solvate to another. Other differences were seen in the case of the THF solvate sample at low 2θ values. These relatively larger differences are likely to be due to the high crystallinty of the sample (not ground). However, the obtained XRPD patterns for all prepared solvates, along with that of the ethyl acetate solvate, are indistinguishable. More strictly speaking, no information can be concluded from the XRPD about the included solvent.

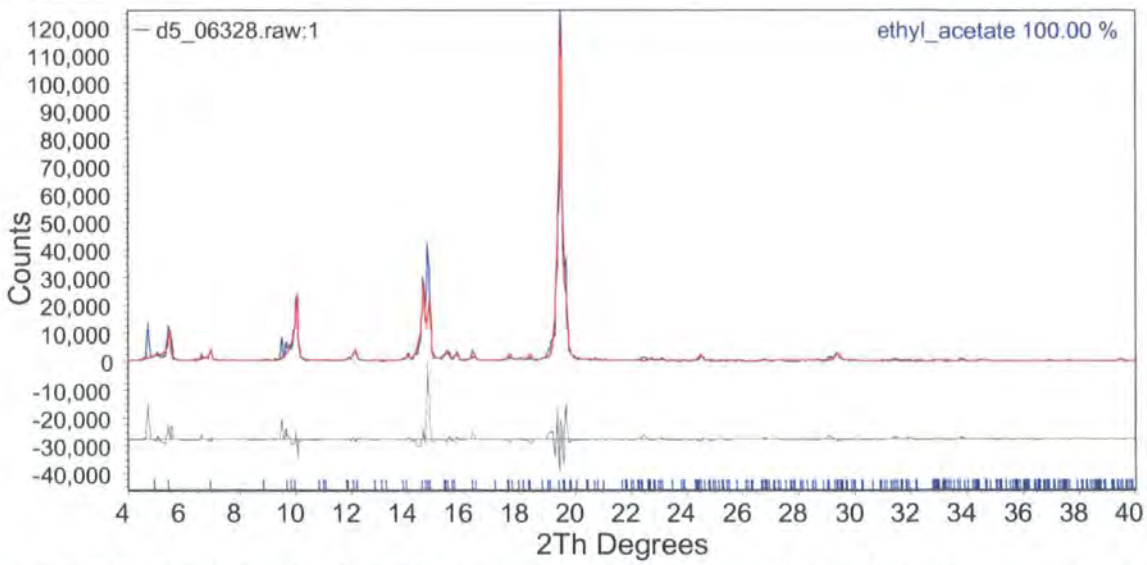

Figure 4.45. Diffractogram for the THF solvate sample. The red trace is the calculated powder pattern for the ethyl acetate solvate.

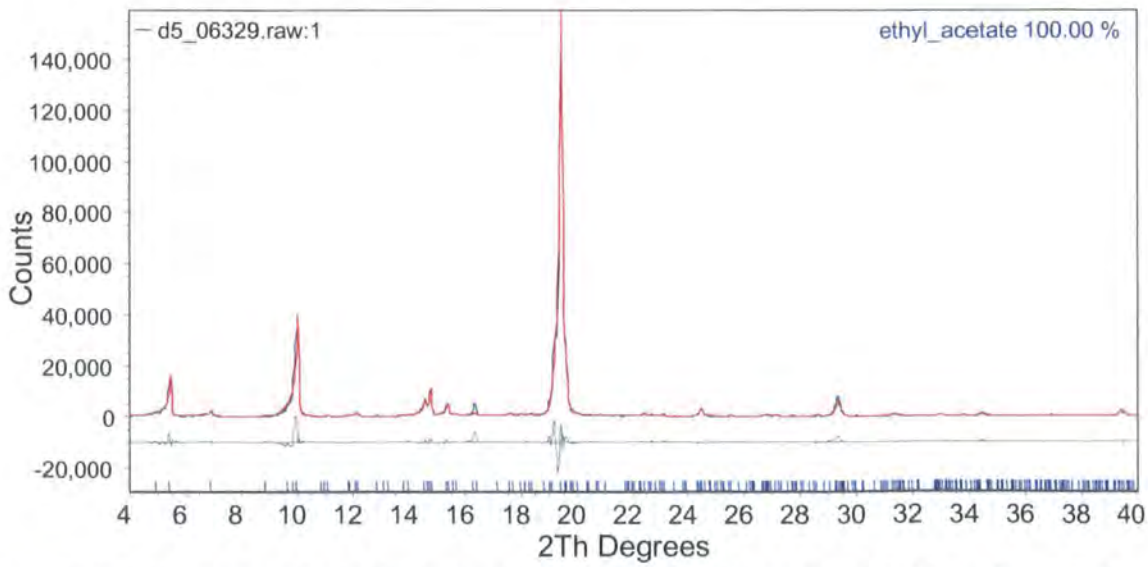

Figure 4.46. Diffractogram for the THF solvate (prepared with additional water). The red trace is the calculated powder pattern for the ethyl acetate solvate.

4.4.2.2 Single crystal XRD characterisation

Table 4.9 summarises the crystallographic data for the newly prepared finasteride solvates. The solvates are isomorphous (also with the ethyl acetate solvate); all having orthorhombic lattice symmetry, $P2_12_12_1$ space groups, two molecules in the asymmetric unit and an empirical formula of bis-finasteride monohydrate monosolvate (Figure 4.47). Moreover, the solvent molecules are highly disordered inside a channel along the *a* crystallographic axis (Figure 4.48). Clearly the channel structure allows ready ingress of molecules of moderate size and it is anticipated that many other solvate hydrates may be prepared. The water molecules appear to be essential to maintain the open channel structure.

Although the dioxane solvate was mentioned in the scientific literature[2], full characterisation was not done (only FT-IR and ^{13}C CPMAS NMR). Hence, the author was not aware of the presence of water in the solvate.

The two molecules (referred to as molecule 1 and molecule 2, containing carbon atoms 1-25 and 26-50, respectively) inside the asymmetric unit are connected with strong intermolecular hydrogen bonding, from the lactam side of ring A, forming a dimer (Figure 4.49). The NH group in the lactam side is a hydrogen bonding donor while the carbonyl group of the lactam side is an acceptor. Such hydrogen bonding was reported[1] for all finasteride forms in the literature where as the amide NH was reported to be uninvolved in hydrogen bonding due to the steric effect of the tert-butyl group.

Figure 4.50 shows the network formed between water and finasteride molecules in the dioxane solvate. It is also representative of the IPA, ethyl acetate and THF solvates. The water molecules in finasteride monohydrate solvates act as bridge, through intermolecular hydrogen bonding, linking finasteride molecule dimers. Water is involved in three hydrogen bonds; being a hydrogen bond donor to lactam group O atoms on two finasteride molecules below, and a hydrogen bond acceptor from the peptide N atom from the finasteride molecule above it (Figure 4.50).

Whilst the water molecules are shown to be strongly fixed in the crystal structure, the solvent disorder in the solvates is severe; hence the dioxane, IPA and THF molecules could not be located as recognizable molecular entities in the Fourier difference maps. A similar degree of solvent disorder was found in the isomorphous ethyl acetate solvate[7]. As a consequence of that NMR and other techniques were consulted (see the next section 4.4.3) in order to quantify the solvents.

Table 4.9. Obtained single XRD data for the prepared finasteride hydrate solvates

Composition	**Finasteride dioxane solvate**	**Finasteride IPA solvate**	**Finasteride THF solvate**
Empirical Formula	$2\ C_{23}H_{36}N_2O_2 \cdot H_2O \cdot C_4H_8O_2$	$2\ C_{23}H_{36}N_2O_2 \cdot H_2O \cdot C_3H_8O_1$	$2\ C_{23}H_{36}N_2O_2 \cdot H_2O \cdot C_4H_8O_1$
Gross formula	$C_{50}H_{82}N_2O_7$	$C_{49}H_{82}N_2O_6$	$C_{50}H_{82}N_2O_6$
Molecular Weight (amu)	823.2	795.2	807.2
Crystal dimensions (mm^3)	0.12 × 0.16 × 0.28	0.16 × 0.20 × 0.20	0.20 × 0.20 × 0.20
Crystal system	orthorombic	orthorombic	orthorombic
Space group	$P2_12_12_1$	$P2_12_12_1$	$P2_12_12_1$
a (Å)	8.1110(7)	8.1132(3)	8.1317(3)
b (Å)	18.0856(16)	17.9012(8)	17.7767(7)
c (Å)	35.512(3)	35.6948(15)	35.7349(15)
V ($Å^3$)	5209.4(8)	5184.2(4)	5165.7(4)
Z	4	4	4
Z'	2	2	2
T (K)	120	120	120
Calculated Density (g/cm^{-3})	1.050	1.019	1.038
μ (mm^{-1})	0.07	0.07	0.07
Number of observed reflections	6298	3772	3529
Number of parameters refined	595	528	524
R_{int} (%)	3.5	2.2	1.5
R (%) for $I > 2\sigma$	11.3	7.1	8.1
wR (%)	25.5	17.0	19.1

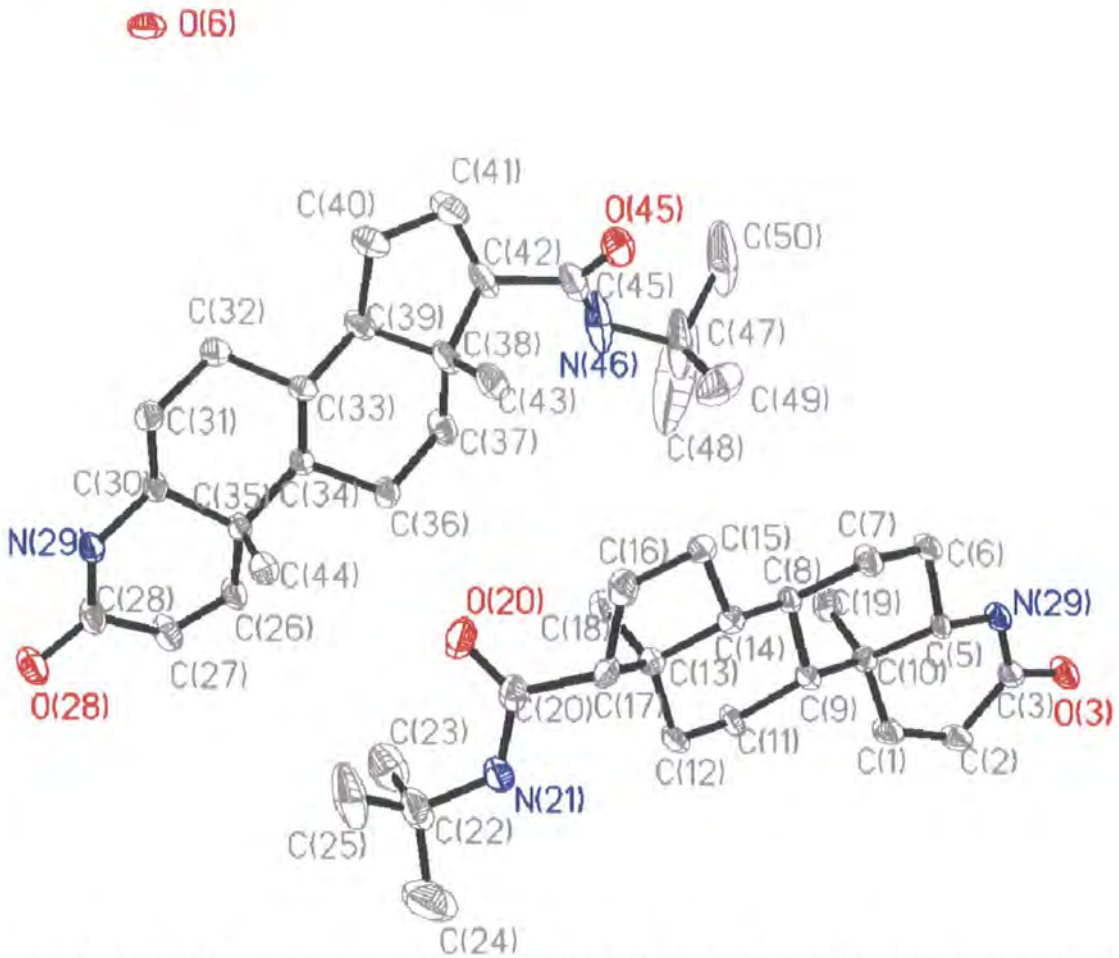

Figure 4.47. Molecular structure and atom numbering scheme for finasteride dioxane hydrate solvate. The atomic displacement parameters are drawn at 50% probability. Disordered solvent and hydrogen atoms have been omitted from the picture for clarity. The same numbering scheme was used for the isomorphous IPA and THF solvates.

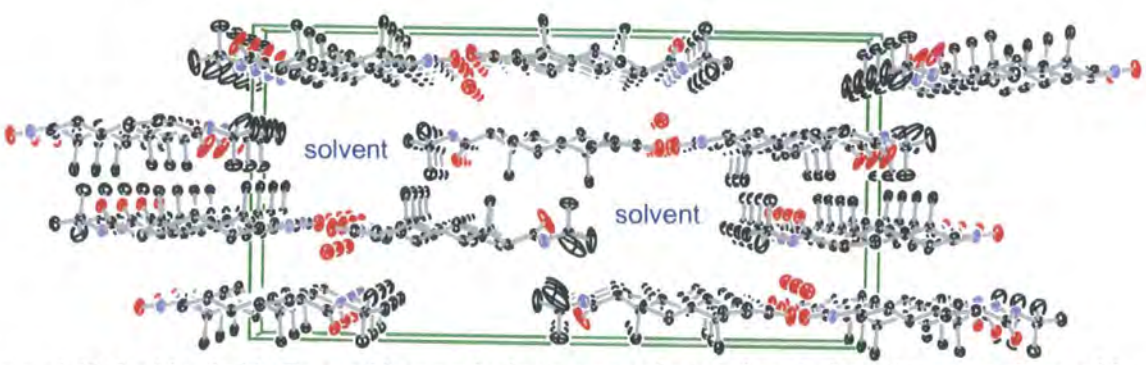

Figure 4.48. Packing in bis-finasteride monohydrate monosolvates viewed along the *a* crystallographic axis.

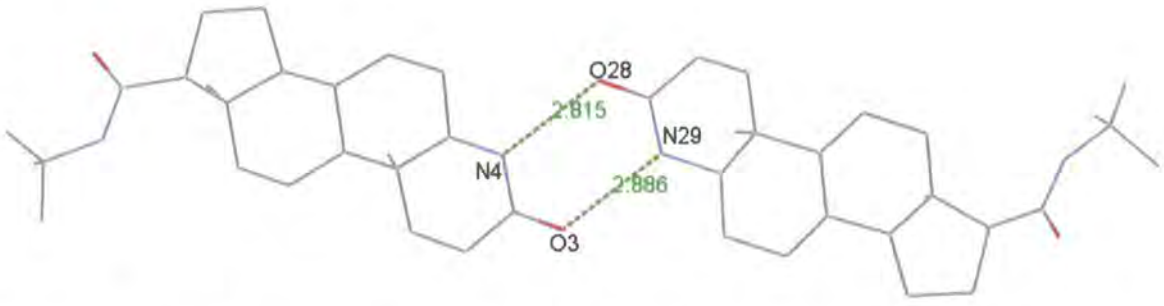

Figure 4.49. Dimers formed between crystallographically independent finasteride molecules through N-H...O hydrogen bonding

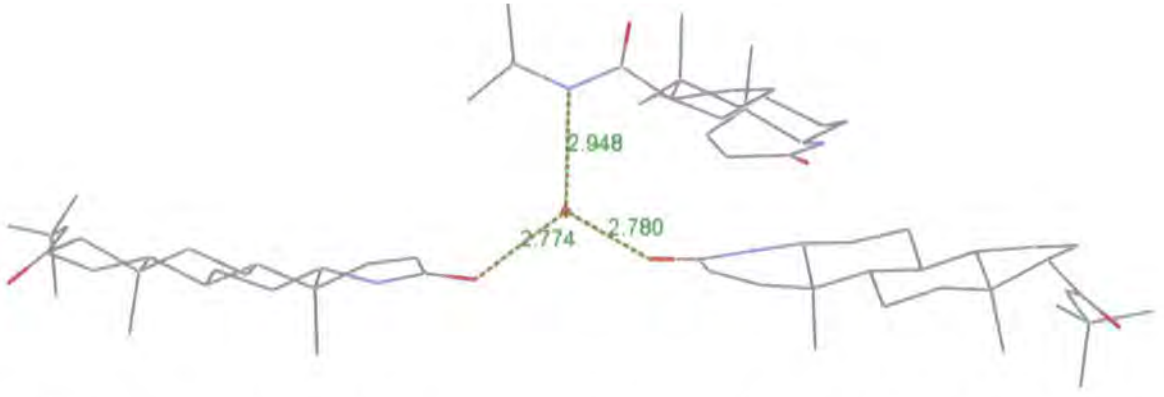

Figure 4.50. Hydrogen bonding between water and finasteride molecules in bis-finasteride monohydrate solvates.

4.4.3 NMR and Thermal Analysis Characterisation

The ^{13}C CPMAS NMR spectra for the IPA, dioxane, THF and THF-water (sample#2) solvates are shown in Figure 4.51 , Figure 4.52 and Figure 4.53, respectively. The spectra confirmed the uniqueness of each form by the presence of peaks assigned to the solvents. The assignments were based on solution-state chemical shifts for the IPA and dioxane solvates. In the case of the THF solvate, a ^{13}C direct pulse (DP) NMR spectrum (Figure 4.54) was obtained to determine the mobile component peaks. The ^{13}C CPMAS spectrum for the THF sample with additional water (sample#2) was found to be the same as that of the first sample of the THF solvate (without water in the preparation). It can be concluded that the addition of water does not affect the formation of the THF solvate.

Distinct ^{1}H MAS NMR spectra for each of prepared solvates were observed, as shown in Figure 4.55, Figure 4.56 and Figure 4.57. The peaks due to the solvents were assigned according to solution-state results.

Since the solvents cannot be quantified from single crystal XRD analysis, quantitative solution-state ^{1}H NMR experiments were carried out for each of the prepared samples. A water spiking procedure was used for the determination of the water peak in the spectra. In cases where the

water peak is overlapped with other genuine finasteride peaks, the quantitation was done by subtractions (after spiking integral minus normal spectrum integral).

In the case of the IPA solvate (Table 4.10), the calculated ratio of water can be inaccurate since the signals for the OH protons from IPA and water are overlapped. The IPA peak at 1.2 ppm was not used in the calculation because of interference from finasteride peaks in that region. As per the ratio of 0.5 for both IPA and water the expected TGA loss is 9.5% which is close to the observed loss of 9.8 % (Figure 4.58).

Table 4.10. Quantitative analysis obtained from solution-state ^{1}H NMR for the IPA solvate.

Chemical shift/ δ_H	Solvent/ assignment	Integral	Molar ratio/ finasteride
4.04	IPA/ CH(septet)	0.55	0.55
~ 1.9	Water+ OH of IPA(broad)	1.24-0.55=0.69*	0.3

* The water peak was overlapped with peaks of finasteride. After spiking of water the peak was resolved, hence the integral was subtracted.

For the dioxane hydrate solvate case (Table 4.11), as per the ratios of 0.7 of dioxane and 0.4 of water, the expected TGA loss is 15.6% while the observed loss is 13.2 % (Figure 4.59). The % loss expected according for a 0.5 ratio of both components is 12.5.

Table 4.11. Quantitative analysis obtained from solution-state ^{1}H NMR for the dioxane solvate.

Chemical shift/ δ_H	Solvent/ assignment	Integral	Molar ratio/ finasteride
3.70	dioxane/ CH_2(septet)	5.9	0.7
1.9	water	2.10-1.36= 0.74*	0.4

*The water peak was overlapped with peaks of finasteride. After spiking of water the peak was resolved, hence the integral was subtracted.

In the same manner, the THF solvate was examined (Table 4.12). As per the ratios calculated, the TGA loss is expected to be 14.1% while the observed loss is 13.0 %(Figure 4.60). However, the theoretical %TGA loss for a 0.5 ratio of both components is 10.8.

Table 4.12. Quantitative analysis obtained from solution-state ^{1}H NMR for the THF solvate.

Chemical shift/ δ_H	Solvent/ assignment	Integral	Molar ratio/ finasteride
1.85	THF/ CH_2(multiplet)	2.62	0.7
3.74	THF/ CH_2O(multiplet)	2.61	0.7
1.9	water	2.36-1.10= 1.26*	0.6

*The water peak was overlapped with peaks of finasteride. After spiking of water the peak was resolved, hence the integral was subtracted.

From the above, it is realised that the observed TGA loss% for both the IPA solvate and the THF-ethyl acetate solvate (ethyl acetate sample #1) is close, within experimental error, to the expected loss calculated on the bases of the ^{1}H NMR data and a 0.5 ratio of solvent and water (Table 4.13). In the ethyl acetate hydrate solvate case, the loss expected for a 0.5 ratio is higher by about 2% than the observed and that calculated according to the ^{1}H NMR data. On the other hand for the dioxane and THF solvates, the loss expected according to the ^{1}H NMR data is higher than the others because the ratio of dioxane was calculated to be 0.7 rather than 0.5. The diethyl ether solvate is shown to be out of the trend as the expected loss% calculated on a 0.5 ratio is significantly lower than the observed

loss but the observed loss is almost similar to the loss due to 2 molecules of diethyl ether and one molecule of water (2:2:1 of finasteride: diethyl ether: water) which is 18.2%.

It is worth mentioning here that the molecular weight range for all the examined solvates is between (60.1-88.1 g/ mol), where the molecular weights of dioxane and ethyl acetate are similar (88.10 and 88.11 g/ mol, respectively) and the molecular weights of THF and diethyl ether are close (72.11 and 74.0 g/ mol, respectively).

Table 4.13. TGA data comparison for the prepared finasteride solvates.

sample	Observed TGA loss%	Expected TGA loss% as per solution-solution-sate experimental results	Expected TGA loss% as per 0.5 ratio of solvent and water
Diethyl ether solvate	17.9	-	10.9
Ethyl acetate sample#1 (THF +ethyl acetate)	10.8	10.5	10.8(THF + water alone)
Ethyl acetate solvate	10.3	10.6	12.5
IPA solvate	9.8	9.3	9.5
Dioxane solvate	13.2	15.6	12.5
THF solvate	13.0	14.1	10.8

A distinct DSC thermogram was obtained for each solvate (Figure 4.61, Figure 4.62 and Figure 4.63). The thermograms obtained for the dioxane and THF solvates (Figure 4.62 and Figure 4.63) were similar to that of the ethyl acetate solvate except that the broad-minor endothermic event is shifted to higher temperatures (from about 45.8 °C to 76-77 °C). An interesting DSC thermogram for the IPA was obtained where two endothermic events seen at 68.8 °C and 102.2 °C. It can be concluded for this result that the escape of IPA and water from the crystals is not simultaneous which means that a purely hydrate form may intervene and thus can be synthesised. The same conclusion can be obtained from the TGA thermogram (Figure 4.58) of the IPA where two merged steps were observed. To check this phase transformation, variable temperature experiment either on the solid-state NMR or on the XRPD should be carried out.

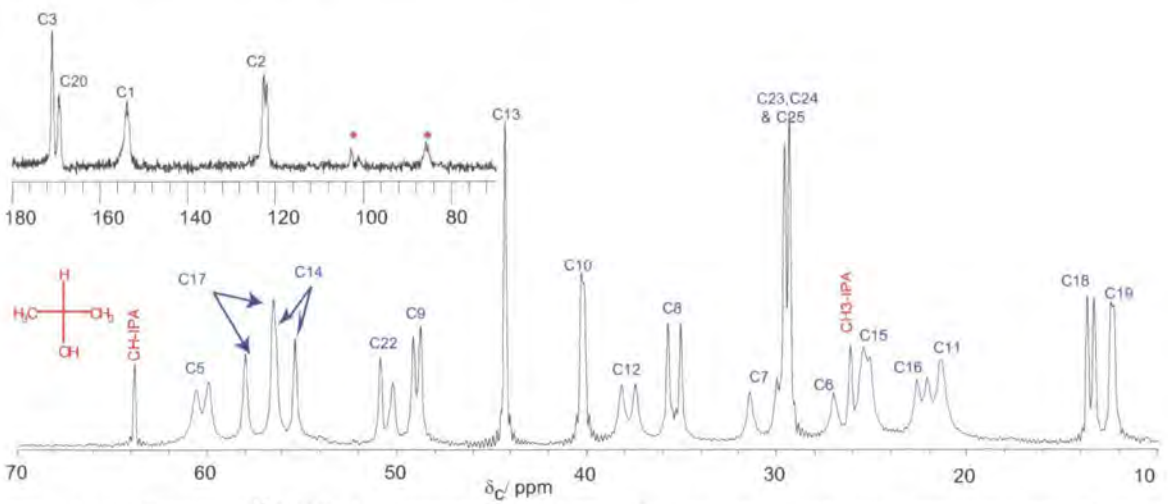

Figure 4.51. Obtained ^{13}C CPMAS spectrum for the IPA solvate. Asterisks represent spinning side bands. The spectrum was acquired for 40 ms with proton decoupling power of 55 kHz.

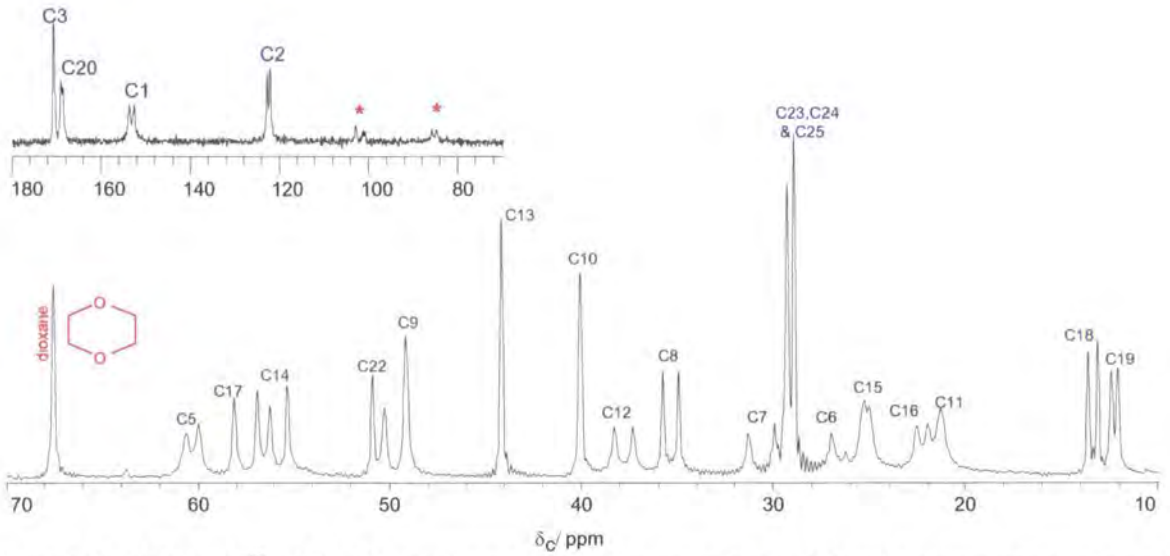

Figure 4.52. Obtained ^{13}C CPMAS spectrum for the dioxane solvate. Asterisks represent spinning side bands. The spectrum was acquired for 40 ms with proton decoupling power of 58 kHz.

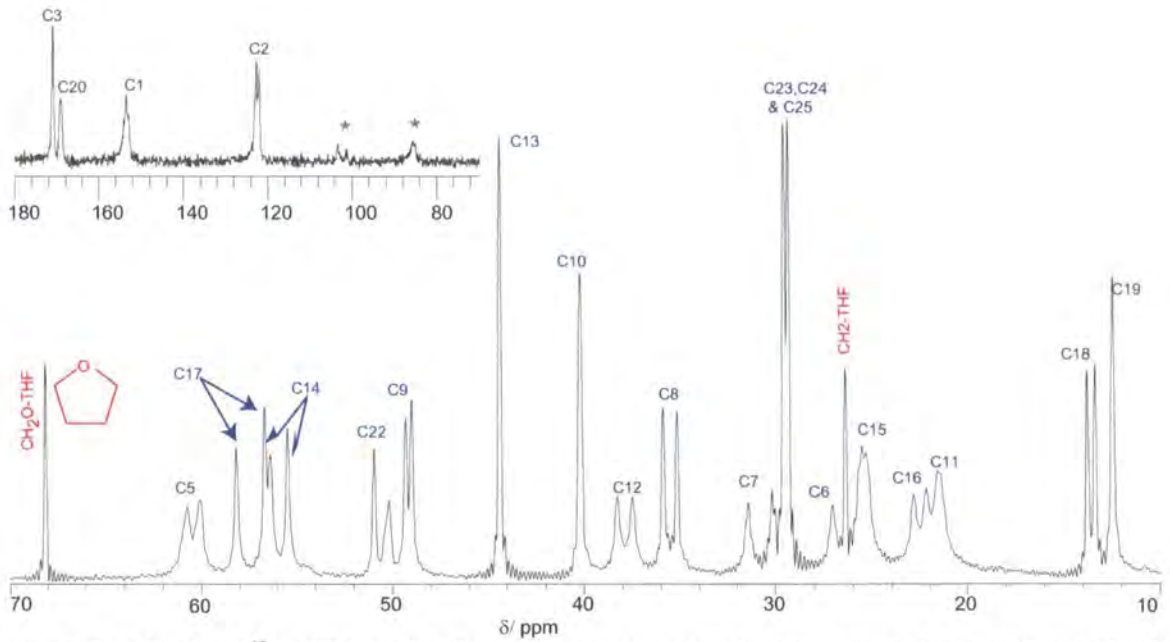

Figure 4.53. Obtained ^{13}C CPMAS for the THF solvate. Asterisks represent spinning side bands. The spectrum was acquired for 40 ms with proton decoupling power of 55 kHz.

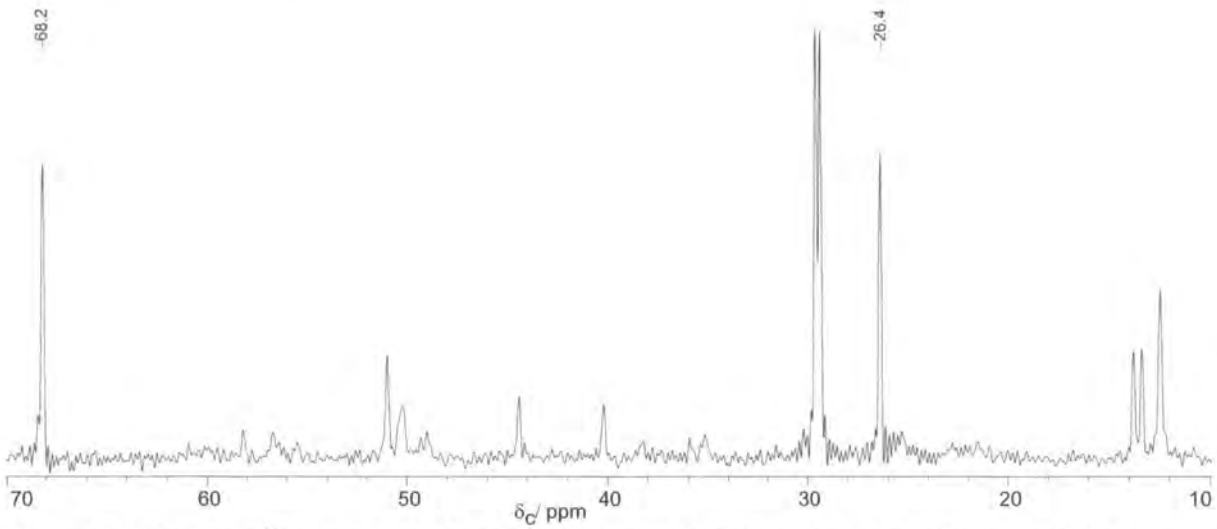

Figure 4.54. Obtained ^{13}C direct pulse (DP) NMR spectrum for the THF solvate. Chemical shifts were shown for peaks due to the THF solvate.

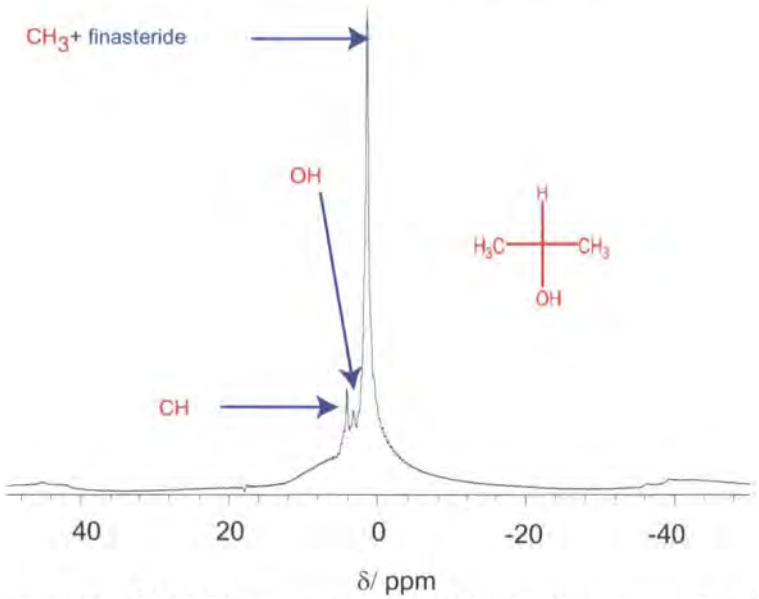

Figure 4.55. Fast MAS ^{1}H NMR spectrum obtained for the IPA solvate. The MAS rate is 20 kHz.

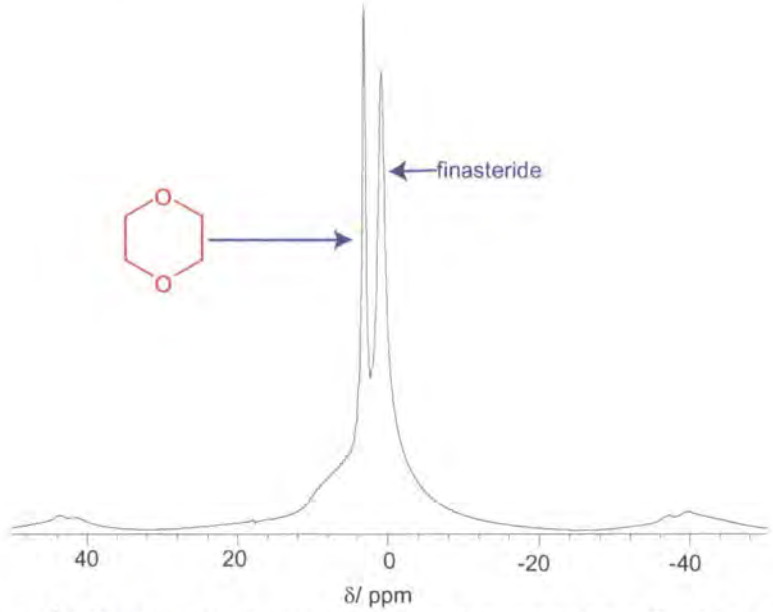

Figure 4.56. Fast MAS ^{1}H NMR spectrum obtained for the dioxane solvate. The MAS rate is 20 kHz.

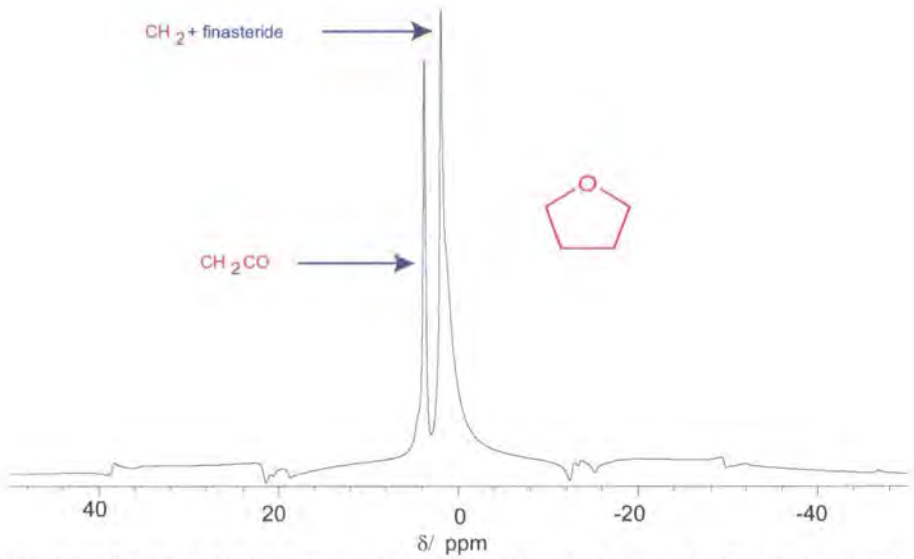

Figure 4.57. Obtained ^{1}H MAS NMR spectrum for the THF solvate sample. The MAS rate is 8.5 kHz.

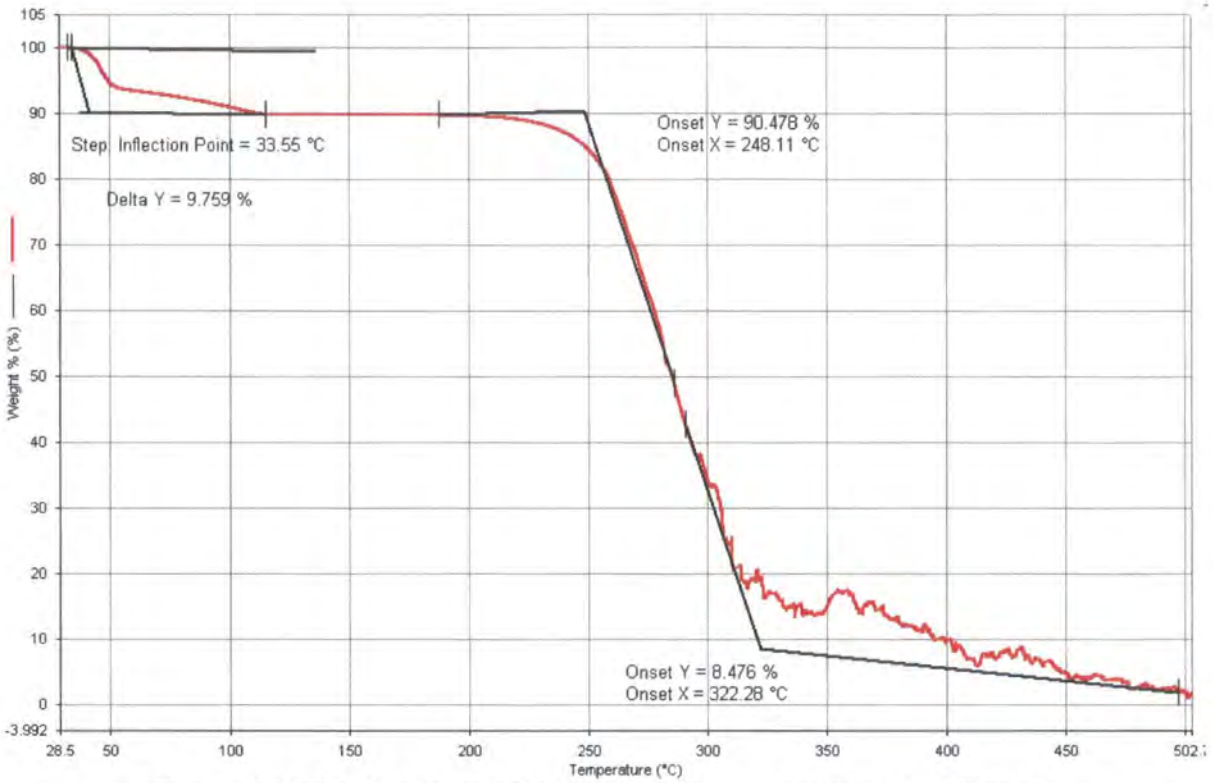

Figure 4.58. TGA thermogram for the IPA solvate at a heating rate of 2°C/ min.

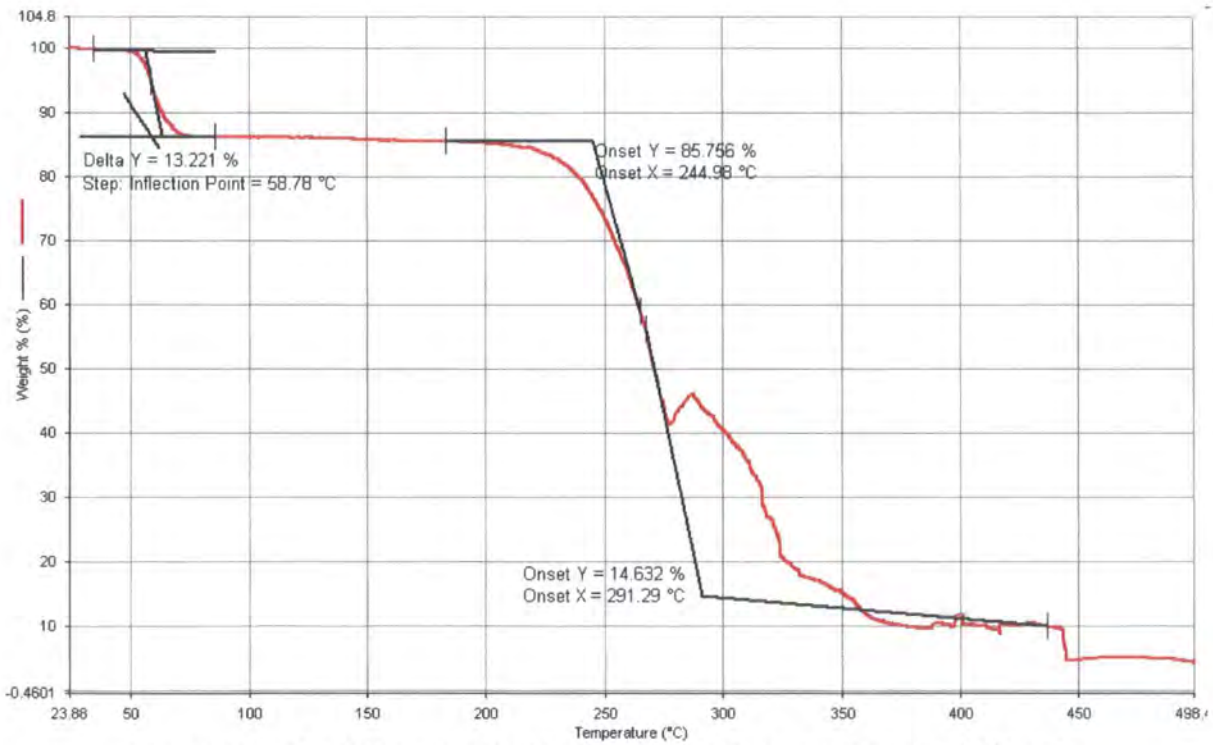

Figure 4.59. TGA thermogram for the dioxane solvate at a heating rate of 2°C/ min.

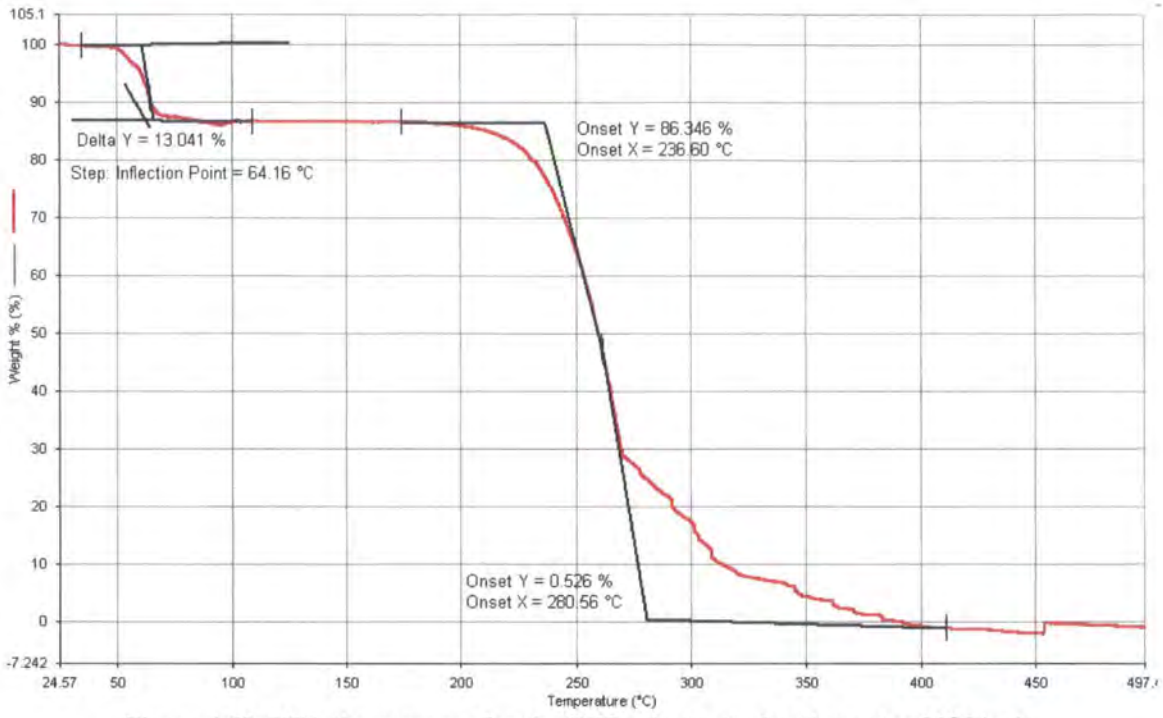

Figure 4.60. TGA thermogram for the THF solvate at a heating rate of 2°C/ min.

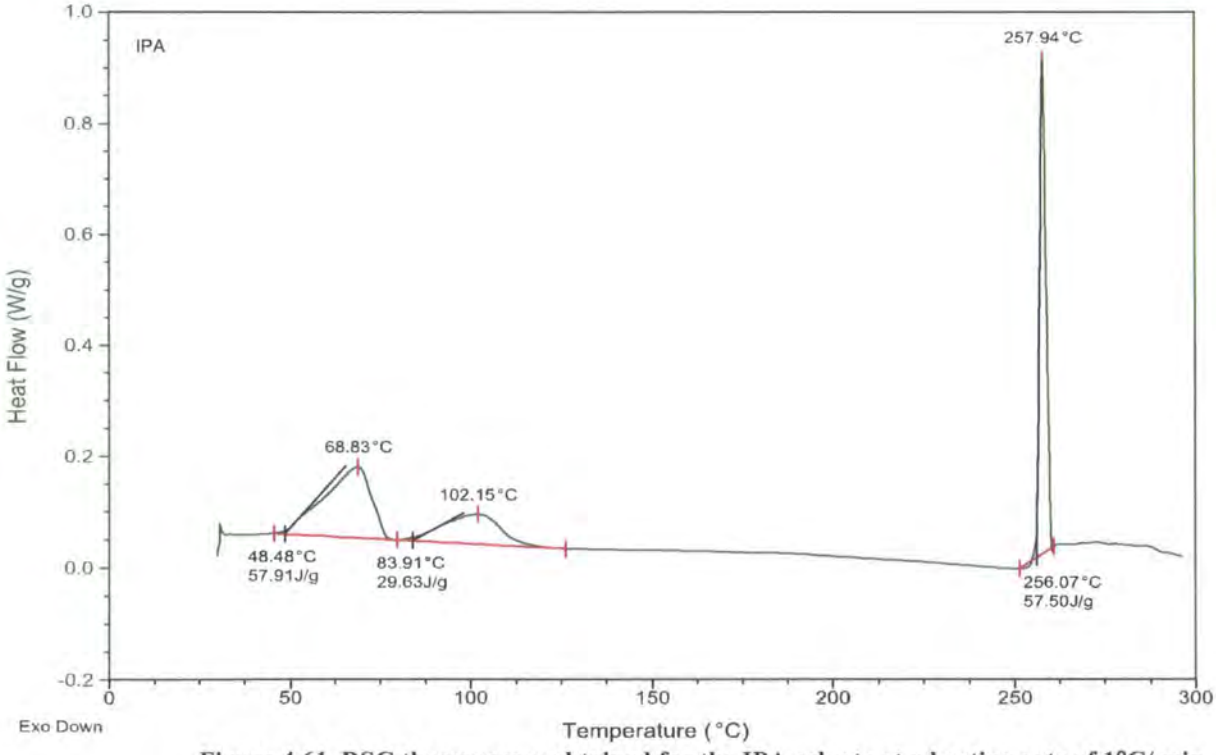

Figure 4.61. DSC thermogram obtained for the IPA solvate at a heating rate of 1°C/ min.

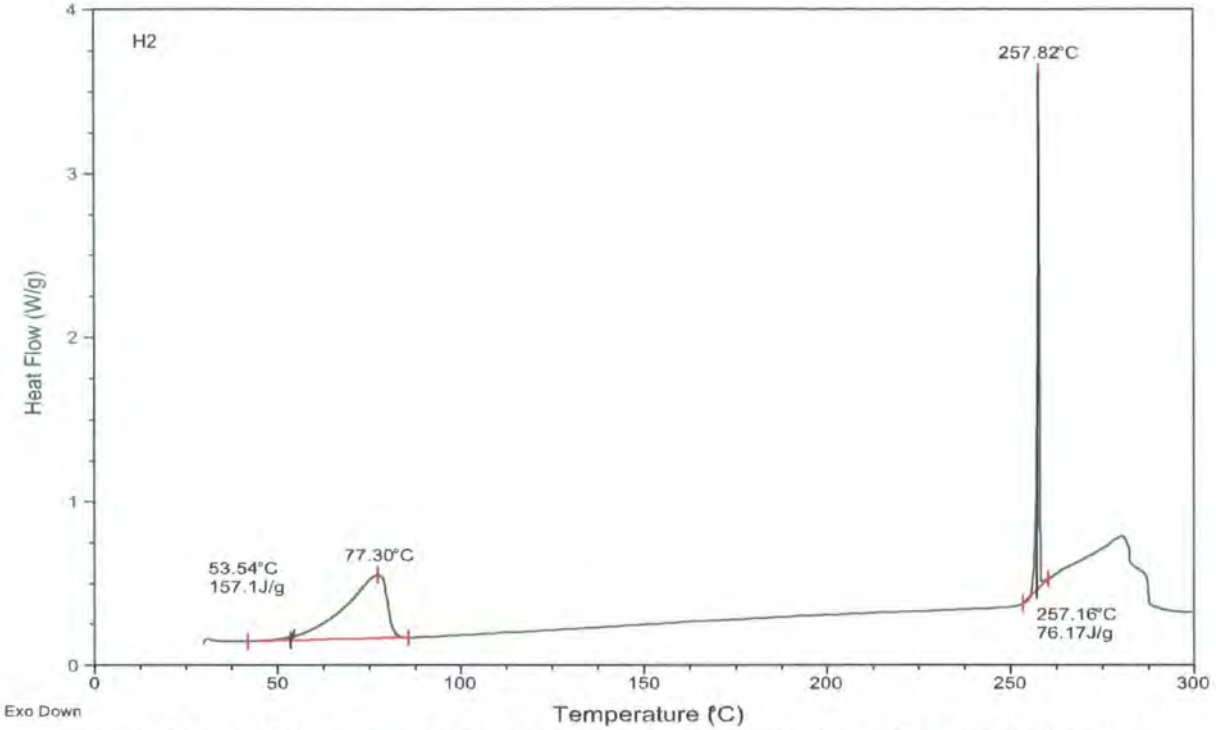

Figure 4.62. DSC thermogram obtained for the dioxane solvate at a heating rate of 1°C/ min.

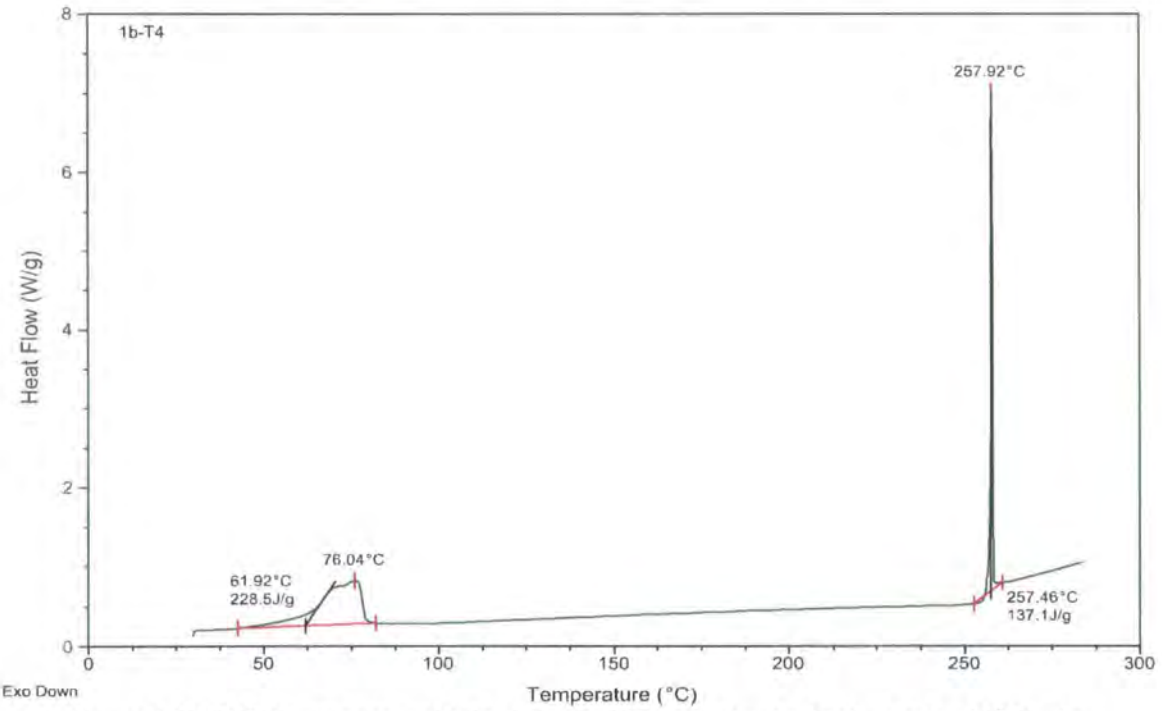

Figure 4.63. DSC thermogram obtained for the THF solvate at a heating rate of 1°C/ min.

4.5 Characterisation of form X

An unknown sample was shown, by ^{13}C CPMAS NMR (Figure 4.65) and XRPD (Figure 4.64), to be a mixture of form I, form II and an additional phase. No information is available about the preparation of this sample except that the sample was stored for several years at RT. Peaks matching those of the reported "form III" in the patent are found in the observed pattern (Table 4.14) of this sample, though some of the peaks are overlapped with the calculated peaks of both forms I and II. This agreement in 2θ values is the same as in the case of the prepared form III trial#2. Nevertheless, the ^{13}C CPMAS NMR spectra for the two samples are different. The ^{13}C CPMAS NMR spectrum for this new form (form X) suggests that it has one molecule in the asymmetric unit. Consequently, the ^{13}C chemical shifts of form X were compared with form I since both are similar in this aspect. This form is either a new anhydrous form or a new hydrate form since the solution-state ^{13}C NMR spectrum of this sample showed no extra peaks. The existence of water in the sample (hydrate) was not fully investigated. The solution-state ^{1}H NMR spectrum did not show any clear contribution of water.

The following were found when comparing form I and form X chemical shifts (Table 4.15) with the solution-state chemical shifts; C1, C2, C3, C7, C8, C18 and C20 have the same chemical shifts difference trend though variations of more than 1 ppm are seen between the two forms. Among these carbons C3 is more deshielded in form X than for form I which indicates that the carbonyl group of the lactam side in form X is forming a stronger hydrogen bonding than form I. Also, C20 is deshielded more in form X which might suggest that the peptide group side is involved in hydrogen bonding, unlike the case of form I. C10 has a similar chemical shift difference in both cases, while C11, C13, C14 and C17 are steady in all three cases (along with the solution-state shifts). C9, C12 and the t-butyl group carbons are more deshielded in form X than form I. In fact, the t-butyl group carbons in form I have a similar chemical shift for that of the solution state, which further suggests the involvement of the peptide group in hydrogen bonding. On the contrary; C5, C19 and C22 are more deshielded in form I than in form X. However, for the last two sets of carbons form X has a similar trend as in the prepared solvates case (Table 4.18) where the chemical shifts are more deshielded than form I. Consequently, it can be suggested that although the prepared solvates and form X are different in number of molecules in the asymmetric unit, they might be similar in the hydrogen bonding profile. For C6, C15 and C16 the comparison was not established since they were not assigned properly for form X due to lack of resolution.

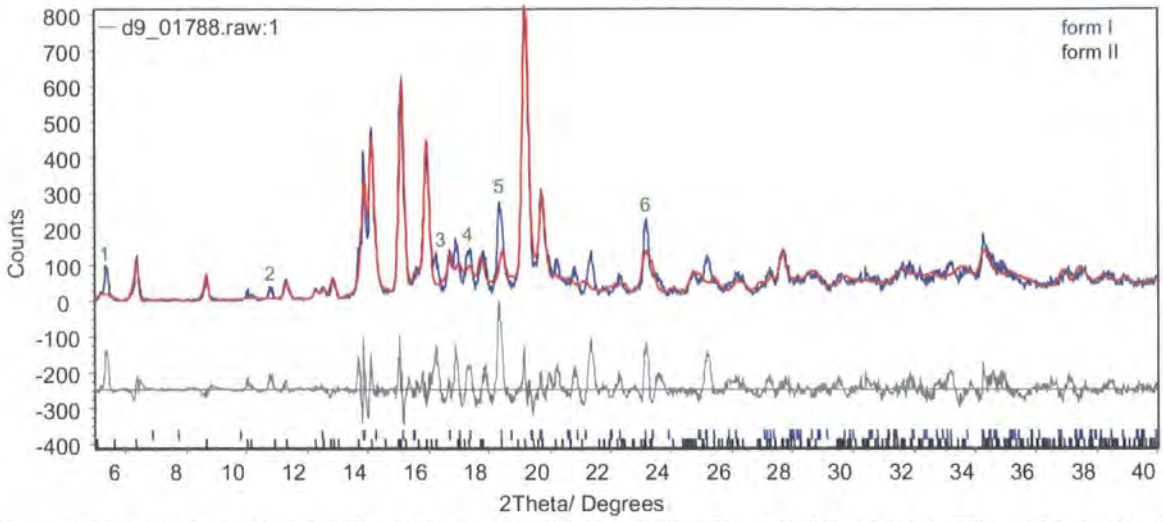

Figure 4.64. Diffractogram for the mixture sample containing form X (blue trace). The red trace is the calculated powder pattern for forms I and II. Numbered peaks match with the reported peaks for the claimed "form III".

Table 4.14. Distinct 2θ values of form X compared with the reported values.

Peak number	2θ values/ d-spacings of numbered peaks	Corresponding 2θ values/ d-spacings of form III[4,5]
1	5.4/16.36	5.3/ 16.67
2	10.7/ 8.29	10.7/ 8.29
3	16.2/ 5.52	16.1/ 5.56
4	17.3/ 5.18	17.2/ 5.21
5	18.3/ 4.90	18.2/ 4.93
6	23.1/ 3.92	23.0/ 3.94

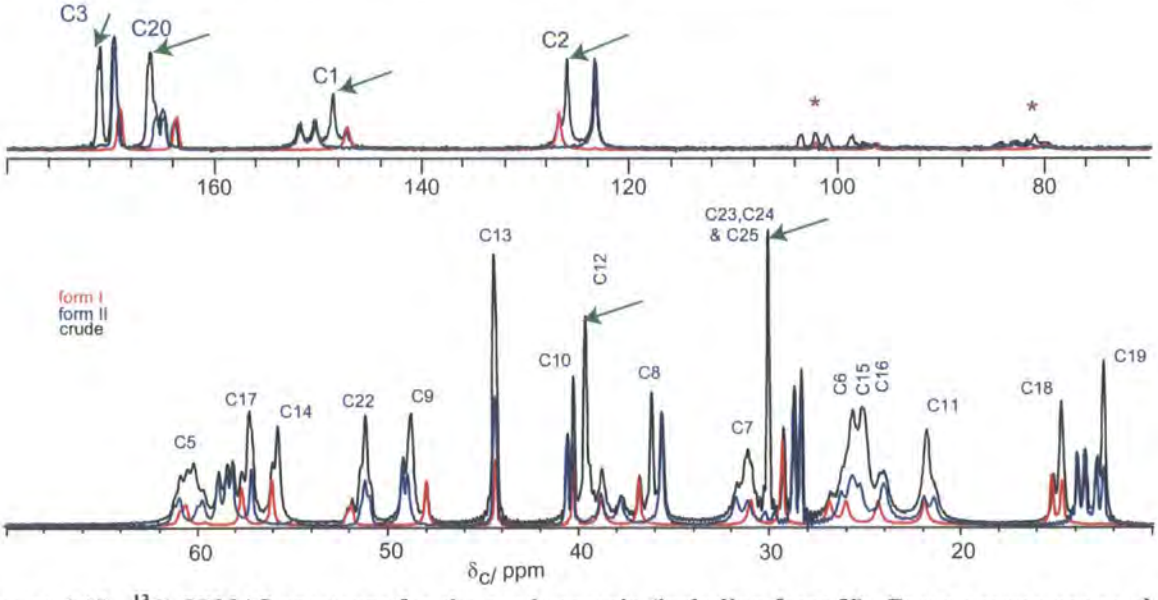

Figure 4.65. ^{13}C CPMAS spectrum for the crude sample (including form X). Green arrows are used to show the distinct peaks due to form X. Asterisks represent spinning side bands.

Table 4.15. ^{13}C chemical shifts (δ_C/ ppm), giving a comparison between solution-state, form I and form X. The differences between solution state and the two other forms solid-state chemical shifts are given in parentheses ($\delta_{solution\ state} - \delta_{solid\ state}$). Differences smaller than 0.5 are omitted from the table.

Carbon number	Solution State ($CDCl_3$)	Form I	Form X
1	151.11	146.9(4.2)	148.6(2.5)
2	123.25	126.9(-3.7)	126.1(-2.9)
3	166.89	169.3(-2.4)	171.1(-4.2)
5	59.88	60.6(-0.7)	60.3
6	26.12	26.8(-0.7)	25.2 or 25.8
7	29.66	30.6(-0.9)	31.2(-1.5)
8	35.54	36.8(-1.3)	36.2(-0.6)
9	47.82	48.0	48.9(-1.1)
10	39.62	40.2(-0.6)	40.3(-0.7)
11	21.48	21.9	21.7
12	38.66	38.8	39.7(-1.0)
13	44.16	44.3	44.5
14	55.87	56.1	55.8
15	24.51	26.0(-1.5)	25.2 or 25.8
16	23.46	24.3(-0.8)	25.2 or 25.8
17	57.67	57.6	57.3
18	13.53	15.2(-1.7)	14.8(-1.3)
19	12.24	14.7(-2.5)	12.5
20	171.84	164.3(7.6)	166.4(5.4)
22	51.33	51.9(-0.6)	51.2
23,24 and 25	29.28	29.3	30.1(-0.8)

4.6 Comparative study on finasteride solid forms

The solvent molecules in all solvates were severely disordered inside channels of the crystal structure showing large indistinguishable electron density distribution. However, the ^{13}C CPMAS NMR spectra show considerable differences (Figure 4.66). This fact shows that solid-state NMR can be significantly more sensitive than diffraction experiments, especially when rapid motion or disorder occurs in part of a crystal unit cell.

The differences in chemical shifts of form I from these of the solution state are in agreement with those reported in the literature[1,2]. The significant differences found for carbons sited at ring A were attributed to the involvement of the ring with strong hydrogen bonding which comes from the lactam group side[1,2]. The differences in the assignment of C3 and C20 between solution and solid states were explained[2] by the fact that the carbonyl carbon is deshielded the more it is participating in hydrogen bonds[8].

Peaks due to C9, C19 and the t-butyl group do not show big large differences in chemical shifts among the hydrate solvates but they show variable patterns, where the degree of splitting of the two peaks changes. In a similar manner the C14 and C17 peaks occasionally show four peaks (2 peaks

each) or tend to show triplets(IPA and THF). C22 show two peaks, with the first one being broader. Large variations in the chemical shifts of C1 in all solid forms are found, specifically between from I and II about 3 ppm, but in the solvates case it is even more deshielded (about 2 ppm difference from form II). C3 is more deshielded in the solvates case than for the two anhydrous forms. This change is due to the bigger contribution of the lactam carbonyl in hydrogen bonding in the solvates since they form additional hydrogen bonds with the water molecules. C20 is found to be more deshielded in all solvates than for the two anhydrous forms, where it is known that the carbonyl (from the peptide side) is not contributing to hydrogen bonding. As in the crystal structure of the hydrate solvates, it is expected that C20 is deshielded because of hydrogen bonding with bridging water molecules. Most other peaks have close chemical shifts for all the hydrated solvates.

Preliminary proton spin-lattice relaxation measurements were done on the solvates and on form II (anhydrous). The experiments were carried out at ambient temperature using the 5 mm probe, except for the acetic acid solvate where the 2.5 mm probe was used. The relaxation parameters (T_1) are, within experimental error, the same for both solvent and "host" Table 4.20. The values are also indistinguishable for the solvated and anhydrous forms (form II). This suggests that the relaxation is driven by reorientation of the methyl groups rather than by solvent dynamics.

Stability and phase transformation of the prepared solvates are of interest. A variable (high) temperature experiment was performed on the dioxane solvate, probing the ^{13}C CP MAS spectra (Figure 4.67). At each set temperature, the probe was left for 15 minutes for thermal equilibration and the ^{13}C spectra were 10 minutes long. Saturation recovery experiments were performed at each temperature to calculate T_1 relaxation coefficient under spinning and static conditions. The later relaxation experiments are not reported since the results were found to be not useful. However, the time spent at each temperature point was about 45 minutes. The temperature was increased as shown in Figure 4.67 and the ^{13}C spectrum was checked in the end at ambient temperature. Phase transformation starts at 100°C to the anhydrous form I, and almost all of the dioxane solvate is transformed by 125°C. The water molecules seem to escape simultaneously with the dioxane since no intermediate (between the dioxane solvate and form I) finger print was observed. The post ^{13}C spectrum indicated, as expected, that the transformation from the dioxane solvate to form I is irreversible. It was reported that form I undergoes transformation to form II at higher temperature (about 150 °C) [7]. It was also reported that form II can be prepared by sublimation of the ethyl acetate solvate at about 235 °C and thermal decomposition of the acetic acid solvate occurs at about 175 °C.

Table 4.16. Crystallographic data on finasteride solid forms

Form ID	Form I[1]	form II[1]	acetic acid solvate[7]	ethyl acetate solvate[7]	IPA Solvate[a]	Dioxane Solvate[a]	THF Solvate[a]
Formula	$C_{23}H_{36}N_2O_2$	$C_{23}H_{36}N_2O_2$	finasteride. CH_3COOH	2finasteride. $H_2O.C_4H_8O_2$	2finasteride. H_2O. C_3H_8O	2finasteride. H_2O. $C_4H_8O_2$	2finasteride. H_2O. C_4H_8O
FW	372.6	372.6	432.6	851.2	795.2	823.2	807.2
Lattice Symmetry	orthorhombic	monoclinic	monoclinic	orthorhombic	orthorhombic	orthorhombic	orthorhombic
Space group	$P2_12_12_1$	$P2_1$	$P2_1$	$P2_12_12_1$	$P2_12_12_1$	$P2_12_12_1$	$P2_12_12_1$
a (Å)	6.437(1)	16.387(2)	12.170(l)	8.173(3)	8.1132(3)	8.1110(7)	8.1317(3)
b (Å)	12.712(1)	7.958(2)	8.16521(7)	I8.364(6)	17.9012(8)	18.0856(16)	17.7767(7)
c (Å)	25.929(1)	18.115(5)	13.577(l)	35.65(2)	35.6948(15)	35.512(3)	35.7349(15)
α (°)	90	90	90	90	90	90	90
β (°)	90	107.25(2)	111.630(1)	90	90	90	90
γ (°)	90	90	90	90	90	90	90
Z	4	4	2	4	4	4	4
Z'	1	2	1	2	2	2	2
Unit cell volume ($Å^3$)	2121.7(6)	2256(2)	1254.1(2)	5350(4)	5184.17	5209.34	5165.65
CSD code	WOLXOK02, WOLXOK01	WOLXOK03, WOLXOK[b]	WOLXEA	WOLXIE	To be published	To be published	To be published
Melting Point (°C)	253-256	253-256	255-257	252-255	257	257	257

[a] Obtained at low temperature XRD.
[b] The XRD data was poor in this case

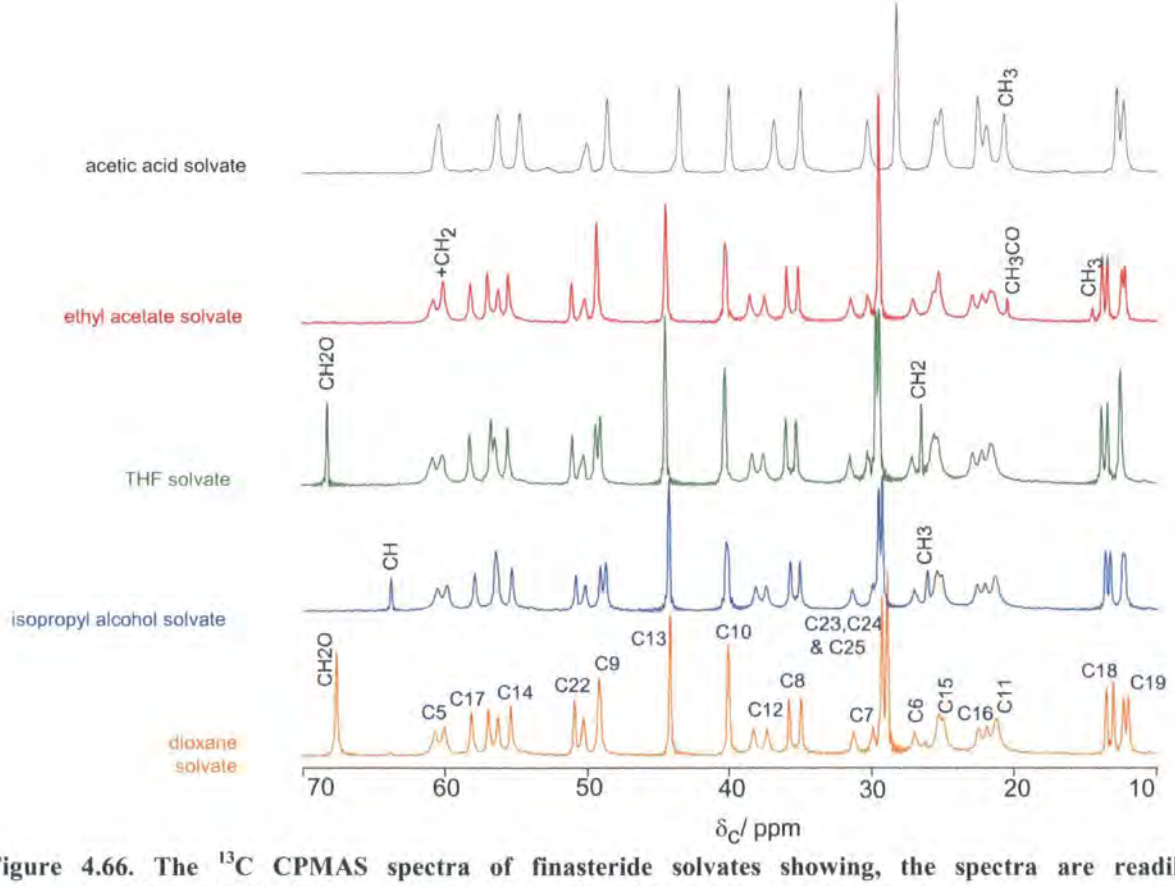

Figure 4.66. The ^{13}C CPMAS spectra of finasteride solvates showing, the spectra are readily distinguished. The low field part of the spectra (carbonyl region) are not shown.

Table 4.17. ^{1}H NMR chemical shifts for examined finasteride solid forms.

Sample	Chemical shift δ_C/ ppm	assignment	Line width at half height(Hz)	MAS condition
IPA	1.4	Finasteride+ IPA CH_3	279	20 kHz at 2.5mm probe
	3.4	IPA-CH	203	
	4.2	IPA-OH	160	
Dioxane	1.0	finasteride	730	
	3.2	Dioxane-CH_2	342	
Acetic acid	-0.1	Acetic acid-CH_3	126	
	1.1	finasteride	473	
	13.3	Acetic acid-OH	502	
THF solvate	1.8+ shoulder at ~1.2	Finasteride+ THF-CH_2	310	8.5 kHz at 5mm probe
	3.7	THF-CH_2O	170	
Ethyl acetate solvate	1.2	Finasteride+ ethyl acetate-CH_3	299	
	2.0	ethyl acetate-CH_3O	110	
	4.2	CH_2	204	
Form II	1.2	finasteride	868	

Table 4.18. Obtained chemical shifts (δ_C/ ppm) for finasteride solid forms. The differences between solution state and solid state chemical shifts of form I are given in parentheses ($\delta_{\text{solution state}} - \delta_{\text{solid state}}$). The differences smaller than 0.5 are not shown in the table.

Carbon Number	Solution State ($CDCl_3$)	Form I	Form II	Dioxane solvate	IPA solvate	THF Solvate	Ethyl acetate solvate	Acetic acid solvate
1	151.11	146.9(4.2)	150.4/151.9	152.5/153.5	154.0 [b]	153.5 [b]	152.8/ 153.7	153.0 [b]
2	123.25	126.9(-3.7)	123.3	122.1/122.7	122.0/122.6	122.1/122.8	122.3/ 122.87	120.9 [b]
3	166.89	169.3(-2.4)	169.7	170.5	170.9	171.0	171.0	170.1
5	59.88	60.6(-0.7)	59.6/60.9	59.9/60.6	59.9/ 60.5	60.1/ 60.8	60.1°/ 60.8	60.4
6	26.12	26.8(-0.7)	26.6	27.0	27.1	27.2	27.1	25.6
7	29.66	30.6(-0.9)	31.1/31.7	29.9/31.3	30.0/ 31.5	30.3/ 31.5	30.3/ 31.5	30.3
8	35.54	36.8(-1.3)	35.6	34.9/35.7	35.1/ 35.8	35.2/ 35.9	35.1/ 35.9	35.0
9	47.82	48.0	48.9/49.2	49.1	48.8/ 49.2	49.1/ 49.4	49.3	48.6
10	39.62	40.2(-0.6)	40.3/40.6	40.0	40.3	40.3	40.3	40.0
11	21.48	21.9(-0.5)	21.3/21.9	21.4[b]	21.4 [b]	21.6 [b]	21.5/ 21.7	22.0
12	38.66	38.8	37.7/38.7	37.3/38.4	37.5/ 38.2	37.5/ 38.5	37.5/ 38.6	36.8
13	44.16	44.3	44.3	44.1	44.3	44.4	44.5	43.5
14	55.87	56.1	57.1/58.1	55.3/56.2	55.4/ 56.5	55.5/ 56.4	55.5/ 56.2	54.7
15	24.51	26.0(-1.5)	25.6	25.1/25.3	25.2/25.5	25.7 [b]	25.3/ 25.7	25.2
16	23.46	24.3(-0.8)	24.0/25.2	22.0/22.6	22.1/ 22.7	22.3/ 22.9	22.3/ 23.0	22.6
17	57.67	57.6	58.3/58.8	56.9/58.2	56.5/ 58.0	56.7/ 58.1	57.0/ 58.2	56.3
18	13.53	15.2(-1.7)	13.5/13.9	13.2/13.6	13.7/ 13.4	13.4/ 13.9	13.5/ 13.9	12.8
19	12.24	14.7(-2.5)	12.5/12.9	12.1/12.3	12.4[s]	12.5 [i]	12.3/ 12.5	12.4
20	171.84	164.3(7.6)	164.9/165.7	168.6,169.0	169.4 [b]	169.0 [b]	168.8[b]	166.7
22	51.33	51.9(-0.6)	50.9	50.2/50.9	50.2/ 50.9	50.3/ 50.9	50.2/ 51.1	50.0
23,24 and 25	29.28	29.3	28.3/28.7	28.9/29.2	29.3/29.6	29.4/ 29.7	29.5	28.3

[b]: broad peak
[i]: intense peak
[s]: small splitting
[o]: overlapped by the CH_2 of the ethyl acetate
Underlined chemical shifts correspond to the chemical shifts assigned for two carbons

Table 4.19. ^{13}C NMR chemical shifts corresponding to the solvent molecules in the examined finasteride solvates.

Sample	Chemical shift δ_C/ ppm	Assignment
IPA	26.2	CH_3
	63.8	CH
Dioxane	67.5	CH_2
Acetic acid	20.7	CH_3
	174.6	C=O
THF solvate	26.5	CH_2
	68.1	CH_2O
Ethyl acetate solvate	14.5	CH_3
	20.5	CH_3O
	60.1	CH_2
	169.2	C=O

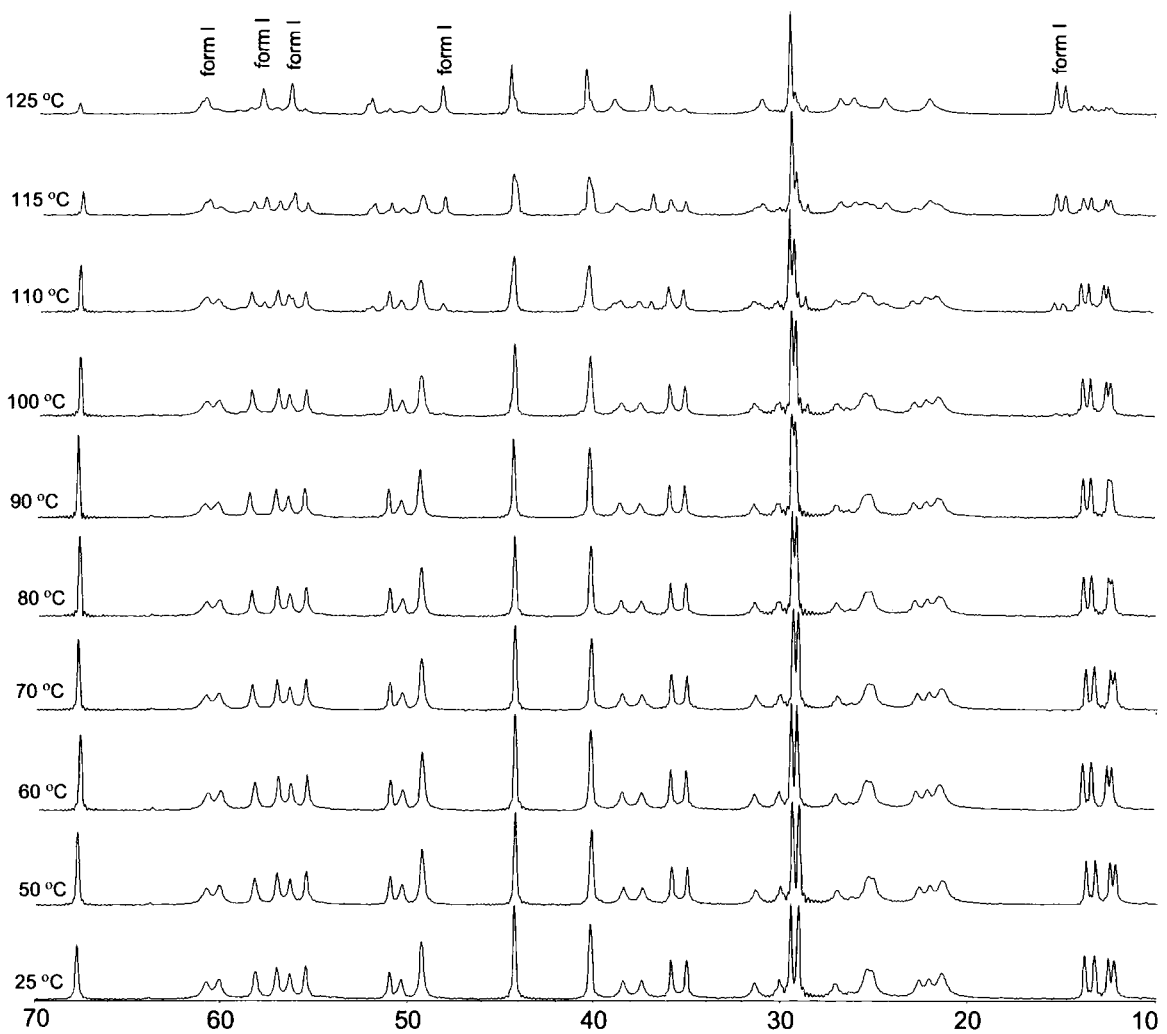

Figure 4.67. ^{13}C CPMAS variable-temperature spectra of the dioxane solvate.

Table 4.20. Proton relaxation measurements obtained under spinning.

Solid form	T_1/ (s) at ambient temperature*		
Dioxane solvate	1.39 ±0.01 (CH_2)	1.36±0.01 (finasteride)	
IPA solvate	1.08±0.02 (CH)	1.10±0.02 (OH)	1.13±0.01 (finasteride+ CH_3)
THF solvate	1.15±0.01 (CH_2O)	1.15±0.01 (finasteride+CH_2)	
Ethyl acetate	1.23±0.01 (**CH_2**CH_3)	1.22±0.01 (CH_3O)	1.20±0.01 (CH_2**CH_3** + finasteride)
Acetic acid solvate	1.12±0.10 (OH)	0.95±0.12 (finasteride)	1.02±0.09 (CH_3)
Form II	0.92±0.01		

*The errors reported in the table are statistical from the plots and the true errors are likely to be larger (general estimate ± 5-10%).

4.7 Conclusions

(i) The methodology reported for the preparation of form III is not reproducible, at least in my hands. It is possible that this "form III" is a solvate of a certain petroleum ether component.

(ii) A diethyl ether solvate was prepared and characterised by XRPD.

(iii) The claimed H1 form in the patent could not be reproduced; in fact each alcohol used leads to different forms.

(iv) The characterisation of finasteride solid forms in the patent by only XRPD led to some deficiencies, while using solid-state NMR the solid forms are readily distinguished.

(v) Three new hydrate solvates were prepared and characterised by XRD and NMR. The solvates were found to be isomorphous. Due to highly disordered solvent molecules the XRD analysis failed to give an estimate of the amount of the included solvent. However, NMR was successively used for this purpose. The data were also compared with the thermal analysis data (TGA).

(vi) A new unknown unsolvated sample was characterised by solid-state NMR.

(vii) An unknown sample was shown, by ^{13}C CPMAS NMR and XRPD, to be a mixture of form I, form II and a third new phase. This new form is expected to be either a new polymorph or a hydrate and it is probably closely related to "form III".

4.8 Future Work

(i) Only a small portion of the diethyl ether solvate sample was prepared. The solvate is to be re-prepared and characterised properly by solid-state NMR.

(ii) Study solvents dynamics inside the solvates by ^{2}H NMR using deuterated samples.

(iii) The two separated DSC events seen for the IPA solvate before melting suggest that a new form can be prepared which can be either a hydrate or an anhydrous IPA solvate.

(iv) As all prepared solvates contained water molecules, trials following a hydrated form are to be carried out.

4.9 References

1. Wenslow RM, Baum MW, Ball RG, McCauley JA, Varsolona RJ 2000. A spectroscopic and crystallographic study of polymorphism in an aza-steroid. J Pharm Sci 89(10):1271-1285.
2. Morzycki JW, Wawer I, Gryszkiewicz A, Maj J, Siergiejczyk L, Zaworska A 2002. C-13-NMR study of 4-azasteroids in solution and solid state. Steroids 67(7):621-626.
3. McCauley JA, Varsolona RJ. 1997. Process for the production of finasteride. United States Patent and Trade Mark Office, ed., US: Merck & Co., Inc.
4. Reddy MS, Rajan ST, Rao MVNB, Vyas K, Reddy SV, Rekha KS. 2005. Novel polymorphic form of 17-beta-(N-ter. butyl carbamoyl)-4-aza-5-alpha-a- ndrost-1-en-3-one and a process for preparing it. United States Patent and Trade Mark Office, ed., US: Dr. Reddy's Laboratories Ltd.
5. Reddy MS, Rajan ST, Rao MVNB, Vyas K, Reddy SV, Rekha KS. 2002. Novel polymorphic form of 17-beta-(N-ter. butyl carbamoyl)-4-aza-5-alpha-a- ndrost-1-en-3-one and a process for preparing it. World Intellectual Property Organization (WIPO), ed.
6. Parthasaradhi R, Bandi, Rathnakar R, Kura , Raji R, Rapolu, Muralidhara R, Dasari, Subash Chander R, Kesireddy. 2004. Novel Crystalline Forms of Finasteride. World Intellectual Property Organization (WIPO), ed.
7. Wawrzycka I, Stepniak K, Matyjaszczyk S, Koziol AE, Lis T, Abboud KA 1999. Structural characterization of polymorphs and molecular complexes of finasteride. J Mol Structure 474:157-166.
8. Ando S, Ando I, Shoji A, Ozaki T 1988. Intermolecular Hydrogen-Bonding Effect on C-13 Nmr Chemical-Shifts of Glycine Residue Carbonyl Carbons of Peptides in the Solid-State. J Am Chem Soc 110(11):3380-3386.

Chapter 5: Solid Forms of Androsterone

5.1 Introduction

Androsterone, $C_{19}H_{30}O_2$; 5α-androstane-3α-ol-17-one, is a male sex hormone (androgen) with functional prostate property. It was proved to be a metabolite of testosterone[1] and has recently been studied as a contributory factor to prostate cancer[2].

Androsterone was chosen for this research as it was structurally a very simple steroid for which literature references suggest the possibility of different solid forms.

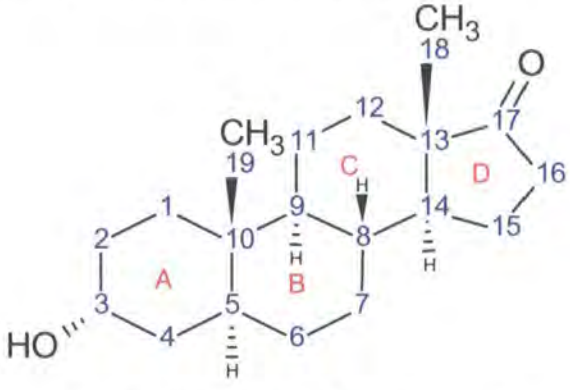

Molecular structure of androsterone

5.2 Literature Review on Androsterone Solid Forms

5.2.1 Androsterone Form 1

Form 1 is the anhydrous form which has been reported in the literature three times. First, the crystal structure (CSD code ANDOON03) was reported by Bernal *et al.*[3] in 1936. Later (in 1966) the crystal structure was redetermined by High *et al.*[4]. Recently, the crystal structure was redetermined again by low temperature single-crystal XRD by Hulme *et al.*[5]. The unit cell parameters and space groups from these studies are shown in Table 5.1. High *et al.*[4] note several unusual geometrical features present in their structure, all of which take more conventional values in the redetermination by Hulme *et al.*[5] . The features are torsion angles between the angular methyl groups, hydrogen bond angle and length and C-C and C-H bond lengths. The differences between the two structural determinations were attributed[5] to the difference in temperature at which the data sets were collected and the superior nature of the determination on a modern diffractometer.

Form 1 crystals were grown by slow evaporation from a solution of ether in the first two references[3,4] while Hulme *et al.*[5] reported their crystals to be grown from slow evaporation from a solution of absolute ethanol.

Form 1 has a melting point of 186°C and it has two symmetry-related molecules (Z=2) in the unit cell bonded head to tail by hydrogen bonding connecting the hydroxyl group (ring A) with the

carbonyl group (ring D) of a second molecule, see Figure 5.1. The crystal structure has a hydrogen bonded chain structure, with the chains propagated parallel to the b crystallographic axis by the 2_1 screw axis, see Figure 5.1.

Table 5.1. Unit cells reported for androsterone form 1.

Reference	CSD Code	Space Group	a (Å)	b (Å)	c (Å)	α (°)	β (°)	γ (°)
Bernal *et al.*[3], 1936	ANDOON03	$P2_1$	9.45	7.70	11.95	90	111	90
High *et al.*[4], 1966	ANDOON	$P2_1$	9.56(2)	7.90(3)	11.78(2)	90	111.37(3)	90
Hulme *et al.*[5], 2006	‡	$P2_1$	9.4045(9)	7.9586(8)	11.6746(12)	90	111.274(2)	90

‡ The crystal structure is not yet included in the database.

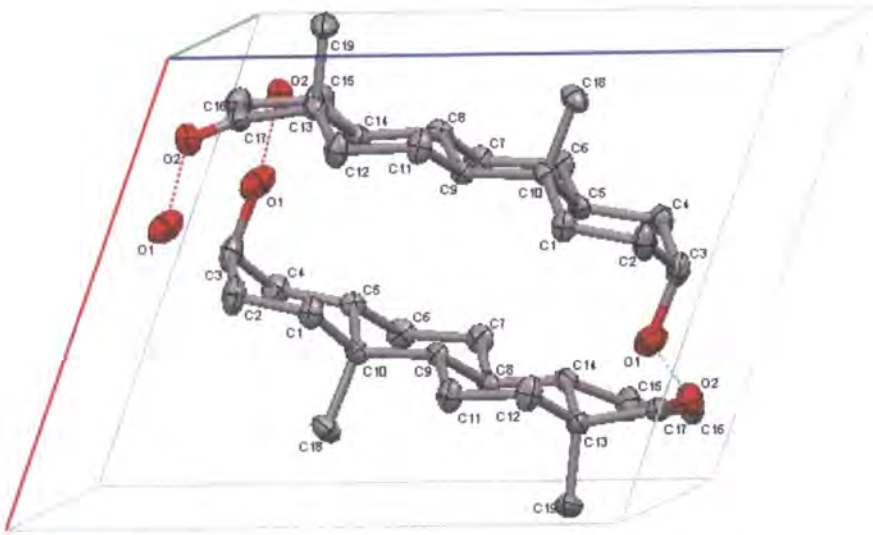

Figure 5.1. Androsterone form 1 crystal structure[5] viewed along the crystallographic *b* axis.

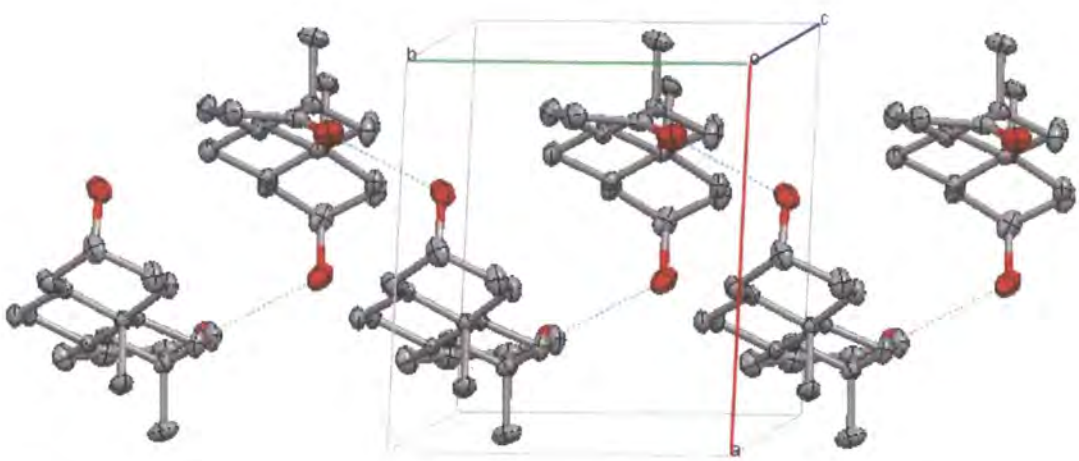

Figure 5.2. Androsterone form 1 crystal structure[5] showing the hydrogen bonding (dotted lines) chain along the crystallographic c axis.

5.2.2 Androsterone Form 2

The unit cell of androsterone form 2 has been reported on two occasions (see Table 5.2), although in neither paper was the full structure determined.

Table 5.2 unit cells reported for androsterone Form 2.

Reference	CSD Code	Space Group	a (Å)	b (Å)	c (Å)	α (°)	β (°)	γ (°)
Banerjee *et al.*[6],1971	ANDOON02	$P2_1/m$	7.20	10.40	22.00	90	100	90
Bouche *et al.*[7],1976	ANDOON01	$P2_1$	7.30	10.40	22.20	90	100	90

A hydrate of androsterone was identified[8] in 1968 by thermal microscopy which desolvated at 80°C. Banerjee *et al.*[6] proposed the possibility of "a second polymorph" of androsterone, and reported a unit cell different to that of form 1, see Table 5.2. The crystals that gave this unit cell were grown from a solution of ether. Bouche *et al*[7]. identified that the crystals grown from ether and dried exhibited an event in the DSC trace at approximately 165°C, which was then followed by the same form 1 melting event at 183-186°C. They identified this as a phase change from a new "Form 2" to Form 1. They also reported that this change could be initiated by grinding. They also suggest this change occurs spontaneously, but slowly, when the "Form 2" crystals are left to stand for a period of time. Because this phase change occurs well above the desolvation temperature of the hydrate, there is no suggestion that this phase change is related to the hydrate. This subtle phase change was not observed by either thermal microscopy or infrared spectroscopy. The thermal behaviour (DSC events) of this new form did not change even after drying the crystals under vacuum for 24 hours. Powder diffraction was used to provide a unit cell reported as" form 2", which on the one hand is different from that of form 1 and the hydrate identified by thermal microscopy[9] and on the other hand concurred with the unit cell published by Banjeree *et al.*[6] for his proposed form 2, see Table 5.2.

The recent work by Hulme *et al.*[10] (next section) shows that this form cannot be reproduced and the unit cell parameters reported correspond to those of a different form (a hemihydrate).

5.2.3 Androsterone Hemihydrate[10]

Kuhnert-Brandstatter *et al.*[9] first identified a hydrate of androsterone by thermal microscopy, desolvating at 80°C. Bouche *et al.* [7] replicated the desolvation of the hydrated form first identified by Kuhnert-Brandstatter *et al.*[9] at 80°C. In this case the crystals were grown by evaporation from 70% ethanol solution at room temperature. Recently, large plate crystals grown from a solution of androsterone in wet ethanol were found to have similar unit cell parameters (Table 5.3) as reported for form 2[6,7] (Table 5.2). However, it was reported by Hulme *et al.*[10] that the structure with this unit cell is a hemihydrate, with two androsterone molecules and a water molecule in the

asymmetric unit. They believe it is likely to be the "hydrate" identified already in the literature[6,7] which desolvates at 80°C and melts at about 185°C (melting point of form 1).

Table 5.3. Unit cell of androsterone hemihydrate.

	Space Group	a (Å)	b (Å)	c (Å)	α (°)	β (°)	γ (°)
Hulme *et al.*[5]	$P2_1$	7.4288(8)	10.289(1)	22.174(2)	90	97.553(2)	90

The water molecules form three strong intermolecular hydrogen bonds between three androsterone molecules; being a donor for two androsterone molecules from their ring D carbonyl group sides and an acceptor from a third molecule from the hydroxyl group side of ring A, see Figure 5.4. The water molecules form another two weak hydrogen bonds of C-H...O type (C65-H65B... O91 and C16-H16A... O91). The two independent androsterone molecules are connected head-to-tail (ring A and ring D) by intermolecular hydrogen bonds O51-H51...O2. The water molecules were found to lie inside a channel along the *a* crystallographic axis (Figure 5.5).

Thermal analysis for androsterone hemihydrate showed that the dehydration takes place between 70-115 °C (shown by the DSC event) along with a mass loss of 3.2% (shown by TGA). These data are close to the dehydration temperature reported in the literature[7,9] and the calculated mass loss of a hemihydrate (3%) respectively. The DSC data reported for the hemihydrate form indicate that it transforms to form 1 after dehydration, which was also reported for the hydrate form in the literature[7]. It was also reported that there is a small endotherm at 150°C between the desolvation and melting point events which was suggested to be the event reported by Bouche *et al.*[7]. The phase transformation to the anhydrous form 1 was further confirmed by variable temperature XRPD, though the there was no evidence of phase transformation at 150°C as seen by DSC[10]. The latter DSC event was suggested to be "a subtle relaxation in the crystal structure of the newly dehydrated phase".

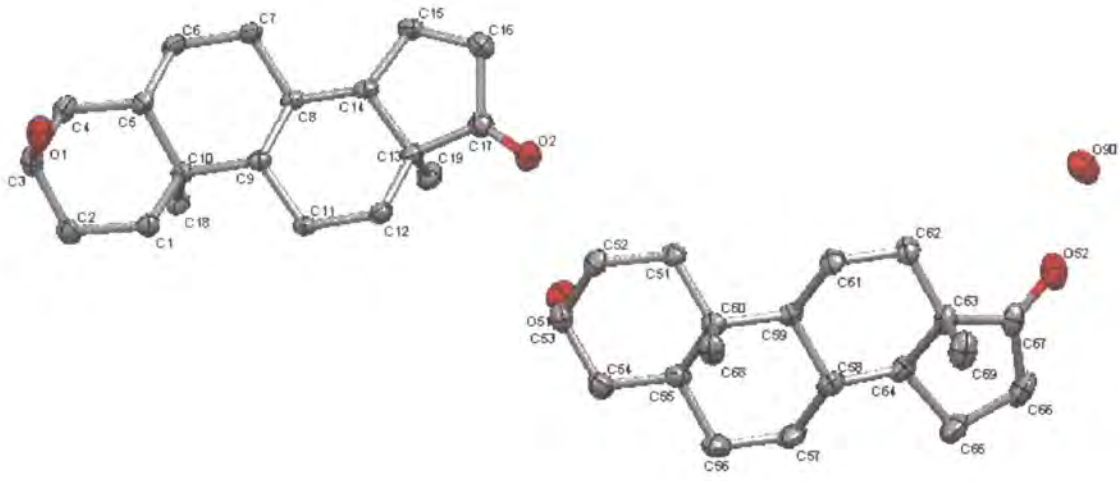

Figure 5.3. Molecular structure and atom numbering for the androsterone hemihydrate asymmetric unit.

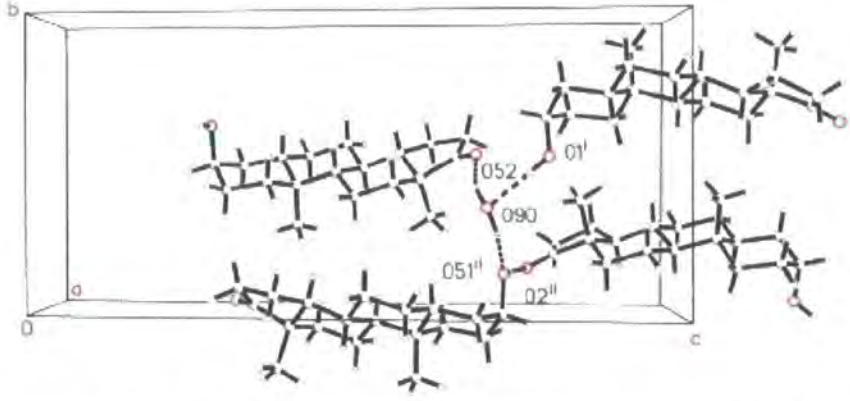

Figure 5.4. Hydrogen bonds in the androsterone hemihydrate crystal structure[10] O90 represents a water oxygen.

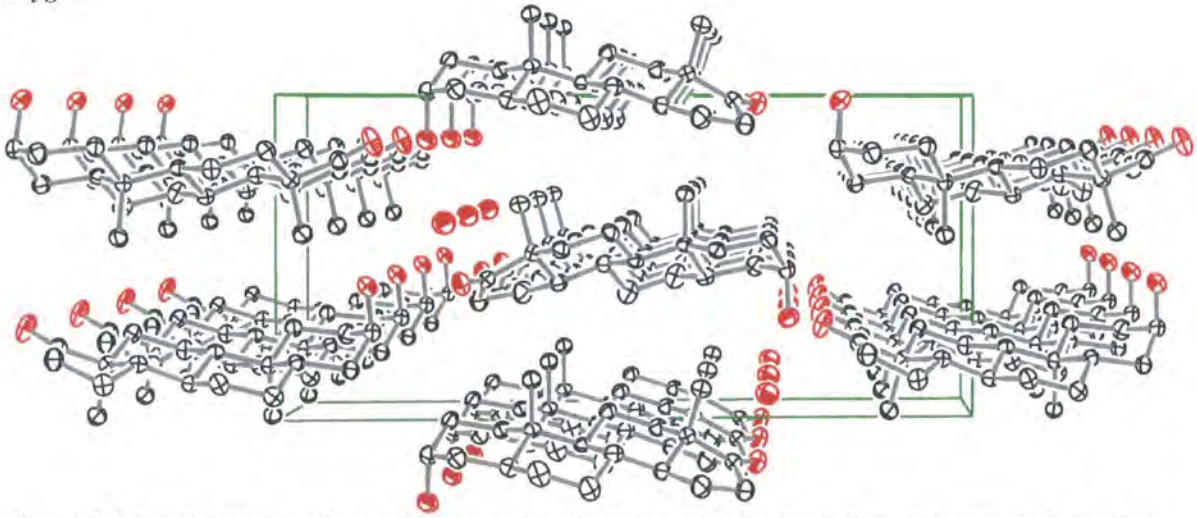

Figure 5.5. Crystal packing for androsterone hemihydrate, with the view along the *a* crystallographic axis showing water molecules inside channels.

5.3 Materials Studied

-Form 1: A sample of androsterone form 1 was provided courtesy of Dr. R. W. Lancaster. Another sample of androsterone form 1 was obtained from Sigma-Aldrich.

-Androsterone hemihydrate: A sample was provided courtesy of Dr. R. W. Lancaster. Other samples were prepared as per the literature[10] and found to be of the same form.

-"Form 2": 150 mg of androsterone form 1 was dissolved in diethyl ether and heated until saturation. The solution was kept to evaporate slowly at room temperature (B# LB1/ 13).The analysis of the sample by both XRPD and ^{13}C CPMAS showed that it is identical to form 1, which is consistent with the work by Hulme *et al.*[10] where they could not reproduce form 2.

5.4 Characterisation of Androsterone Form 1

The sample from Sigma-Aldrich was examined by XRPD and found to be of pure form 1 (Figure 5.6). The sample contains large crystallites; hence a portion of the sample was crushed before examination. However, some differences are still found between the calculated and observed powder pattern indicating the presence of severe preferred orientation. The sample was examined on a glass slide which is responsible for the broad hump in the base line of the observed pattern.

The purity of the sample was further confirmed by the ^{13}C CP MAS NMR spectrum (Figure 5.7). The spectrum shows peaks due to only one form and a single peak is observed for each carbon expected from the crystal structure of form 1 (Z'=1). The chemical shift assignments appearing in the spectrum will be explained in section 5.6.2. The two samples mentioned in section 97 were found to be identical by comparing their ^{13}C CP MAS NMR spectra.

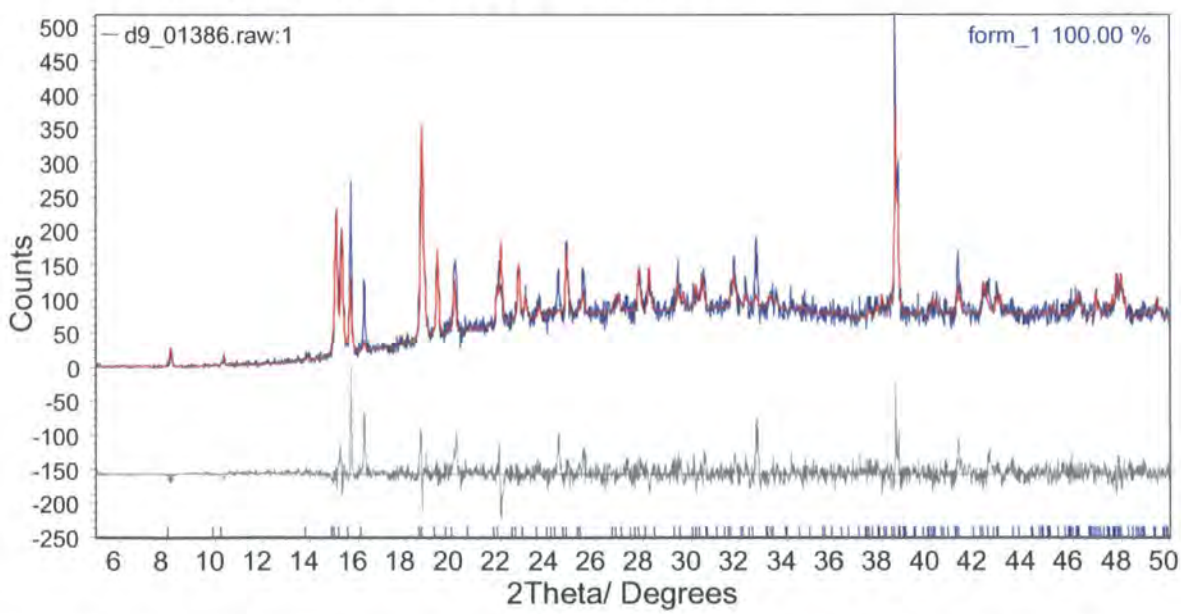

Figure 5.6. Rietveld fitting of the observed diffractogram of form 1 with the calculated powder pattern. The sample was smoothly crushed and examined on a glass slide.

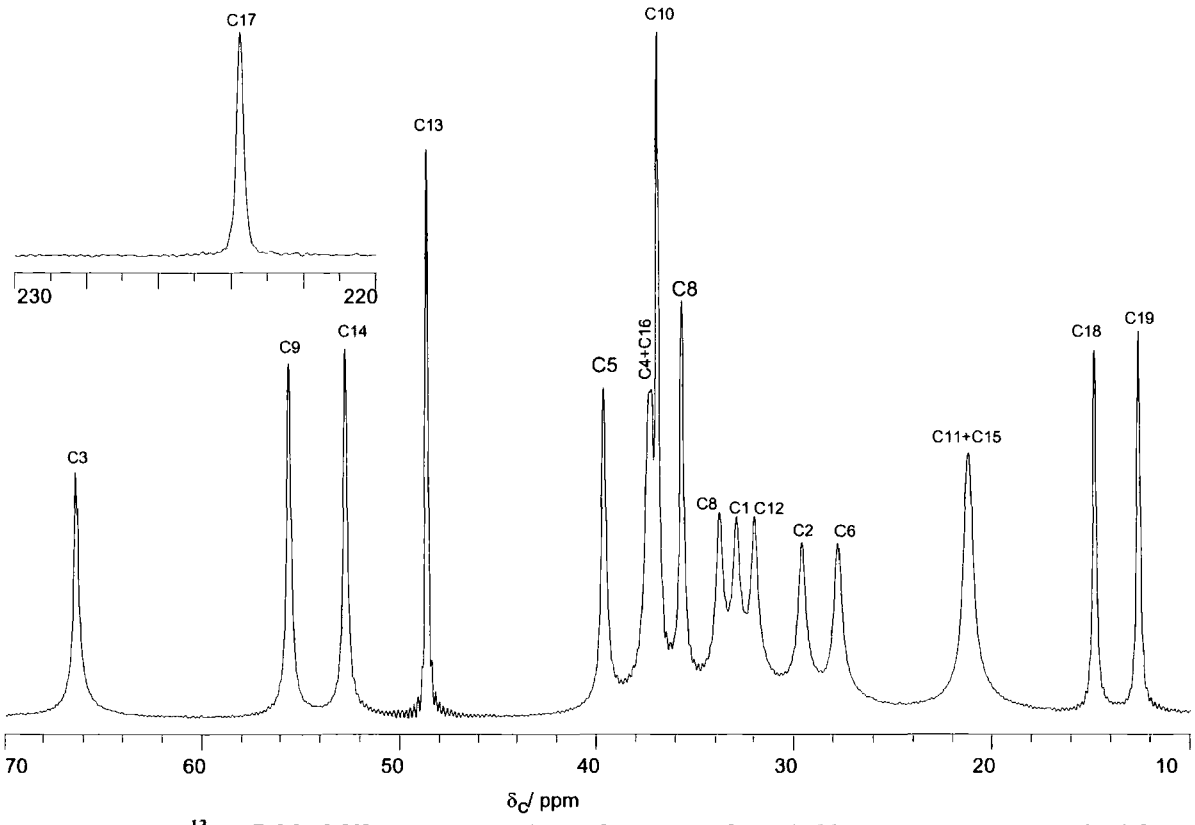

Figure 5.7. The ^{13}C CP MAS NMR spectrum for androsterone form 1. The spectrum was acquired for 40 ms with proton decoupling power of 58 kHz.

5.5 Characterisation of Androsterone Hemihydrate

The sample obtained from Dr. Lancaster was examined by XRPD as is (without grinding or crushing) and showed several differences (Figure 5.8) between the observed and calculated patterns. As in the case of the form 1 sample, such differences are due to the large crystallites of the sample, which results in preferred orientation. Since the hemihydrate form undergoes transformation to form 1 by heat[10], grinding was performed under liquid nitrogen. Consequently, the differences in the Rietveld fitting were minimised to a remarkable extent (Figure 5.9).

The ^{13}C CPMAS NMR readily distinguishes between the two forms (form 1 and the hemihydrate form). Clear differences between the two spectra were observed (Figure 5.10). The obtained spectrum of the hemihydrate was consistent with the crystal structure since nearly all non-equivalent carbons showed two peaks, indicating that the hemihydrate form has two molecules in the asymmetric unit (Z'=2). The spectrum of the hemihydrate form also shows minor peaks that correspond to form 1 peaks, indicating that the sample examined contains impurities of form 1. The peaks observed in the CH_2 peaks region (25-35ppm) were quite broad due to the low dipolar decoupling power used. However, the decoupling power was not increased further since the acquisition time was long (75 ms), thus potentially leading to over-heating of the probe.

A variable-time XRPD was carried on androsterone hemihydrate although a variable-temperature (VT) XRPD was already done by Hulme *et al.*[10]. However, different results were

obtained in terms of the stability of the form. The hemihydrate form was found to be unstable at room temperature whereas in the literature it was found to be stable up to higher temperatures (full transformation took place between 65-130°C). The transformation to form 1 occurred within 24 hours at 25°C. Figure 5.11 shows data sets collected every 14 minutes. Quantitative Rietveld analysis (Figure 5.12) shows the kinetics of form 1 formation.

The sample subjected to VT XRPD in the literature was not ground at all, whereas in my variable time experiment the sample was ground under liquid nitrogen. Hence, the instability could be attributed to either the fine particle size of the sample or the act of grinding.

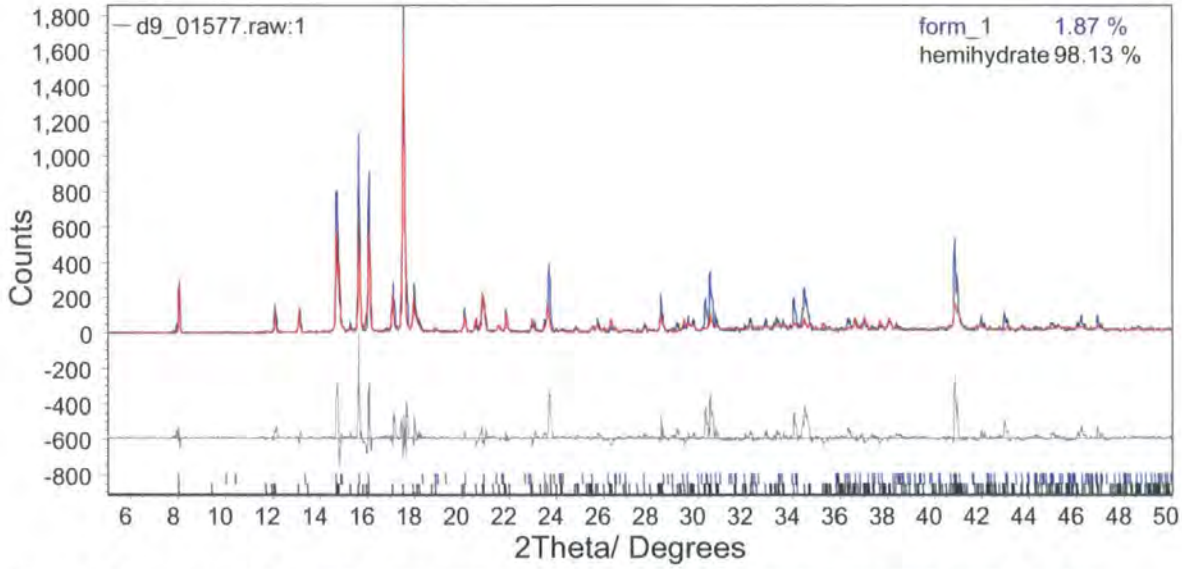

Figure 5.8. The Rietveld fitting of the observed diffractogram for the hemihydrate form with the calculated powder pattern. The sample was examined as received on a silicon slide.

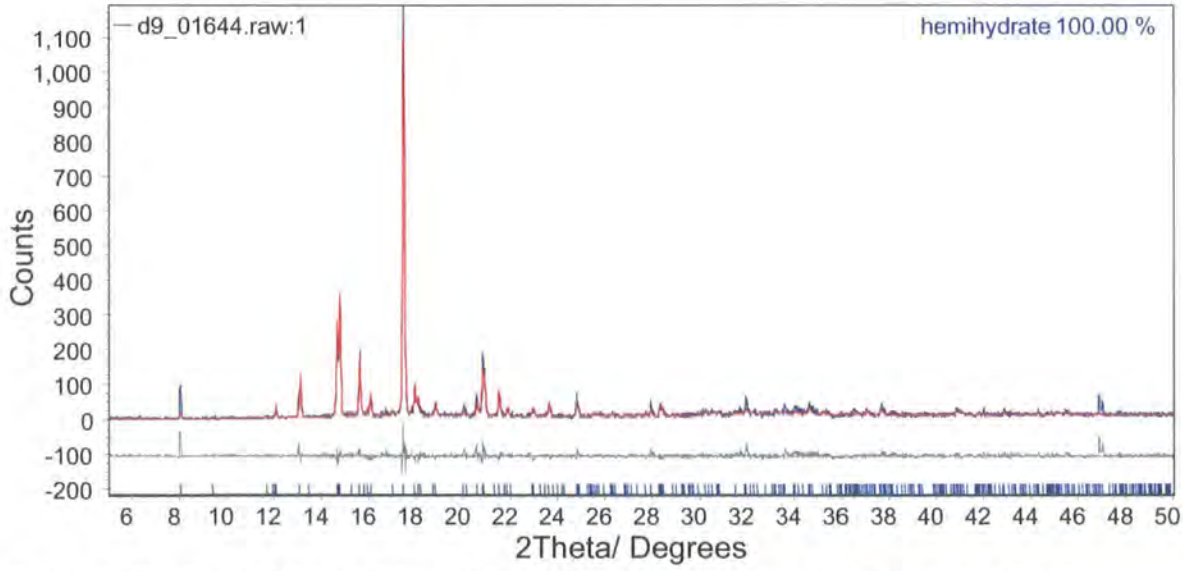

Figure 5.9. The Rietveld fitting of the observed diffractogram of the hemihydrate form with the calculated powder pattern. The sample was examined on a silicon slide after grinding under liquid nitrogen.

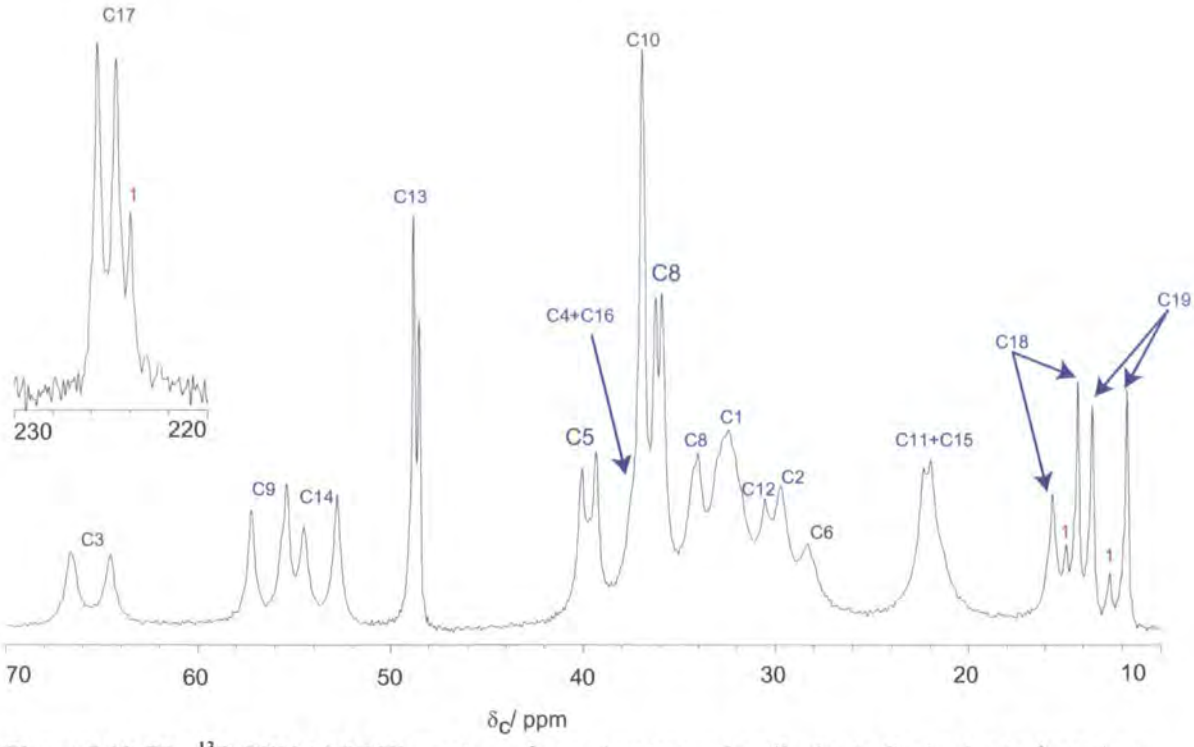

Figure 5.10. The ^{13}C CPMAS NMR spectrum for androsterone hemihydrate. Peaks due to form 1 are assigned by "1". The spectrum was acquired for 75 ms with proton decoupling power of 56 kHz.

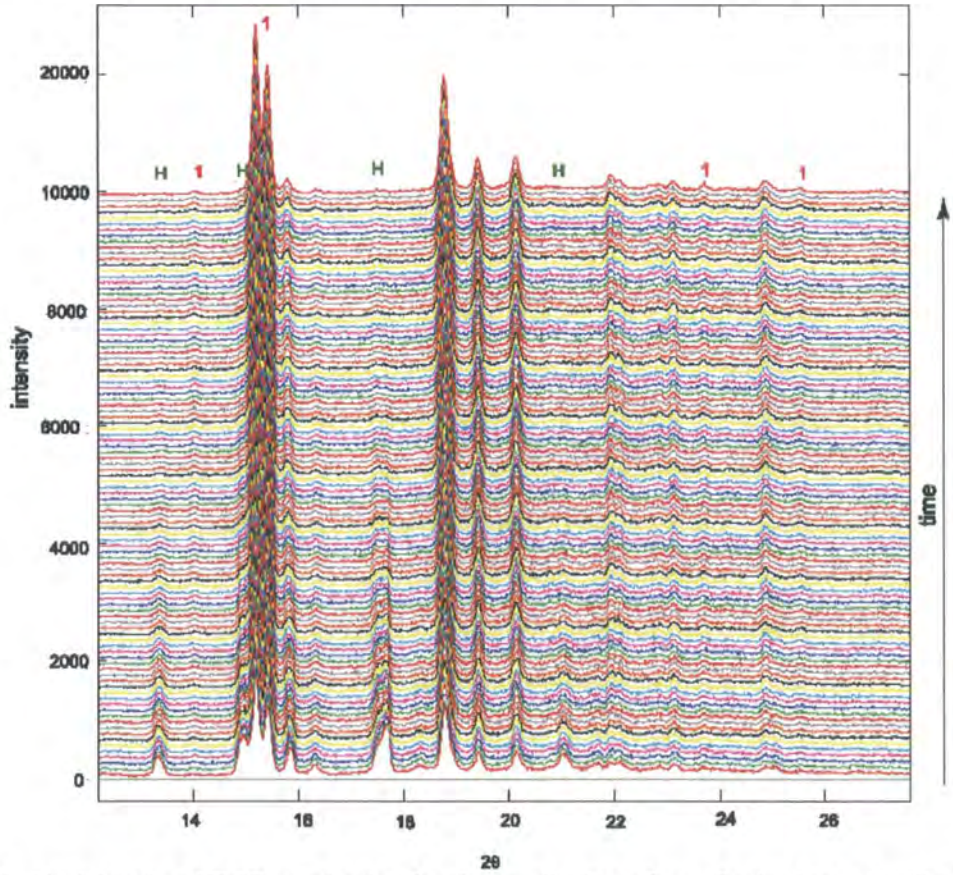

Figure 5.11. Variable time XRPD monitoring for the hemihydrate form. Peaks due to hemihydrate (H) and form 1(1) are labelled.

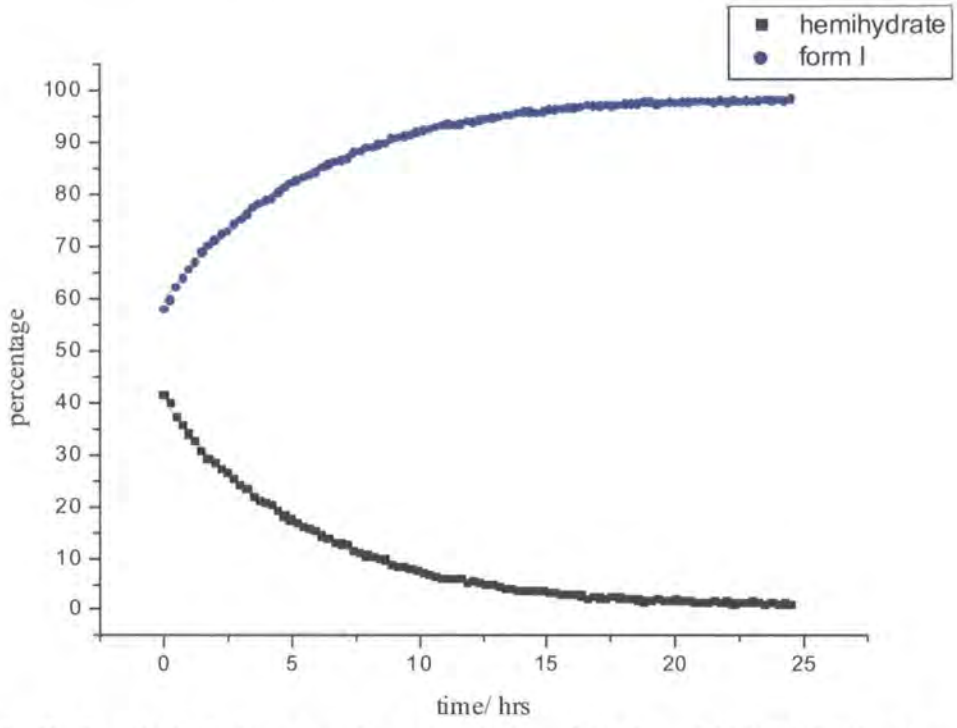

Figure 5.12. The hemihydrate form transformation to form 1 by time at 25 °C. Initially, the sample contained 41.7% of the hemihydrate form and 58.3% of form 1. The scans were recorded every 14 minutes. The data were fitted with the exponential function $y= y_0+ A_0 exp(-kt)$.

5.6 ^{13}C Chemical Shift Assignments of Androsterone Solid Forms

The solid-state assignments are done on the basis of the solution-state results. The latter assignments were made in the literature[11] in 1977 but the authors assigned two carbons to the same chemical shift (C10 and C16) due to lack of resolution. Consequently, the solution-state ^{13}C NMR spectrum of androsterone was re-examined. The two unresolved peaks were separated in the obtained spectrum. The following section illustrates the experiments carried out to fully assign the peaks.

5.6.1 Solution-state ^{13}C Chemical Shift Assignments

Figure 5.13 shows the androsterone ^{13}C NMR spectrum. 2D NMR experiments were used to assign the chemical shifts in the range of 35-36 ppm (including the resolved peaks of C10 and C16).

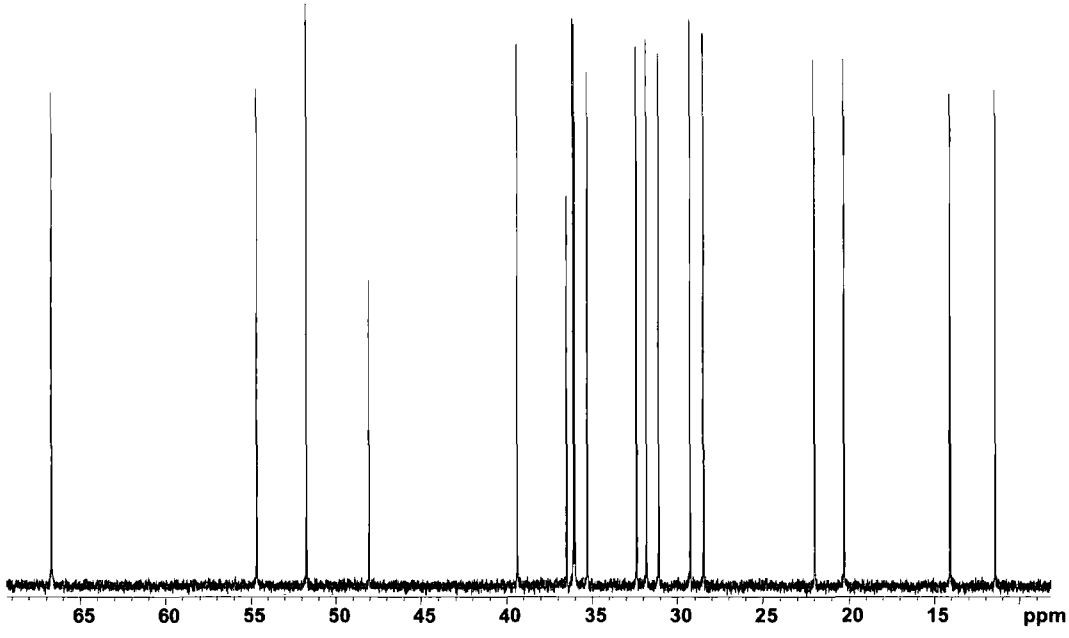

Figure 5.13. Androsterone solution-state ^{13}C NMR spectrum.

5.6.1.1 2D NMR (HMBC, HSQC and NOESY)

As seen in Table 5.4, carbons 8, 10 and 16 are indistinguishable. However, C10 is quaternary, which can be spotted from the HSQC spectrum (36.5 ppm), see Figure 5.14. The other two carbons are of CH_2 type. In the NOESY spectrum, the proton at C3 correlate with protons on C2 and C4 (Figure 5.15) and the latter protons (at C2 and C4) correlate with C4 (36.0 ppm) in the HMBC spectrum (Figure 5.16), leaving the carbon at 36.1 ppm to be C16. C16 can also be confirmed by its correlation, in the HSQC and HMBC spectra, with the deshielded proton (the quartet at about 2.5 ppm), which in turn correlates with the carbonyl (C17) in the HMBC (Figure 5.17). Table 8 shows the new chemical shift assignments.

Table 5.4. Final ^{13}C chemical shift assignments.

Carbon Number	Chemical shifts (δ_c/ ppm)
C19	11.4
C18	14.1
C11	20.3
C15	22.0
C6	28.5
C2	29.3
C7	31.1
C12	31.8
C1	32.4
C8	35.3
C4	36.0
C16	36.1
C10	36.5
C5	39.4
C13	48.1
C14	51.7
C9	54.7
C3	66.7
C17	221.0

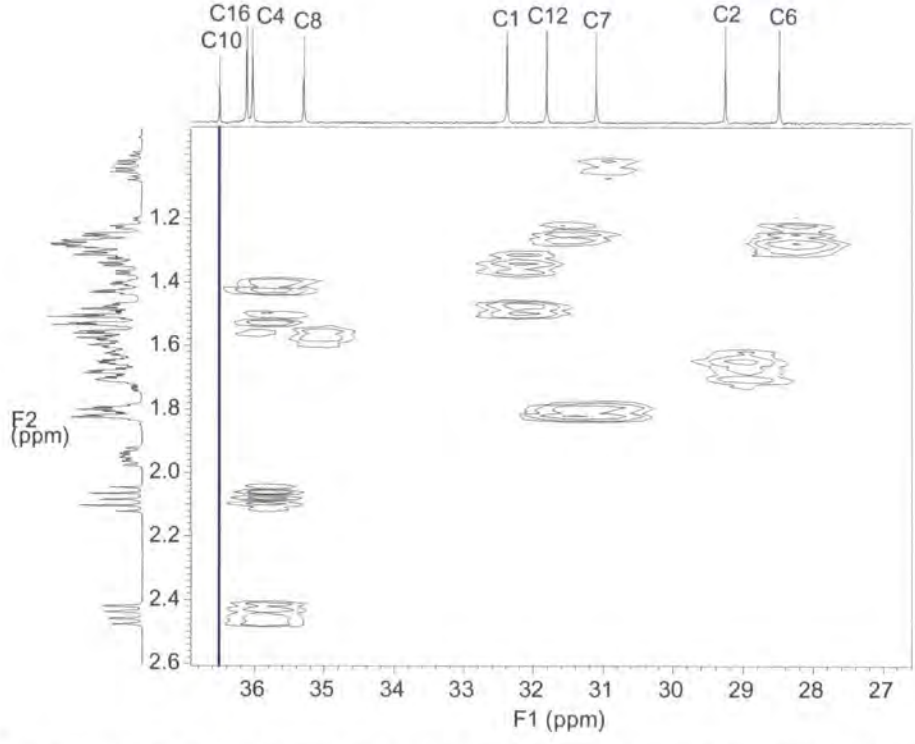

Figure 5.14. Androsterone HSQC spectrum, showing that C10 does not correlate with any proton.

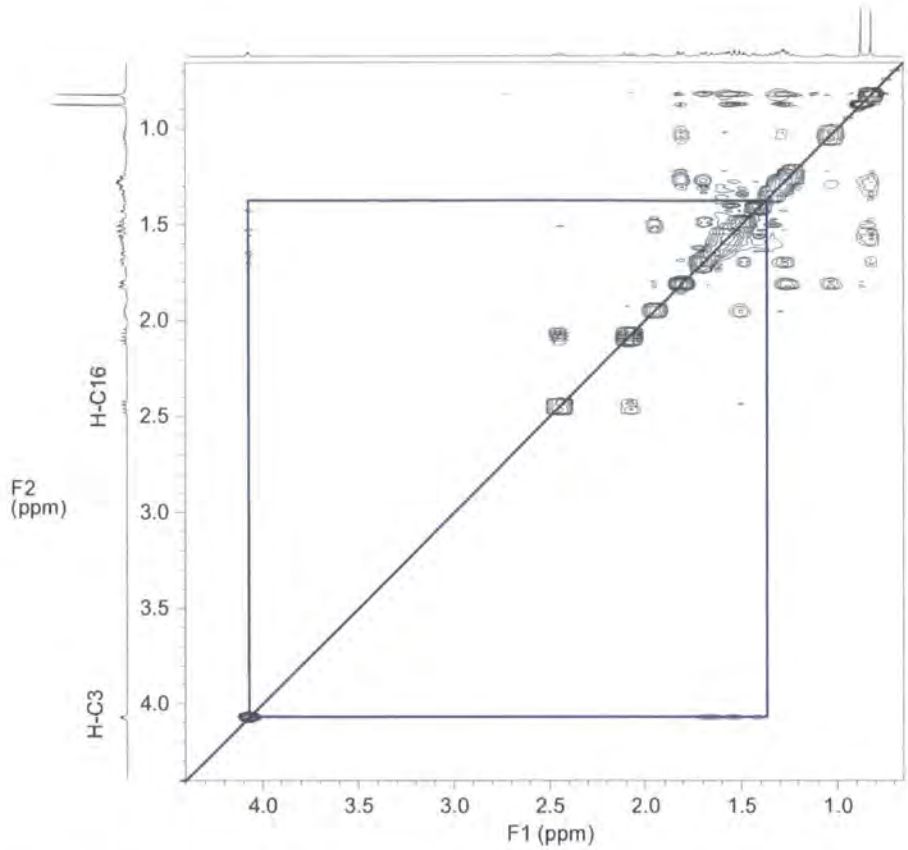

Figure 5.15. Androsterone NOESY spectrum, showing that the proton at C3 (4.1 ppm) correlates with protons apart from C16 protons (1.5-2.0 ppm).

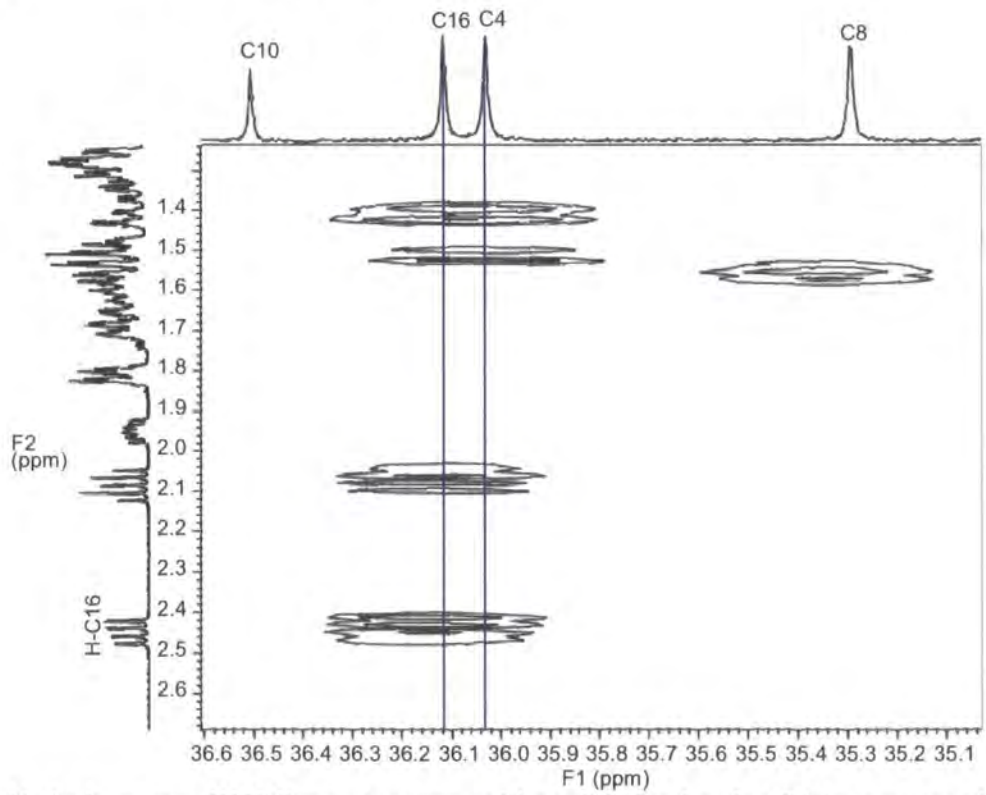

Figure 5.16. Androsterone HMBC spectrum (zoomed-in scale), showing that C4 does not correlate with protons which correlate with the protons at C3 in NOESY. C16 correlates with the deshielded proton at C16.

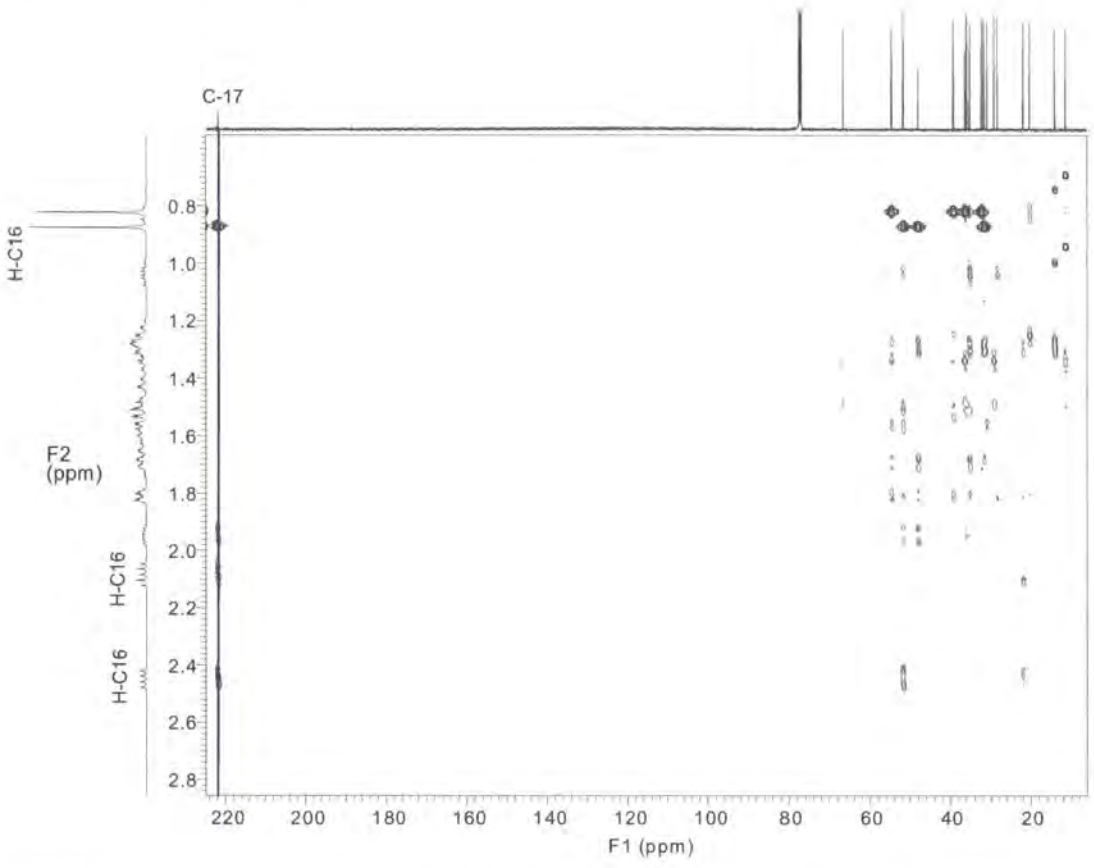

Figure 5.17. Androsterone HMBC spectrum showing that protons at C16 correlate with C17 (carbonyl).

5.6.2 Solid-state ^{13}C Chemical Shift Assignments

The ^{13}C CPMAS spectra (Figure 5.7 and Figure 5.10 of form 1 and the hemihydrate form, respectively) were assigned on the basis of the solution-state chemical assignments, dipolar dephasing and selective population inversion experiments. ^{13}C chemical shifts from the solution state helped in the assignment of most of the peaks in the solid-state spectrum, with some uncertainty in the region between 28-40 ppm. The assignments were done for androsterone form 1 and after that the hemihydrate form was assigned (as far as possible) accordingly. Table 5.5 includes the assignments for androsterone form 1 and the hemihydrate form chemical shifts.

5.6.2.1 Dipolar Dephasing and Selective Population Inversion Experiments

By using the dipolar dephasing experiment, which observes the methyl and quaternary carbons only, carbons C10, C13, C17, C18 and C19 were assigned easily (Figure 5.18).

The spectra obtained from the Selective Population Inversion experiment differentiate between the CH_2 and CH groups. The CH_2 peaks disappear or become negative by increasing the inversion time (Figure 5.18 and Figure 5.19), leaving the other peaks positive, though CH peaks diminish in intensity. Very long inversion times will turn the CH peaks negative though the CH_2 peaks are inverted faster. This was observed with 50 μs inversion time; see C8, C5, C14, C9 and C3 in Figure 5.18 as examples.

Table 5.5. Solid-state ^{13}C chemical shift (δ_c/ ppm) assignments for androsterone forms .The differences between solution state and solid-state chemical shifts are given in parentheses ($\delta_{solution\text{-}state} - \delta_{solid\ state}$).

Carbon No. (carbon type)	Solution-state	Form1	Hemihydrate form
C19(CH_3)	11.4	12.7 (-1.3)	11.7/13.5 (-0.3/-2.1)
C18(CH_3)	14.1	14.9 (-0.8)	14.3/15.6 (-0.2/-1.5)
C11(CH_2)	20.3	21.2	22.0 (1.7)
C15(CH_2)	22.0	21.2	22.0
C6(CH_2)	28.5	27.9 (0.6)	28.3 (0.2)
C2(CH_2)	29.3	29.7 (-0.4)	29.7 (-0.4)
C7(CH_2)	31.1	32.1 (-1.0)	30.5 (0.6)
C12(CH_2)	31.8	33.0 (-1.2)	32.4 (-0.6)
C1(CH_2)	32.4	33.9 (-1.5)	34.0 (-1.6)
C8(CH)	35.3	35.7 (-0.4)	35.8/36.2 (-0.5/-0.9)
C4(CH_2) [a]	36.0	[b] 37.2 (-1.5)	37.5 (-1.2)
C16(CH_2) [a]	36.1	[b] 37.4 (-1.4)	37.5 (-1.3)
C10(C)	36.5	37.0 (-0.5)	36.9 (-0.4)
C5(CH)	39.4	39.7 (-0.3)	39.3/40.0 (0.1/-0.6)
C13(C)	48.1	48.7 (-0.6)	48.5/48.8 (-0.4/-0.7)
C14(CH)	51.7	52.8 (-1.1)	52.8/55.0 (-1.1/-3.3)
C9(CH)	54.7	55.7 (-1.0)	55.4/57.2 (-0.7/-2.5)
C3(CH)	66.7	66.4 (0.3)	64.5/66.4 (2.2/0.3)
C17(C=O)	221.0	223.9 (-2.9)	224.7/225.7 (-3.7/-4.7)

[a] observed only as a negative peak in the Selective Population Inversion experiment.
[a] very small resolution between the two peaks.

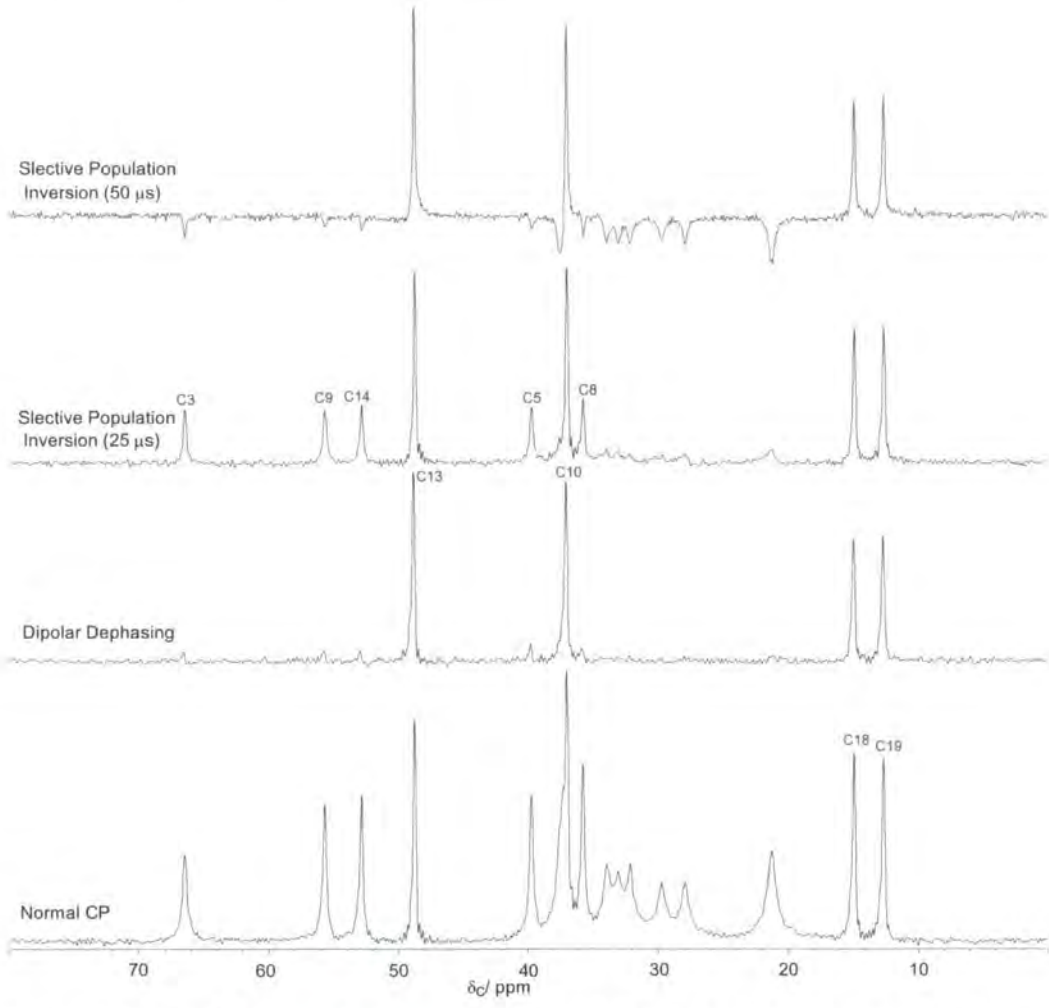

Figure 5.18. This shows ^{13}C spectra of androsterone form 1 obtained with different "editing" pulse sequences. Dipolar Dephasing show quaternary and methyl carbons while Selective Population Inversion invert the CH_2 peaks (null or negative according the inversion time).

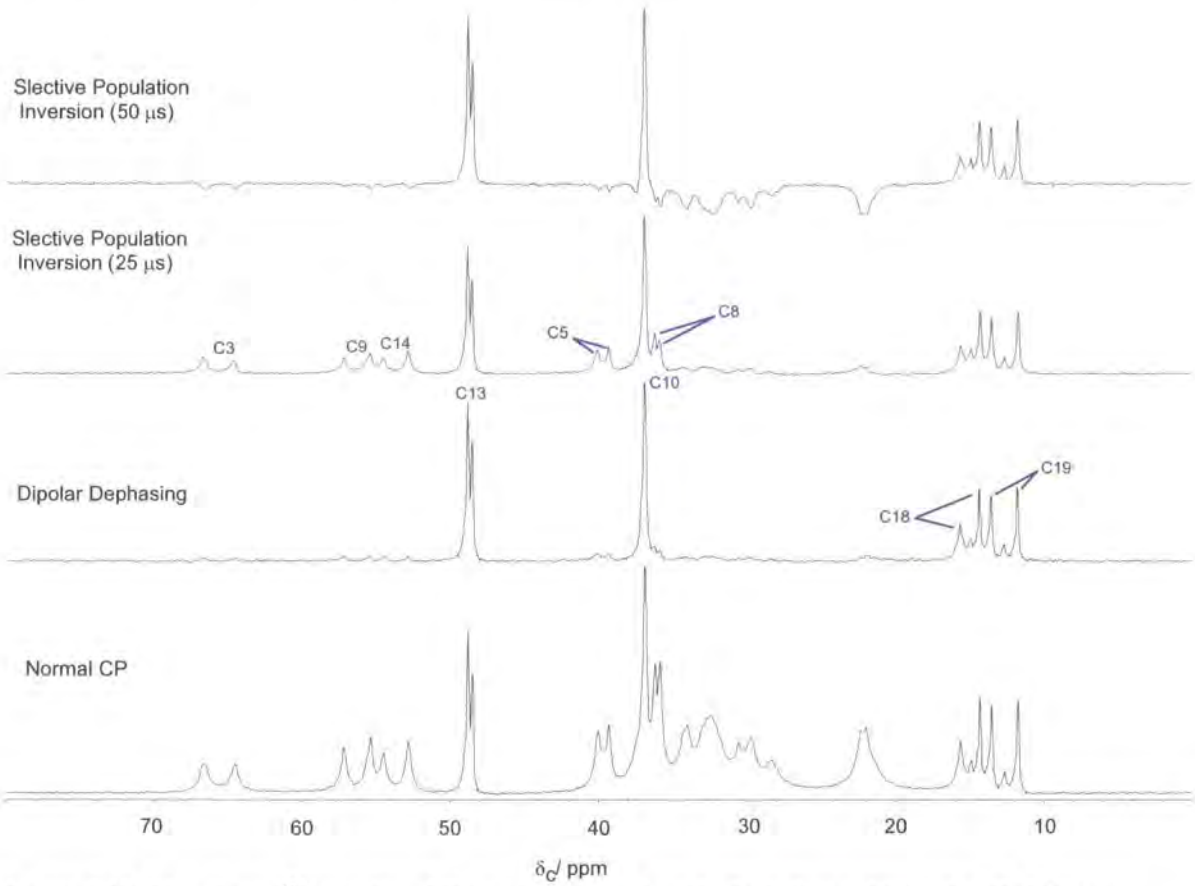

Figure 5.19. This shows ^{13}C spectra of the androsterone hemihydrate form obtained with different "editing" pulse sequences. Dipolar Dephasing show quaternary and methyl carbons while Selective Population Inversion invert the CH_2 peaks (null or negative according the inversion time).

5.7 Conclusions

A solution-state ^{13}C NMR spectrum of better resolution, than that in the literature, was obtained and the chemical shifts were assigned properly by 2D NMR. Androsterone hemihydrate form and form 1 were identified by ^{13}C CPMAS and their chemical shifts were assigned on the basis of solution-state chemical shifts and using special solid-state NMR pulse sequences (Dipolar Dephasing and Selective Population Inversion). Noticeable differences (>1.0 ppm) in chemical shifts between the solution-state and form 1 are mostly related to carbons sited at rings A and D of androsterone. The carbons in these rings are expected to be the most affected by the head-to-tail hydrogen bonding; hence the effect on their chemical shifts. C4, C10 and C16 chemical shifts were found to be in a different order than for the solution-state, of which C4 and C16 have significant chemical shift changes (~1.2 ppm). Although C3 is strongly involved in hydrogen bonding in form 1, the difference in chemical shift is small. In the case of the hemihydrate form, the difference is much clearer. On the other hand, the carbonyl (C17) is significantly deshielded in the solid-state. Carbons 11 and 15 show a single overlapped peak in the solid-state spectrum, though the peaks are separated in the solution-state. Other significant differences are found for some carbons not located

at either ring A or D. It is worth pointing out here that the two forms are of similar ring conformation, see Figure 5.20.

The hemihydrate transformation to form 1 by time was monitored using XRPD. Such transformation was also encountered while running some solid-state NMR experiments, where peaks due to form1 started to appear as function of time.

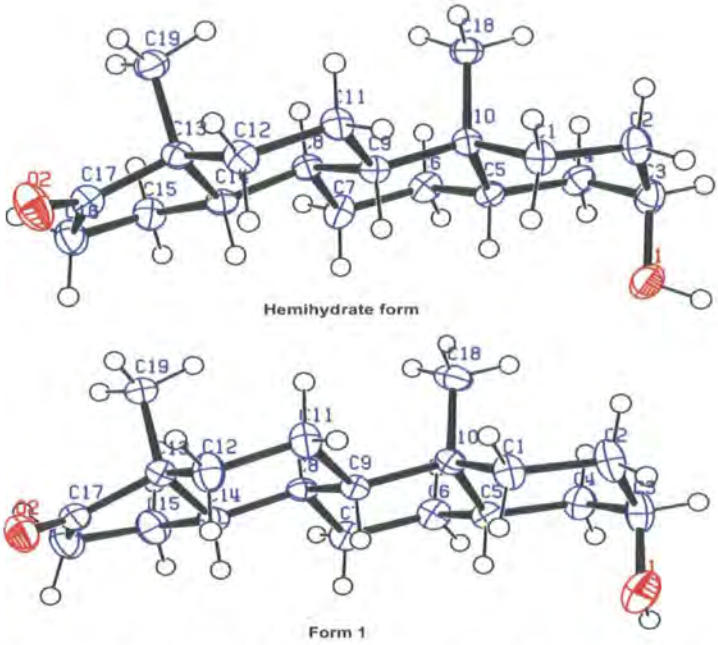

Figure 5.20. Androsterone form 1 and the hemihydrate form showing the similarity of the ring conformations.

5.8 Future Work

Preliminary ^{1}H MAS NMR work on androsterone solid forms was carried out. Signals from neither hydrogen bonding nor the water molecule in the hydrate form were resolved, probably because of the low resolution (two broad lines) obtained. It is planned to record the ^{1}H and ^{2}H MAS NMR of samples of the hemihydrate, with deuteration of the water and exchangeable hydrogens, in order to study molecular dynamics.

5.9 References

1. Hammond G 1978. Endogenous steroid levels in the human prostate from birth to old age: a comparison of normal and diseased tissues. J Endocrinol 78(1):7-19.
2. Mohler JL, Gregory CW, Ford OH, III, Kim D, Weaver CM, Petrusz P, Wilson EM, French FS 2004. The Androgen Axis in Recurrent Prostate Cancer. Clin Cancer Res 10(2):440-448.
3. Bernal JD, Crowfoot D 1936. Z Kristallogr 93:464.
4. High DF, Kraut J 1966. The crystal structure of androsterone. Acta Crystallographica 21(1):88-96.
5. Hulme A, Lancaster R, Cannon H 2006. Clarification of the crystalline forms of androsterone. CrystEngComm 8:309-312.
6. Banerjee A 1971. Crystal Data of Androsterone, C19h30o2. Zeitschrift Fur Kristallographie Kristallgeometrie Kristallphysik Kristallchemie 134(1-2):152-&.
7. Bouche R, Draguetbrughmans M 1976. Steroid Polymorphism .1. Androsterone. Mikrochimica Acta 2(3-4):403-409.
8. Kuhnert-Brandstatter M, Grimm H 1968. Differentiation of Pseudopolymorphic Crystal Forms Containing Solvents and Polymorphic Modifications in Steroid Hormones .2. Mikrochimica Acta (1):127.
9. KuhnertB.M, Grimm H 1968. Differentiation of Pseudopolymorphic Crystal Forms Containing Solvents and Polymorphic Modifications in Steroid Hormones .2. Mikrochimica Acta (1):127.
10. Hulme AT, Lancaster RW, Cannon HF 2006. Clarification of the crystalline forms of androsterone. Crystengcomm 8(4):309-312.
11. Blunt JW, Stothers JB 1977. C-13 Nmr-Studies .69. C-13 Nmr-Spectra of Steroids - Survey and Commentary. Organic Magnetic Resonance 9(8):439-464.